**THESE**

Présentée à l'Université Louis Pasteur Strasbourg I
pour obtenir le titre de:

Docteur de l'Université Louis Pasteur de Strasbourg

Par

**Shin-Hong SHIAO**

# Molecular and Cellular Basis of Interactions between *Anopheles gambiae* and *Plasmodium berghei*

Soutenue le 16 mars 2005 devant la commission d'examen:

**Prof. Robert SINDEN**
Biological Sciences Department, Imperial College of Science, London

**Prof. Dominique WACHSMANN**
Laboratoire d'Immunologie et de Biochimie Bacterienne, Strasbourg

**Dr. Laurent RENEA**
Département d'Immunologie, Institut de Cohane, Paris

**Prof. Fotis KAFATOS**
European Molecular Biology Laboratory, Heidelberg

**Prof. Jules HOFFMANN**
Institut de Biologie Moléculaire et Cellulaire, Strasbourg

**Dr. Elena LEVASHINA**
Institut de Biologie Moléculaire et Cellulaire, Strasbourg

# Abstract

*Anopheles* mosquitoes are important vectors of human malaria, which is caused by *Plasmodium* parasites in the sub-Sahara. The transmission of this disease is initiated by an infectious bite of an *Anopheles* mosquito. The parasite undergoes massive losses during its development in the mosquito, suggesting that mosquitoes are able to mount a potent immune response against the parasite. However, the cellular and molecular mechanisms of mosquito-parasite interactions are not completely understood. We first established an *in vitro* co-culture system using a mosquito hemocyte-like cell line of *A. gambiae* and chose a thioester-containing protein 1 (TEP1), which acts as an opsonin and promotes phagocytosis of bacteria by hemocytes, as a candidate to study its role in mosquito-parasite interactions.

We demonstrated that the mosquito cells in the co-culture system responsed to the parasite presence by activation of general immune responses, including the induction of synthesis of antimicrobial peptides and phagocytosis. As no specific interactions between TEP1 and the ookinetes could be detected, we concluded that our *in vitro* model is unsuitable for TEP1 functional analysis. By using a double-stranded RNA (dsRNA) silencing technique and phenotype assays, we demonstrated that the binding of TEP1 to *Plasmodium* parasites mediates their killing in the mosquito midgut. These results document the important role of mosquito immune responses, especially those mediated by hemocytes, in the establishment of vectorial capacity in *A. gambiae.*

We performed transmission electron microscopy to follow the development of *P. berghei* parasites in the *A. gambiae* midgut. We observed that the majority of *P. berghei* ookinetes invade the mosquito midgut before complete polymerization of the peritrophic matrix. Moreover, during the invasion, ookinetes preferentially take an extracellular route to migrate across the midgut. This conclusion is important as it suggests that during midgut invasion parasites are rather facing hostile environlment of the extracellular space than the cytoplasmic milieu of the epithelial cells.

We demonstrated that the previously described filamentous zone surrounding melanized parasites is composed of polymerized actin and renamed it the “actin zone”. The formation of the actin zone occurs when parasites are dead or dying, suggesting that the actin zone is not associated directly with parasite killing. The silencing of *TEP1* by dsRNA abolishes the formation of the actin zone in both susceptible and refractory mosquitoes, suggesting that TEP1 could be the genetic determinant of this structure. Therefore, a model of actin-based parasite clearance is proposed: the parasite is first killed by a *TEP1*-dependent mechanism, and subsequently the parasite is lysed or melanized. Dead or dying parasites are recognized by epithelial cells, and the actin zone is then formed to separate the dead or dying parasites from host tissues.

# Résumé

Le moustique anophèle est le vecteur majeur du paludisme. Cette maladie provoquée par les parasites du genre *Plasmodium* est transmise par une piqûre infectieuse d'anophèle. Le parasite subit des pertes massives pendant son cycle de développement chez l'anophèle, ce qui suggère que les moustiques sont capables de développer une réaction immunitaire efficace contre le parasite. Cependant, les mécanismes cellulaires et moléculaires des interactions entre parasite et anophèle restent mal connus.

Pour aborder cette étude, nous avons commencé par établir un système *in vitro* basée sur la culture d'une lignée cellulaire d'anophèles de type hémocytaire, en présence d'oocinètes de *Plasmodium*. Nous avons démontré que, dans ce système *in vitro*, les parasites induisent une réponse immunitaire de type non spécifique comprenant, entre autres, la synthèse de peptides antimicrobiens et la phagocytose.La protéine à motif thioester, TEP1, agit en tant qu'opsonine chez l'anophèle et favorise la phagocytose des bactéries par les hémocytes. Après avoir vérifié que notre lignée cellulaire était capable de produire une protéine TEPI fonctionnelle pour la phagocytose, nous avons utilisé ce système pour étudier la fonction de TEP1 dans la réponse antiparasitaire. Contrairement à la situation observée *in vivo*, nous n'avons cependant pas détecté de liaison directe entre TEP1 et la surface des oocinètes et conclu que le modèle *in vitro* était peu adapté à l'analyse fonctionnelle de TEP1.

Nous avons alors développé la technique d'invalidation des gènes par l'ARN double brin (dsRNA) chez l'anophèle adulte et avons pu démontrer que la liaison de TEP1 sur la surface des parasites induit leur élimination dans le tube digestif du moustique. Ces résultats montrent le rôle crucial des réactions immunitaires de l'anophèle vis-à-vis du parasite.

Nous avons utilisé la microscopie électronique à transmission pour suivre le développement du parasite *P. berghei* chez *A. gambiae* et avons observé que la majorité des oocinètes envahit les cellules épithéliales du moustique avant la polymérisation complète de la matrice péritrophique. De plus, ces oocinètes prennent préférentiellement un itinéraire extracellulaire pour migrer à travers le tube digestif. Cette observation est très importante, car elle démontre que les parasites sont confrontés à l'environnement hostile de l'espace extracellulaire du tube digestif plutôt qu'au milieu cytoplasmique des cellules épithéliales.

Enfin, nous avons démontré que la dite "zone filamenteuse" qui entoure les parasites mélanisés se compose d'actine polymérisée. Nous l'avons renommée «zone d'actine». La formation de cette zone se produit lorsque les parasites sont morts ou mourants, ce qui suggère qu'elle n'est pas directement responsable de la mort des parasites. L'invalidation de *TEP1* par la technique du dsRNA supprime la formation de la zone d'actine, ce qui montre l'implication, directe ou indirecte, de TEP1 dans cette structure. Nous proposons ainsi un modèle d'élimination parasitaire: le parasite est d'abord tué par un mécanisme dépendant de TEP1, puis, subit une lyse ou mélanisation. Les cellules épithéliales identifient les parasites morts ou mourants et se protègent par polymérisation d'actine dans la zone de contact.

# Acknowledgements

First of all I would like to thank Prof. Jules Hoffmann for giving me the opportunity to work in his laboratory, in an excellent scientific environment and for his continuous support. It is always an exciting hour to work in the field of innate immunity and vector biology. Thank you for contributing so much to the establishing of the mosquito group thus allows us to work without any fear of disturbance in the rear.

I am very grateful to Prof. Fotis Kafatos for accepting me in his laboratory, this period was very important for me as it open the world of mosquito functional genomics. Thank you for your generous support during my stay at EMBL, and for your interest in my work.

I would like to thank Prof. Robert Sinden, Prof. Dominique Wachsmann and Dr. Laurent Renia who accepted to be part of the jury and to critically read my thesis. I would also like to thank Prof. Robert Sinden for generously provide the parasite clones and antibodies.

Most of all, I am greatly indebted to my supervisor Dr. Elena Levashina. I would like to thank her for her patience and her great support and guidance. Thank you Lena, for your enthusiastic discussions, always open your door and listen to anyone of us even there is only some negligible things, and always answer my stupid questions with full patience. In addition, I really appreciate for your great help in my thesis. It is really a wonderful time to work with you.

This work has benefited from diverse collaboration and I would like appreciate those who have been involved. I would like to thank Prof. Daniel Zachary for teaching me the discipline of electron microscopy and for fruitful discussions. I gratefully thank Dr. Heinz Schwarz and Dr. Gareth Griffiths for drawing our attention to the ultrastructural study. Thanks to the members of the TEP team at EMBL: Dr. Stephanie Blandin and Dr. Luis Moita, for their kindness, sharing materials and ideas. Also thanks to Dr. George Christophides for his kind collaboration with the microarray analysis. I thank Dr. Stefan Wyder, with whom I share ideas and fruitful discussions, regardless of scientific or non-scientific merit. Many thanks to Dr. Miranda Whitten, for her critical reading of the manuscript, and thanks to Christelle for her help with the translation of the French part of my thesis.

Thanks also to the members of Prof. Hoffmann's lab, and especially to Dr. Christine Kappler for her kindness and help with everything I asked, to David and Francine for their assistance at the beginning of my thesis, and to the members of the mosquito group: Cecile, Nicolas, Martine, Malou, Marie-Eve and Annika for their kind cooperations. I would also like to thank the members of the Kafatos' lab for their kind welcome and assistance during my stay in Heidelberg.

Special thanks to the electron microscope group at the Institut Fédératif de Recherche de Neurosciences de Strasbourg: Prof. Yannick Bailly, Dr. Anne-Marie Haeberlé and Valérie Demais for their assistance.

The most important and grateful thanks will go to my family, my parents, my brother, my wife Yu-Lan and my daughter Michelle, for their love, endless support and their encouragement. And Thanks to my friends in Taiwan and in Strasbourg who continuously pray for me.

Thanks Lord for everything.

# Table of Contents

**Chapter 4. The role of actin in parasite clearance in *Anopheles* mosquitoes**



**General Discussion**



**Résumé de Thèse en Français**



**Materials and Methods**

# GENERAL INTRODUCTION

## 1. Malaria

Malaria probably originated in Africa and fossils of mosquitoes up to 30 million years old show that the vector for malaria was present well before the earliest recorded history. *Plasmodium* parasites are highly specific, using man as the main vertebrate host and *Anopheles* mosquitoes as the vectors. This specificity of the parasites also points towards a long and adaptive relationship with our species (reviewed by Sinden 2002).

At present, at least 300 million people are affected by malaria globally, and there are between 1 million and 3 million malaria deaths per year. Malaria is generally endemic in the tropics, with extensions into the subtropics. Malaria in travelers arriving by air is now an important cause of death in non-malarious areas, and this is not helped by ignorance or indifference of travelers to prophylaxis. Distribution varies greatly from country to country, and regionally within the countries themselves, as the flight range of the vector between suitable habitats is fortunately limited to a maximum of 3 km (Gwadz and Collins 1996).

In 1990, 80% of the global malaria cases were in Africa, with most of the remainder clustered in nine countries: India, Brazil, Afghanistan, Sri-Lanka, Thailand, Indonesia, Vietnam, Cambodia and China. *Plasmodium falciparum* is the predominant malaria parasite species responsible for 120 million new cases and up to 1 million deaths per year globally. It is the *P. falciparum* species which has given rise to the formidable drug resistant strains emerging in Asia. In 1989, the World Health Organization (WHO) declared malaria control to be a global priority due to the worsening situation, and in 1993, the World Health Assembly urged member states and WHO to increase control efforts. As well as control measures, such as spraying with DDT, coating marshes with paraffin (to block *Anopheles* mosquito larvae spiracles), draining stagnant water, and the widespread use of bed nets, research into the biology and microbiology of malaria enables a methodical search for better vaccines and a possible cure in the fight against malaria (Gwadz and Collins 1996).

In addition, support for fundamental, applied and operational research aims to develop new technical tools, such as new drugs and vaccines, but also new strategies to control the vectorial capacity of mosquitoes. The past few years have witnessed the emergence of techniques that allow stable genetic transformation of mosquitoes. By genetic engineering, mosquitoes could be rendered refractory to parasite infection by the expression of an exogenous compound inhibiting parasite development (Ito et al., 2002), by the mis-expression of a mosquito molecule essential to parasite development or by the fine-tuning of already existent mosquito immune defence. Although at present the ecological consequences of a release of genetically engineered mosquitoes, even when sterilized, are very difficult to

foresee, it provides an attractive tool to modulate mosquito vectorial capacity. Nevertheless, to design novel strategies and to assess the associated potential efficacy and risk, a more thorough understanding of mosquito-parasite interactions at the molecular level is required. In spite of more than 100 years of research, our understanding of *Anopheles-Plasmodium* interactions is still lacking important molecular and cellular insights into the finely-tuned host-parasite interactions.

## 2. Malaria parasite and mosquito vector

Insect resistance to infectious agents is essential for their own survival and also for the health of the plants, animal and human populations with which they closely interact. Several major human diseases are spread by insects and are rapidly emerging as a result of the development of insecticide resistance in vectors and drug resistance in parasites. Malaria is the most important and threatening of these diseases. Most of these cases occur in poorly developed countries, where the lack of environmental management of the vector habitat, the major public health infrastructures and the unavailability of curative and preventive drugs contribute to the spread and of the disease.

Studies initiated by Ross and Grassi, clearly demonstrate that malaria is caused by *Plasmodium*, a unicellular apicomplexan protozoan, which is transmitted to humans by mosquitoes. During its asexual lifecycle in the human host, *Plasmodium* differentiates through several developmental stages, which can dramatically alter the physiology of the host, leading to fever and chills, to severe anaemia and in the worse case to brain damage and death. Of the four species that are known to cause human malaria, *P. vivax* and *P. falciparum*, are the most common. The former species accounts principally for malaria in Southeast Asia, India and Central/South America, while the by far more dangerous *P. falciparum* species is found mostly in Africa.

The parasites are transmitted with infective bites by female mosquitoes, after the completion of the sporogonic cycle that takes places in the insect vector. The spread of malaria is intimately linked to the success of the cycle within the insect vector. Although the parasites have to pass through several bottlenecks and suffer severe losses in the mosquito, transmission rates can be very high in malaria endemic areas where several hundreds of infective bites can affect one person. Several mosquito species can serve as natural vectors for malaria. Three main features however, define the transmission capacity of a species: 1. support of the parasite life cycle, 2. the habitat and feeding behaviour and 3. the average lifespan of the vector. Historically, in many areas where malaria has been eradicated, effective control was achieved by targeting the vector and transmission rates through the use of insecticides and the eradication of mosquito breeding sites, concomitant with the application of well-designed prophylactic

programs.*Anopheles gambiae* is the natural vector of *P. falciparum* in sub-saharian Africa. The adults of this species are notorious for their highly anthropophylic feeding preference and indoor resting behaviour. Unfortunately, the control of this species is hampered by the nature of the seasonal breeding sites, characterised by small depressions, which are difficult to eliminate or to treat. For these reasons, the understanding of the molecular and cellular basis of vector-parasite compatibility and the biology of cellular and molecular interactions between mosquito and *Plasmodium* insect-stages will be a substantial aid in the development of effective control strategies.

### 3. Brief overview of the *Plasmodium* life cycle

The malaria parasite takes many forms during its complex life cycle, alternating invasive and replicative stages, both in the vertebrate host and in the anopheline vector. An overview is presented in Figure 1. Sporozoites are injected with the saliva of a female mosquito into a vertebrate host with an infective bite. They rapidly invade hepatocytes to escape from the blood stream of the host. After successful

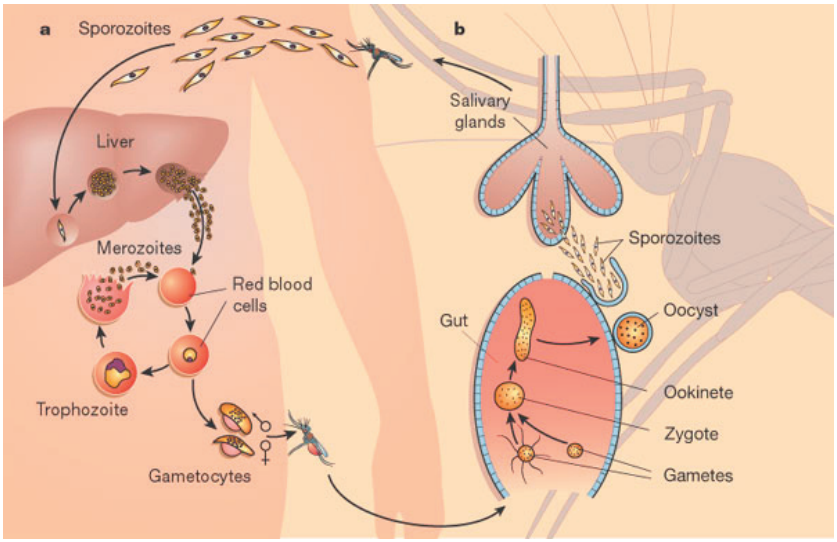


**Figure 1. Lifecycle of the malaria parasites**
To successfully complete its lifecycle, *Plasmodium* has to be transmitted to the vertebrate host by a mosquito vector. Critical differentiation steps of the parasites occur both in the vertebrate host and in the vector. The completion of the asexual cycle and the sporogonic cycle are necessary to perpetuate the malaria parasite survival (adapted from Wirth, 2002).

invasion of the hepatocytes, single sporozoites can develop up to 20,000 merozoites, which rupture the hepatocytes and enter the bloodstream. Then the asexual erythrocyte cycle begins, with the merozoites invading the red blood cell (RBC).

After invasion of the RBC, merozoites mature from ring forms to schizonts, which are periodically released into the bloodstream by rupture of the RBC and which are able to invade new erythrocytes. Schizonts are released during a period of 48-72 h post infection, depending on the species of malaria parasite, and this triggers the pathological onset of recurring fevers. A number of erythrocytic stages differentiate into gametocytes, which can be ingested by the mosquito through a blood meal. Gametocytes give rise to sexual gametes, which fertilise in the midgut of the mosquito. Zygotes develop into

motile, banana shaped ookinetes, which penetrate the midgut epithelium 24 h after blood ingestion. The ookinete transforms then into an oocyst, in which sporogony takes place. After maturation of the oocyst, several thousands of sporozoites are released in the mosquito hemocoele, and then invade the salivary glands. They are finally transmitted to a new vertebrate host with an infective bite.

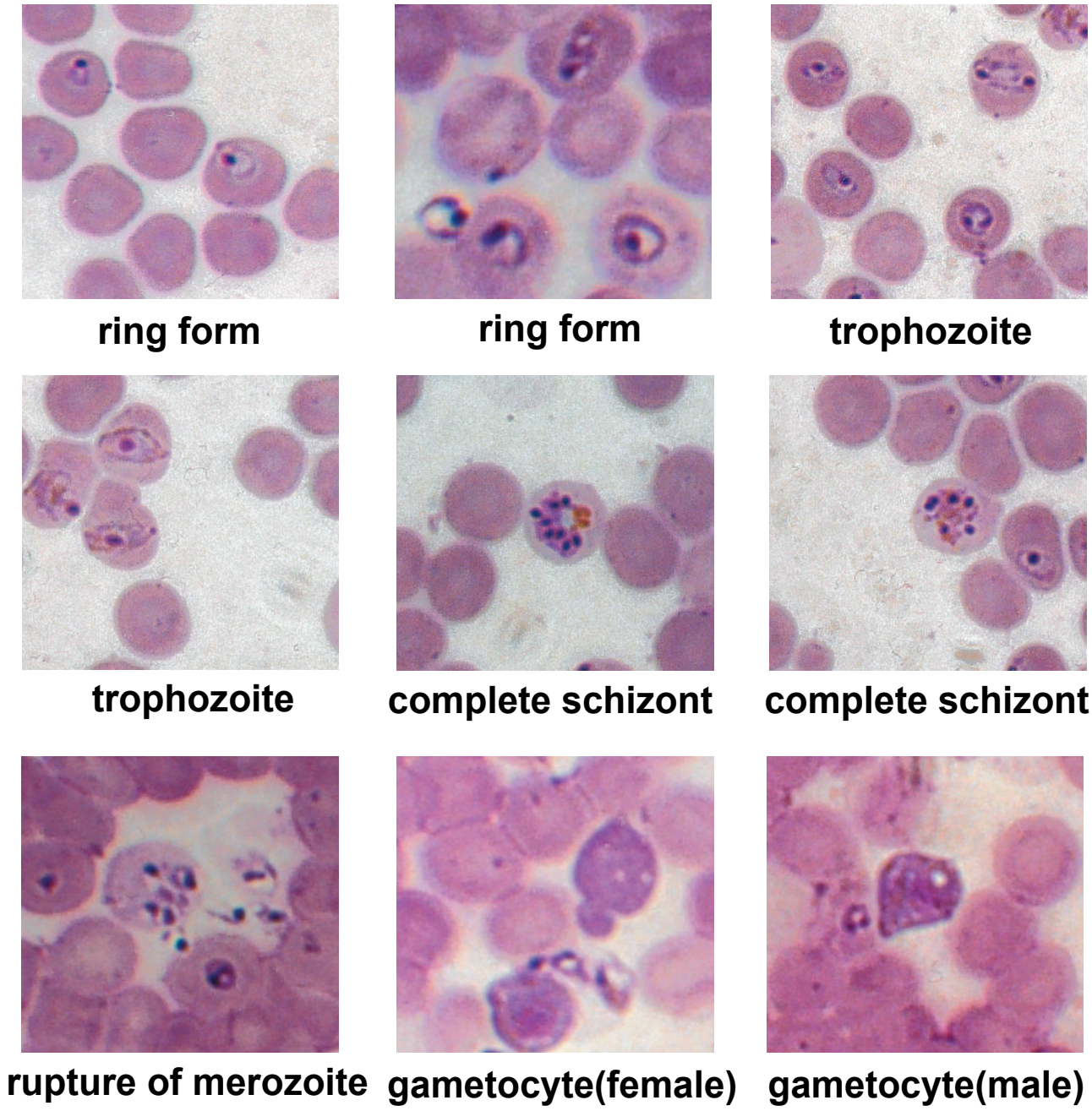


**Figure 2. The erythrocytic stages of *P. berghei* parasite in the mammalian host**
The asexual erythrocytic cycle begins with merozoites invading the red blood cell (RBC). After invasion of the RBC, merozoites mature from ring form, to trophozoites to schizonts. A number of erythrocytic stages differentiate into gametocytes, which can be ingested by the mosquito through a blood meal.

**The asexual cycle in the mammalian host**

Sporozoites are transmitted to a vertebrate host by the bite of an infected *Anopheles* mosquito. The sporozoites enter hepatocytes shortly after inoculation into the blood circulation. Sporozoite invasion of hepatocytes requires the interaction of surface proteins of the sporozoite and host cell. Recently, a protein called sporozoite microneme protein essential for cell traversal (SPECT), which has a membrane attack complex/perforin (MACPF)-related domain has been shown to be involved in breaching of the liver sinusoidal cell layer before entering hepatocytes (Ishino et al., 2004). In the hepatocytes, sporozoites develop into exoerythrocytic (preerythrocytic) stage schizonts during the next 5-10 days, depending on the *Plasmodium* species. *P. vivax, P. ovale* and *P. cynomolgi* have a dormant stage, named the hypnozoite, which may remain in the liver for weeks before the development of preerythrocytic schizongony (Krotoski et al., 1982 and reviewed by Fujioka and Aikawa 2002). This results in relapses of malaria infection. *P. falciparum* and *P. malariae* have no persistent phase. A preerythrocytic schizont contains 10,000 to 30,000 merozoites, which are released into the blood circulation and invade the RBC. Merozoites develop within the RBC through ring, trophozoite and schizont stages (erythrocytic schizogony) (Figure 2). The parasite modifies its host cell in several ways to enhance its survival. Erythrocytes containing segmented schizonts eventually rupture and release the newly-formed merozoites, which then invade new erythrocytes. Erythrocyte invasion by merozoites is dependent on the interactions of specific RBC membrane receptors with molecules on the surface of the merozoite. First, merozoite attachment and orientation towards erythrocytes may involve adhesion of erythrocyte ligands to merozoite surface molecules, such as merozoite surface protein 1 (MSP-1) or apical membrane antigen-1 (AMA-1). The following tight attachment might be promoted by micronemal compounds such as erythrocyte-binding antigen (EBA-175) or Duffy-binding-like erythrocyte-binding protein (DBL-EBP) (reviewed by Chitnis et al., 2000). The entire invasion process takes about 30 seconds (reviewed by Fujioka et al., 2002).

Concomitantly, a small portion of the parasites differentiate from newly invasive merozoites into sexual forms, termed macrogametocytes (female) and microgametocytes (male). The trigger for this alternative developmental pathway leading to gametocyte formation is presently unknown. Unlike most viral and bacterial intracellular pathogens, which trigger their own passive uptake by the host cell and form a parasitophorous vacuole in order to be protected from the cytosolic environment, *Plasmodium* invasion appears to be an active process. The parasite has an active actin-based motility system to enter the host cell. Breaching of the host cell plasma membrane is rapidly followed by a repair mechanism and by the exit of the parasite from the cell. Intriguingly this mode of invasion does not result in the formation of an internalization vacuole. Sporozoites traverse the cytosol of several hepatocytes before finally invading a cell, and forming a parasitophorous vacuole, in which they will develop into the next

infective stage (Mota et al., 2001). Migration through several hepatocytes might be beneficial for malaria infections in two ways: by activating sporozoites for infection and by increasing the susceptibility of host hepatocytes (reviewed by Mota et al., 2004).

### Sporogonic cycle in the mosquito vector

The sporogonic cycle (Figure 3) involves a series of complex differentiation and developmental steps that the parasite has to undertake to overcome a hostile environment within the vector (reviewed by Sinden, 1999).

As all nonautogenic insects, mosquitoes rely on a blood meal to induce oogenesis. A study on the female fat body specific vitellogenin gene, which is exclusively expressed after a blood meal, revealed the important link between the mosquito reproduction cycle and pathogen transmission (Raikhel et al., 2002). Only female mosquitoes bite their hosts and are, therefore, solely responsible for the transmission of *Plasmodium* species. Initially, the vector ingests gametocytes with an infective blood meal. Within an hour after blood ingestion, gametogenesis is triggered. This process involves the escape of the gametocyte from the RBC. Male gametocytes undergo a specific differentiation, termed 'exflagellation'. It was postulated that the blood meal contains a potent mosquito-derived factor (formerly named MEF, mosquito exflagellation factor) that triggers gametogenesis leading to the release of 8 motile microgametes (reviewed by Aikawa 1971). The chemical identity of this crucial "ignition key"

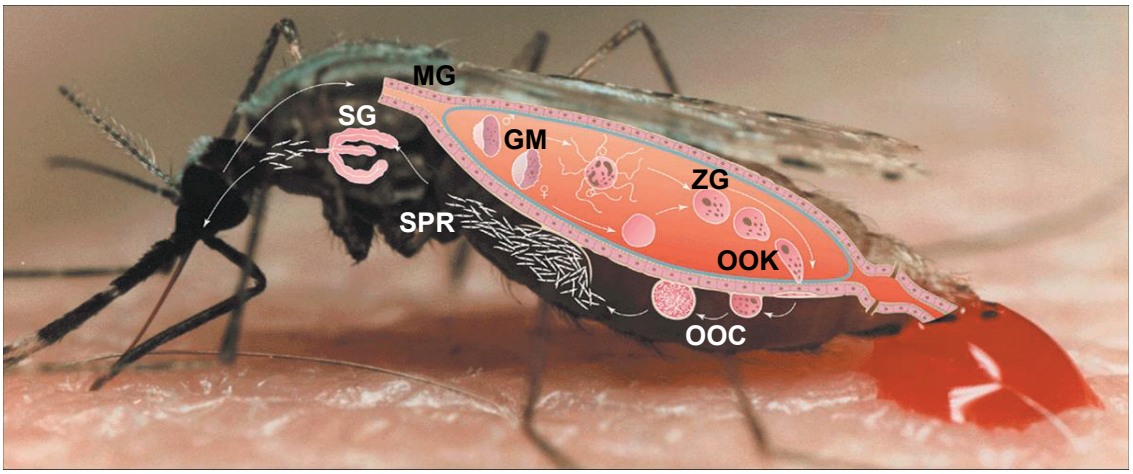


**Figure 3. Sporogonic cycle of *Plasmodim* in mosquito.**
Despite a miracle adaptation to the diverse environments faced in the mosquito, malaria parasites suffer severe losses during the sporogonic cycle. GM: gametocytes, MG: midgut, OOC: oocyst, OOK: ookinete, SG: salivary gland, SPR: sporozoite, ZG: zygote.

(renamed GAF, gametocyte activating factor) has recently been discovered to be xanthurenic acid, a

catabolite of the tryptophan-ommochrome eye-pigment pathway (Billker et al., 1998). Subsequently, the male gametes disperse throughout the blood meal and fertilize the female gametes.

The molecular mechanism of fertilization and putative chemotactic attractions among the gametes are still unknown. In the fertilized female gametes, the haploid nuclei fuse, giving raise to a diploid zygote. Whilst two subsequent meiotic divisions of the nucleus permit the recombination of parental genomes, the cytoplasm is reorganized, and vesicles and intracellular membrane structures become evident (reviewed by Sinden, 1999).

Non-motile zygotes then differentiate into motile ookinetes. Ookinetes have a gliding and contractile nature and are responsible for the penetration of the mosquito midgut epithelium. Ultrastructurally, the ookinete is surrounded by a pellicular complex, composed of two membrane complexes. Beneath the pellicular complex are microtubules, which extend from the anterior to the posterior end. In cross section, the microtubules are regularly arranged, encircling the body of the organism. The anterior end (apical part) of the ookinete is compactly formed by an apical ring and several electron-dense bodies such as rhoptry and microneme (reviewed by Aikawa 1971).

Ookinete migration through the midgut epithelium is a critical step during the lifecycle of the parasites. While thousands of gametocytes can be ingested with a blood meal, normally just a slight number of ookinetes are produced, which suffer additional losses during the epithelium invasion. Accordingly, much effort is put into understanding the biological and molecular mechanisms of these “bottlenecks”, as they are considered to be potential targets for malaria control. Recently, the interest in this essential and intriguing phenomenon has been renewed, and numerous studies have examined the molecular and cellular biology of the invasion process and the interactions of the parasites with the basal lamina of the gut. Upon the successful invasion of the epithelium, ookinetes eventually transform into a spherical oocyst in the space between the epithelium and the basal lamina. Despite several studies in different mosquito species (Meis et al., 1987 and 1989; Shahabuddin and Pimenta 1998; Han et al., 2000; Zieler et al., 2000), there is still some controversy about the subcellular details of midgut invasion. The issue of whether the ookinetes migrate by an inter- or intracellular route is not yet completely resolved, and it was proposed that the route might vary between parasite-vector species combinations (reviewed by Sinden and Billingsley 2001).

Once the ookinetes reach the basal lamina, the process of differentiation into oocysts is initiated. After a period of maturation (10-16 days), the oocyst ruptures and releases several thousands of sporozoites into the hemocoele of the mosquito. Some lines of evidence suggested that the vector immune res-

ponses that are induced at this stage of parasite development, which might play a role in reducing the sporozoite load (Dimopoulos et al., 1998). Nevertheless, the number of released sporozoites is large enough to ensure the completion of the cycle. Mature sporozoites invade only the medial lobe and distal portion of the lateral lobes of the salivary gland (reviewed by Fujioka and Aikawa 2002), suggesting that there is specificity in the sporozoite-salivary gland interaction. A thrombospondin-related anonymous protein (TRAP) is thought to mediate this specificity (reviewed by Menard 2001). TRAP is mainly stored in sporozoite micronemes (Rogers et al., 1992) and accumulates as a cap at the anterior part upon contact with the host cell (Gantt et al., 2000). Synthesis of *Plasmodium* TRAP proteins gradually increases during sporozoite maturation. *TRAP* knockout (KO) mutants are incapable of invading mosquito salivary glands and also cannot invade mammalian hepatocytes *in vitro* (Sultan et al., 1997). Strikingly, *TRAP* KO sporozoites completely lose the typical gliding motility. Genetic studies in *P. berghei* have confirmed that surface TRAP has a direct role in sporozoite gliding (Kappe et al., 1999). It is suggested these proteins regulate gliding motility, and therefore, infectivity of parasites both of the mosquito salivary gland stage and at the liver cell stage in the vertebrate host (reviewed by Menard 2001). Recently, a sporozoite specific gene, upregulated in infective sporozoites gene 3 (UIS3), was reported (Mueller et al., 2005). The parasites with the deletion of *UIS3* showed a severe defect in their ability to complete transformation into liver trophozoites, leading to an inability to establish blood-stage infections *in vivo*.

The sporozoite has an elongated shape. Although haploid sporozoites display somewhat different appearance compared to ookinetes, the organelle distribution is very similar between these two invasive stages. Like in ookinetes, two types of membrane-bound organelles, rhoptries and micronemes, are located at the anterior half of the sporozoite (reviewed by Menard 2001). The pellicle is composed of an outer membrane, double inner membrane and a row of subpellicular microtubules. Sporozoites suffer severe losses in the hemocoele, so that only a certain number reach the salivary glands. Once inside the salivary epithelium, sporozoites traverse the cytoplasm and invade the secretory cavity through the apical membrane of the cells. To be transmitted with an infected bite, sporozoites must reach the salivary duct. Sporozoite entry into the duct might be also strictly motility-dependent (Kappe et al., 2003). The parasite cycle in the mosquito is completed when the mosquito injects infective sporozoites into a new host.

## 4. Mosquito immune responses

During its life cycle within *Anopheles*, the malaria parasite suffers severe losses (Figure 4). On one hand, this reflects the relatively recent evolutionary association between these two organisms proposed by phylogenetic studies (Coluzzi, 1999). On the other hand, it may be a result of parasite exposure to

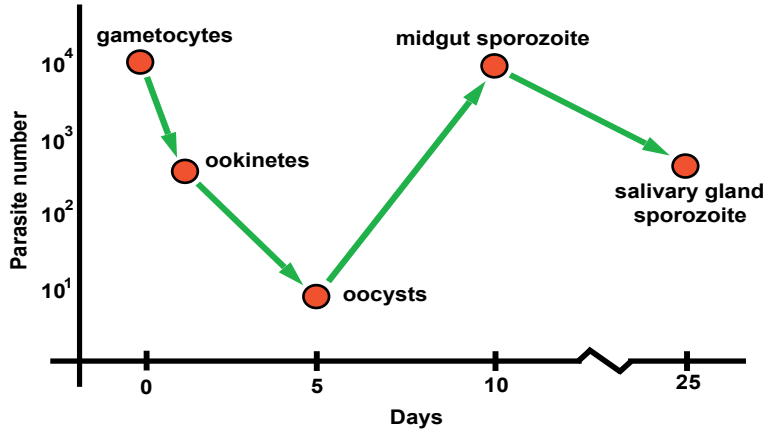


**Figure 4. Parasite losses in the mosquito vector.**
The number of parasites successfully completing the sporogonic cycle is dramatically affected by the hostile midgut environment. Parasite losses are often attributed to the mosquito defense mechanisms (Sinden, 1999).

the innate defence mechanisms of the vector. Mosquitoes, like other insects, are known to mount potent immune responses against invading bacteria, fungi, viruses and parasites (reviewed by Lehane et al., 2004). There is a substantial evidence that the mosquito is able to trigger a series of diverse defence reactions upon *Plasmodium* infection. These defence mechanisms are believed to account for the aforementioned reduction of the parasite loads and may underlie some cases of natural refractoriness. How these defence mechanisms are triggered is still largely unknown. We will first describe principles of insect immunity and then discuss our current knowledge on the mosquito immune defences.

### Insect Innate Immunity

It has long been recognized that insects harbour a powerful and efficient immune system. Pioneering studies by Metchnickov and Cuneot suggested the involvement of hemocytes (insect blood cells) into defence reactions more than a century ago. In recent years, and after a prolonged period of neglect, much progress has been made in understanding the biological and molecular mechanisms that mediate the physiological responses of insects to pathogens. This knowledge converges with the studies of mammalian innate immunity, leading to the concept that innate immunity is evolutionary ancient (reviewed by Hoffmann et al., 1999). Innate immunity refers to the first line of host defence that serves to limit the spread of pathogens immediately after infection, but also in directing the successive clonal responses of adaptive immunity in vertebrates (reviewed by Hoffmann et al., 1999). The invertebrate immune response is of a cellular and humoral nature, but it lacks adaptive features. Features of the humoral response, include the recognition of non-self by pattern-recognition receptors and opsonins, leading to the activation of serine protease cascades. The proteolytic cascades promote extracellular melanization and coagulation reactions, or activate intracellular signalling pathways, which control the expression of series of inflammatory and antimicrobial effector molecules (reviewed by Hoffmann et al., 1996). The cellular responses, on the contrary, are mediated by hemocytes, which can phagocytose or encapsulate foreign particles and organisms. Hemocytes also take part in the humoral response, as they express and secrete zymogens, signalling cytokine-like and effector molecules. These reactions are discussed in greater detail below.

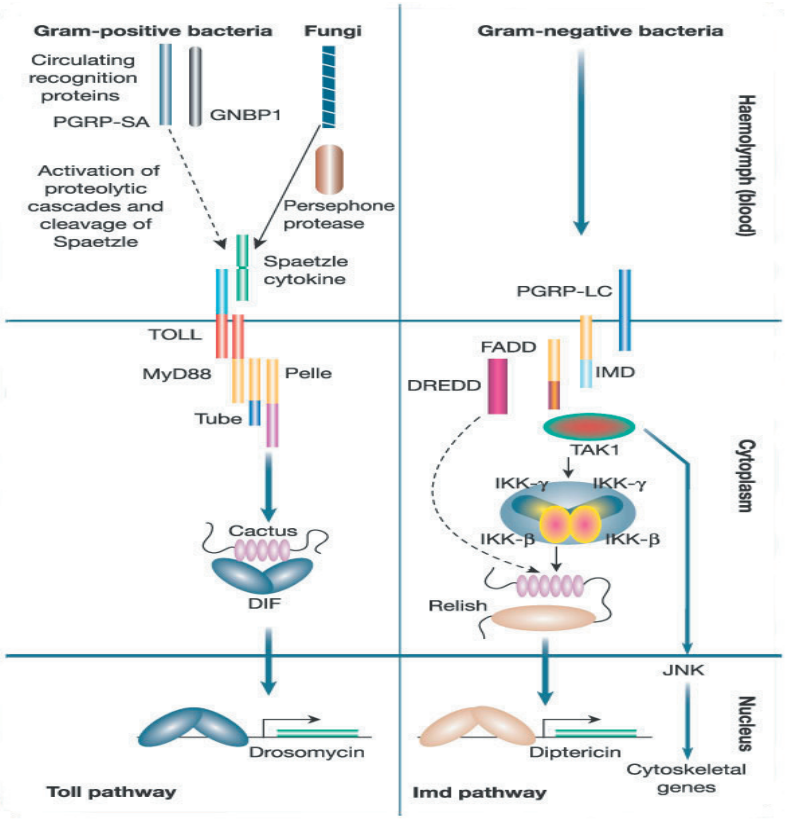


**Figure 5. The Toll and Imd pathways in the control of expression of genes encoding antimicrobial peptides.**
(Toll pathway) Recognition of Gram-positive bacteria and fungi is mediated by two separate extracellular branches that converge to the proteolytic cleavage of Spaetzle. The signal is transduced into the degradation of Cactus and the nuclear translocation of DIF, which activates antifungal and anti- Gram-positive antimicrobial peptide (AMP) genes.
(Imd pathway) Gram-negative bacteria are most probably recognized by a receptor complex involving PGRP-LC, which activates two transduction cascades, leading either to the translocation of Relish into the nucleus and activation of anti Gram-negative AMPs, or to the activation of the expression of cytoskeletal genes through a JNK cascade. (Adapted from Hoffmann, 2003).

### Humoral immune responses

The humoral response has received considerable attention, and much is known about the nature and the regulated expression of antimicrobial peptides. These bioactive molecules are primarily produced by the insect fat body, a functional analogue of the mammalian liver, and are secreted in the hemolymph upon immune challenge (reviewed by Hoffmann and Reichhart, 1997). The power of *Drosophila* genetics permits the dissection of signalling pathways involved in immunity. The flies produce peptides with diverse antimicrobial activities both in a systemic (fat body) and in a local (epithelium and hemocytes) response fashion. To do so, they make use of two distinct signalling pathways: the Toll pathway and *imd* (immunodeficiency) pathway (Lemaitre et al., 1996; Ferrandon et al., 1998; Khush et al., 2001). When the epithelial barriers are breached and tissues are infected, both cellular and humoral responses of the flies are activated to fight invading pathogens. Gram-positive bacteria are recognized by a receptor complex, which is composed of a PeptidoGlycan-Recognition Protein SA (PRGP-SA) and a Gram-Negative Bacteria binding Protein 1 (GNBP1), and leads to the activation of the Toll pathway (Michel et al., 2001; Gobert et al., 2003). Gram-negative bacteria are recognized by a receptor complex involving another recognition molecule, PGRP-LC, and activates the Imd pathway (Choe et al., 2002, Gottar et a., 2002, Ramet et al., 2002). The Toll signalling pathway was originally characterized as a regulator of dorso-ventral polarity in the developing embryo (Nusslein-Volhard and Wieschaus 1980).

Lately it was shown to regulate the antifungal response of the fly as demonstrated by *Toll*-deficient mutants that are susceptible to fungal infection and by the compromised induction of the *Drosomycin* gene, which encodes a potent antifungal peptide (Lemaitre et al., 1996). In addition to antifungal peptides, Toll also regulates the expression of some antibacterial peptides and *Toll* mutants are also sensitive to Gram-positive bacteria infections. However, *Toll*-deficient flies are not susceptible to infection by Gram-negative bacterial, indicating that another pathway regulates this response. This pathway, which was named Imd after a mutation that compromized flies survival to Gram-negative bacteria, regulates the expression of antimicrobial peptides via Relish, a Rel/NF-κB transcription factor. To date, the two pathways do not appear to share any intermediate molecules (Figure 5).

**Cellular immune responses**

Cellular responses are mediated by blood cells and include phagocytosis and encapsulation. In *Drosophila* larvae, there are at least three classes of morphologically distinguishable hemocytes: plasmatocytes, lamellocytes and crystal cells (Meister and Lagueux, 2003). Phagocytosis is performed by plasmatocytes, which are the most abundant hemocytes, while encapsulation is carried out by lamellocytes.

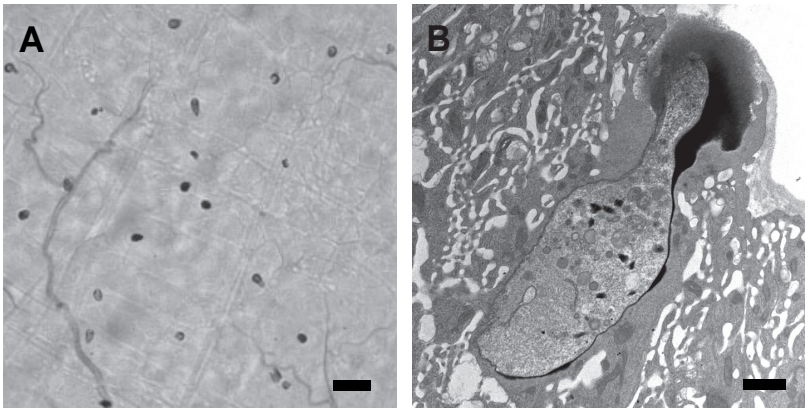


**Figure 6. Melanotic encapsulation of parasites.**
A. Melanized ookinetes are visible on the midgut of refractory L3-5 females 48 h post infection. B. Electron micrograph of a melanized ookinete in the midgut of the L3-5 mosquito 33 h post infection. Scale bars in micron: (A) 10; (B) 1.

Finally, crystal cells are thought to mediate melanization of encapsulated bodies in a reaction called melanotic encapsulation. In *Drosophila* adults, the only blood cell type present is the plasmatocyte (reviewed by Meister 2004). Phagocytosis is a cellular process in which blood cells recognize, internalize and destroy microbial invaders (reviewed by Aderem and Underhill, 1999). Initial binding of opsonic ligands to the microorganism appears to be necessary for its recognition by the phagocytic cell. A receptor involved in the phagocytosis of Gram-negative bacteria in *Drosophila* is the Imd pathway mediator - PGRP-LC, indicating that a link might exist between humoral and cellular immune reactions (Ramet et al., 2002). In *Anopheles*, a member of the ThioEster-containing Protein family, TEP1, acts like an opsonizing complement factor by binding to and promoting phagocytosis of bacteria (Levashina et al., 2001). Encapsulation is a second type of cellular reaction that targets large invaders such as eggs of pa-

rasitoid wasps in *Drosophila*. In this reaction, multiple layers of lamellocytes attach to the surface and, by extending long lamellae, spread over and inactivate the invader, which then dies by asphyxiation or is attacked by free radicals (Nappi and Vass, 1998). Often, the next step involves local activation of the ProPhenoloxidase (PPO) cascade, possibly initiated by crystal cells (Meister and Lagueux, 2003). Melanin, synthesis of which is catalyzed by activated PO, cross-links cellular mass in a melanin capsule.

## 5. Mosquito immune response and malaria transmission

Historically, the first description of the mosquito immune response to parasites was reported by Ross in 1898, who described "black spores", corresponding to melanotic encapsulated parasites. The melanotic encapsulation of *Plasmodium* reflects a complex relationship between vector and parasite. In some laboratory strains, as well as in field-collected mosquitoes, only a few parasites are encapsulated, while the rest develop normally. Genetically selected strains of mosquitoes which are completely refractory to parasites were established in several laboratories and provided a powerful tool for dissection of mechanisms involved in the elimination of parasites. The best known is the L3-5 strain selected by Collins and colleagues (Collins et al., 1986). This strain melanotically encapsulates *P. cynomolgi* B ookinetes as they traverse the midgut epithelial cells (Figure 6). The reaction is thought to be catalysed by soluble components present in the hemolymph, as ookinetes are first melanized at their apical end facing the basal side of the midgut epithelium 24 h after blood-feeding. The genetic control of the refractoriness involves a quantitative trait loci, named *Plasmodium* encapsulation locus 1 (*Pen1*) and two additional loci, *Pen2* and *Pen3* (Zhang et al., 1997, 2003). A critical step in the generation of melanin involves the cleavage of prophenoloxidase (PPO) to active phenoloxidase (PO) by a serine protease. The large number of PPO genes identified in the mosquito (and in other insect genomes) might reflect multiple functions of melanization which is not only involved in encapsulation of invading microorganisms (reviewed by Cerenius et al., 2004). In fact, it is also involved in the sclerotization and tanning reaction of the egg shell and the pupal and imago cuticle, as well as in wound healing. It is believed that PPO activation is triggered by soluble recognition molecules capable of binding to microbial surface moieties. Several recognition molecules, such as peptidoglycan, β-1.3-glucan and lipopolysaccharides, have been linked to PPO activation in invertebrates (reviewed by Ochiai and Ashida 2000, Cerenius et al., 2004). The activated PO enzyme catalyses the hydroxylation of tyrosine to DOPA, which then oxidizes to dopachrome, leading finally to the synthesis of the melanin precursor indolequinone (reviewed by Beernsten et al., 2000).

In addition to melanization, another parasite killing mechanism in the mosquito midgut has been reported for another refractory strain of *A. gambiae* selected by K. Vernick and collaborators (Vernick et al., 1995). This strain eliminates *P.gallinaceum* ookinetes by lysis. The ookinetes appear to be initially

vacuolated and subsequently lysed while still in the cytoplasm of the midgut epithelial cells. Genetic analysis of this line suggested that the refractory mechanism is controlled by a single dominant esterase locus, *Est*. The esterase locus is located in the 2La region (divisions 23–26 of ovarian nurse cell polytene chromosome 2L), whereas *Pen1* has been mapped to chromosome 2R, division 8C/D (Zheng et al., 2003). Although refractory strains provide good models to study molecular mechanisms of refractoriness, genes involved in these processes have not been conclusively identified.

## 6. Thioester-containing proteins

Thioester-containing proteins (TEPs) appeared early in animal evolution: members of this family have been identified in such diverse organisms as nematodes, insects, molluscs, fish, birds and mammals (reviewed by Levashina et al., 2002). In vertebrates, these proteins play important roles in immune responses as components of the complement system (factors C3/C4/C5), or as universal protease inhibitors, in the case of the α2-macroglobulins (α2Ms). TEPs are characterized by homologous sequence features, including a unique intrachain β-cysteinyl-γ-glutamyl thioester bond and a propensity for multiple conformationally sensitive binding interactions (Chu and Pizzo, 1994), which define their functional properties. The thioester bond mediates covalent attachment of the molecules to activate self and non-self surfaces (complement factors), or covalent and non-covalent cross-linking to attacking proteases (α2Ms). The thioester is highly reactive and is readily hydrolysed by water when exposed. To avoid precocious inactivation, the thioester bond is protected by a shielded environment in the native protein (Salvesen et al., 1981; Sim and Sim, 1981).

Activation of the TEPs requires exposure of the thioester bond, which is achieved through a proteolytic cleavage either by a specific “convertase” protease complex (in the case of complement factors) or by attacking proteases (α2Ms). The proteolytic activation of the complement factors generates two products, a small anaphylatoxin fragment without the thioester (C3a, C4a and C5a), and a larger fragment that binds covalently to target surfaces via the hydrolysis of the thioester. Both cleavage products have signalling properties via specific interactions with receptors or effector molecules. Anaphylatoxins spread in the vicinity of complement activation and act as chemoattractants to recruit macrophages to the site of infection. Binding of the larger fragment targets pathogens for phagocytosis or for destruction by lysis, mediated by a membrane attack complex. In the case of α2Ms, proteolytic activation triggers a major rearrangement of the protein that has two important consequences. First it triggers the trapping of the attacking protease within the protein, therefore denying the protease active site access to its substrates. Second, it exposes the C-terminal recognition domain, which can then mediate the clearance of the protease-reacted α2M from the circulation by receptor-mediated endocytosis (reviewed by Blandin and Levashina, 2004).

The completion of the genome sequencing of *D. melanogaster* and *A. gambiae* provided a unique opportunity to analyze phylogenetic relationships between complement factors, α2Ms and insect TEPs (reviewed by Blandin and Levashina, 2004). Six TEP homologues are identified in *Drosophila* (Lagueux et al., 2000). Within these six TEPs, four contain a conserved thioester motif, whereas *TEP5* and *TEP6* exhibit a modified sequence (Crowly et al., 1993; Lagueux et al., 2000). The transcription of *TEP1*, *TEP2* and *TEP4* is strongly upregulated by bacteria challenge in larvae while *TEP2* and *TEP4* are induced by immune challenge in adults. Besides, *TEP1* and *TEP4* are expressed in larval and adult hemocytes, respectively. It is proposed that *Drosophila* TEPs might play a role in promoting phagocytosis, however, no experimental evidence is available to date (reviewed by Meister et al., 2003).

The fruitfly *D. melanogaster* is a model of choice to study fundamental biological processes due to the exceptional experimental possibilities offered by this insect, including a myriad of molecular and genetic tools and the availability of the complete genome sequence. Recent advances in the development of tools for functional gene analysis and the completion of the genome sequencing validate *A. gambiae*, as a powerful model to address mechanisms of vectorial capacity in medically important insect vectors. The interest of this model is highlighted by the fact that the protozoan parasite has to evade two related but distinct immune systems, those of the vertebrate host and of the mosquito. Insects are able to mount rapid and efficient responses, which are reminiscent of innate immune defences of vertebrates. Since insects lack an adaptive immune response, they represent a valuable model to dissect functions of thioester-containing proteins.

### Thioester-containing proteins in *A. gambiae*

The *A. gambiae* genome contains 19 homologues of TEP genes (Christophides et al., 2002). Among these, four gene pairs display characteristic features of haplotypes (TEP1-TEP16, TEP5-TEP17, TEP6-TEP18 and TEP8-TEP19) and, therefore, might representrather polymorphic variations than closely related but distinct genes. Consequently, the TEP family in *A. gambiae* is likely to be represented by a total of 15 TEPs. TEP1 is a typical thioester-containing protein of the mosquito and has been characterized in more detail (Levashina et al., 2001; Blandin et al., 2004). This protein contains a signal peptide-like hydrophobic N-terminal segment characteristic of secreted proteins, and a canonical thioester motif, which is followed 100 amino acids downstream by a catalytic histidine residue. The C-terminal part displays a cysteine signature, characteristic of the *Drosophila* Teps. The TEP1 protein is glycosylated and secreted into the hemolymph by mosquito hemocytes. In the hemolymph, TEP1 is present as a full-length form of approximately 165 kDa and as a smaller fragment of 80 kDa (Levashina et al., 2001), indicating a constant low level of proteolytic cleavage of the protein. Interestingly, the same

type of cleavage can be induced by both wounding and bacterial challenge. It is unknown whether cleavage occurs during activation or subsequent inactivation of the molecule.Functional studies of TEP1 were performed using a mosquito hemocyte-like cell line, established by H.-M. Müller (Catteruccia et al., 2000; Müller et al., 1999). Mosquito cells *in vitro* secrete TEP1 into the conditioned medium, where it is readily detected by affinity-purified rabbit polyclonal antibodies recognizing both the full-length and the C-terminal fragment of the molecule (Levashina et al., 2001). The functionality of the thioester bond in TEP1 is supported by denaturation-dependent autocatalytic fragmentation experiments. Heat treatment of the conditioned medium leads to the appearance of a new C-terminal fragment of 50 kDa, resulting from fragmentation of the molecule at the thioester site. Methylamine treatment completely prevents this autocatalytic fragmentation (Levashina et al., 2001).

Mosquito cultured cells show phagocytic activity against latex beads and bacteria (Dimopoulos et al., 1999). Interestingly, this activity can be enhanced by pre-treating Gram-negative *Escherichia coli* with the conditioned cell medium, before exposing the bacteria to the mosquito cells (Levashina et al., 2001). Double-stranded RNA knockdown of *TEP1* or methylamine treatment of the conditioned medium both decrease the efficiency of bacteria uptake by 50%. These experiments demonstrate that a thioester protein of a protostome opsonises Gram-negative bacteria for phagocytosis and, therefore, displays an ancient complement-like function (Levashina et al., 2001). Exprssion of *TEP1* was upregulated upon infection with bacteria and after infectious blood meal. However, at the time when I started my thesis project, little was known about the role of TEP1 in the antiparasitic responses.

## 7. Goals of the present study

As discussed above, *Plasmodium* invasion activates immune responses of the mosquito vector. These responses are believed to play an important role in reducing parasite numbers during parasite sporogonic life cycle and, therefore, might be actively involved in establishment of vector competence. Thus, the identification of the molecular and cellular mechanisms leading to parasite recognition and activation of immune responses is a key step in understanding how the vector limits parasite loads. This project focused on the characterisation of the molecular and cellular basis of host-parasite interactions between *A. gambiae* and *P. berghei* with a particular emphasis on the development of tools for functional gene analysis.

**1. Development of an *in vitro* system functional analysis of interactions between mosquito cells and *P. berghei***

The study of any pathogenic organism is hampered by the absence of either an appropriate animal model or of a culture system. Before the development of an *in vitro* method for the laboratory maintenance of *P. falciparum*, malaria research was severely disadvantaged. Here, we attempted to adapt an co-culture system of the *A. gambiae* hemocyte-like cell line with the sporogonic stages of *P. berghei* for functional analysis of mosquito genes *in vitro*. We first characterized mosquito cells - parasite interactions using confocal microscopy and transmission electron microscopy. Further, we compared interactions of a thioester-containing protein 1 with *P. berghei in vivo* and *in vitro*. Finally, we extended our analysis of a co-culture system to a genome-wide transcriptional profiling by cDNA microarrays.

**2. Functional analysis of thioester-containing protein 1 *in vivo***

The first thioester-containing protein 1 (TEP1) identified in the mosquito serves as a complement-like opsonin and promotes phagocytosis of bacteria (Levashina et al., 2001). Is TEP1 also involved in the mosquito immune defences against malaria parasites? To answer this question, we characterized TEP1 - *P. begrhei* interactions during the parasite development in the mosquito using confocal and transmission electron microscopy. For functional analysis of TEP1 in the mosquito we made use of double stranded RNA silencing which was developed in our group (Blandin et al., 2002).

**3. Ultrastructural study of the sporogonic development of *Plasmodium berghei* in *Anopheles gambiae***

The available descriptions of the parasite life cycle in the mosquito remain often contraversal. Development of the parasites within a mosquito host in some cases was demonstrated to vary with the compbination of host-parasite species used for analysis. Moreover, reports on the complete cycle of *P. berghei* within *A. gambiae* are still missing. To gain a better understanding of species-specific mosquito-parasite interactions, we followed *P. berghei* development in the *A. gambiae* midgut by transmission electron microscopy. We further used ultrastructural studies to examine modifications in the midgut structure caused by dsRNA silencing of *TEP1*.

**4. Role of actin in the parasite clearance in *A. gambiae***

*TEP1* dsRNA knockdown results in the better parasite development in *A. gambiae*. At the same time, our ultrastructural analysis of the mosquitoes depleted for TEP1 demonstarted a link between TEP1 presence and formation of a filamentous zone around invading ookinetes. Although the filamentous zone was previuosly observed around melanized parasites, its function and organisation were unknown. Our goal was to provide functional characterization of the filamentous zone using transmission electron and confocal microscopy and dsRNA silencing.

# CHAPTER 1

## Immune responses of a mosquito hemocyte-like cell line to *Plasmodium* parasites in a co-culture model

# INTRODUCTION

When I started my thesis in 2000, the first thioester-containing protein (TEP1) in the mosquito was identified and characterized (Levashina et al., 2001). TEP1 is a hemocyte-specific acute phase glycoprotein, which is proteolytically processed in the mosquito hemolymph shortly after septic injury. Studies on a hemocyte-like mosquito cell line revealed that TEP1 was able to bind to *Escherichia coli* and *Staphylococcus aureus* and that this binding was dependent on a functional thioester bond. Double-stranded RNA (dsRNA) knockout experiments were developed *in vitro* by the group of Prof. F.C. Kafatos to demonstrate that this complement-like protein strongly promotes phagocytosis of three tested Gram-negative bacteria in a mosquito cell line (Levashina et al., 2001). Therefore, we proposed to make use of the same cell line to study mosquito-parasite interactions and, more specifically, to perform functional analysis of TEP1. When we began this project, there were no efficient tools for functional analysis of the parasite-mosquito interactions *in vivo*. *In vitro* co-culture was the best candidate system for us to carry out the functional analysis of parasite-responsive genes.

A drawback in the analysis of the midgut stage of the malaria parasite *in vivo* is the difficulty to examine the detailed biological events that take place in the mosquito midgut. A simplified *in vitro* system would be an indispensable tool for studies of host-parasite interactions (reviewed by Hurd et al., 2003). The *in vitro* system has been mostly used to follow the development of malaria parasite (Reviewed by Hurd et al., 2003). Several authors have reported reproducible methods that supported the development of mosquito stages of malaria parasites, thus enabling remodeling of host-parasite interactions.

The production of ookinetes *in vitro* can be achieved routinely for *P. berghei* and *P. gallinaceum* (Janse et al., 1985). Briefly, parasitized blood drawn from infected rodents or chickens is immediately mixed with pre-cooled RPMI-1640 medium (pH 7.4) containing 10% fetal calf serum (FCS), and is passed through a column (Plasmodifur) to remove white blood cells. The blood is then incubated in a culture flask for 24 h at 20˚C to allow development of ookinetes (for details see Materials and Methods).

The sporogonic cycle of the malaria parasites *P. gallinaceum* and *P. falciparum* were studied *in vitro* by co-culturing with *D. melanigaster* Schneider's S2 cells supplemented with a basement membrane-like gel (Matrigel) (Warburg et al., 1992 and 1993). Ookinetes of *P. gallinaceum* were mixed with *Drosophila* cells at a ratio of 1 ookinete : 20 *Drosophila* cells and seeded onto the Matrigel. The transformation of ookinetes into oocysts and their subsequent growth was observed. Sporozoites were first observed at 10 days of co-culture (Warburg et al., 1992). The formation of sporozoites was also observed at 12 to 16 days of co-culturing the *P. falciparum* ookinetes mixed with *Drosophila* S2 cells in the presence of Matrigel (Warburg et al., 1993). Matrigel most probably substitutes for laminin and collagen type IV, which are the major constituents of the insect basement membranes, and are also present in the oocyst capsules of *P. gallinaeceum*. Therefore, it was suggested that extracellular matrix components might be important for oocyst development (Warburg et al., 1992 and 1993).

Syafruddin and colleagues followed the development of the sexual stages of *P. berghei in vitro* using C6/36 cell line from the mosquito *A. albopictus* (Syafruddin et al., 1992). In their study, ookinetes were incubated in the absence of Matrigel either in acellular culture or with the mosquito cells. In the acellular culture, a number of rounded up ookinetes and young oocysts was observed at 3 days of culturing. No nuclear division was detected even at 6 days of culturing. Co-cultivation of ookinetes with mosquito C6/36 cells led to an intracellular development of ookinetes and young oocysts at day 3 of co-culturing. Some of the intracellular ookinetes were clearly surrounded by vacuoles. No further development of intracellular young oocysts, evidenced by nuclear division and by formation of the oocyst capsule, was detected at 6 days of co-culture.

More complete study compared the development of *P. berghei* ookinetes in co-cultures using Matrigel and three different insect cell lines, including *Drosophila* S2, *A. aegypti* MOS20 and *A. gambiae* 4a-3A (Siden-Kiamos et al., 2000). In the presence of insect cells, development of oocysts was followed for a total of 28 days. The nuclear division was observed only in intracellular oocysts and lasted for up to 21 days in the co-culture with the mosquito 4a-3A cell line. However, no sporozoite development was detected in this system. Authors concluded that Matrigel is not sufficient to enhance the oocyst development. This system was further used to perform functional analysis of the *P. berghei* P25 and P28 surface proteins. For that the development of mutant ookinetes lacking both genes was examined. Normally, the expression of *P25* and *P28* genes, which is first detected in the macrogametes, continues for 6-10 days during oocyst development (Simonetti et al., 1993; Rodriguez et al., 2000). Development of oocyst was compromised only in the *P28* knockout mutants demonstrating that its function is required for the transformation of ookinetes into oocysts or for the early oocyst development. However, the knockout of *P25* had no phenotypic effect in this system.

As mentioned above, ookinetes of *P. berghei* are able to transform into early oocysts in an *in vitro* acellular culture and are situated intracellularly in the co-cultured *A. albopictus* cells (Syafruddin et al., 1992). However, parasite development did not proceed beyond 6 days. Moreover, no nuclear division or oocyst wall formation was detected. Sidén-Kiamos et al. (2000) also described the development of *P. berghei* oocysts intracellularly within a variety of insect cells (*Drosophila* S2, *A. aegypti* Mos20 and *A. gambiae* 4a-3A). By day 7, oocysts were expressing circumsporozoite protein (CSP), the marker of oocyst development (reviewed by Kappe et al., 2003), and some nuclear division occurred by day 21, as determined by DAPI staining. However, thereafter oocysts degenerated and no sporozoite development was observed.

By the time I started my thesis, the techniques for *in vitro* gametogenesis and transformation of ookinetes into early oocysts were well-developed. However, complete *in vitro* development of the mosquito stages of parasites *in vitro* up to the stage of infectiuos sporozoites has been achieved only very recently (Al-Olayan et al., 2002). Our group was interested in interactions of the mosquito proteins with the ookinetes of *P. berghei* and I decided to use the developed techniques for functional analysis of the mosquito genes *in vitro*.

Thioester-containing proteins are acute phase proteins that play an important role in innate immune responses in mammals (reviewed by Volanakis, 1995). Our group demonstrated that bacteria challenge rapidly induces transcription of the mosquito thioester-containing protein 1 (TEP1) resulting in maximum transcript levels after 4-6 h in adult mosquitoes. In addition, the proteolytic cleavage of TEP1 in adult mosquitoes is induced at 3 and 6 h after injection of bacteria (Levashina et al., 2001). The first results of functional analysis of *TEP1* using double-stranded RNA knockdown (dsRNA KD) strongly suggested that TEP1 opsonizes bacteria for phagocytosis. Furthermore, the preliminary results of E. Levashina using TEP1 specific antibodies and confocal microscopy suggested that TEP1 is able to bind to the surface of ookinetes during midgut invasion. However, at that time the significance of this binding was unclear. We speculated that TEP1 might be involved in the mosquito antiparasitic defences. This prompted us to make use of a co-culture system for functional analysis of TEP1 in an *in vitro* model using the Sua 5.1* mosquito cell line in the presence of Matrigel to ensure the development of early oocysts. Several questions were raised:

1. Invasion of the mosquito midgut by the parasites is a critical step for parasite development. However, how parasites invade the mosquito cells remained largely unknown. No mosquito epithelium-like cell line was available to date. Can the *in vitro* co-culture system based on the mosquito hemocyte-like cell line serve as a model to study the parasite-mosquito interactions?

2. *In vitro* co-culture systems have been used to follow the parasite development as described above. In these systems, both extracellular and intracellular parasite development was observed. However, whether ookinetes actively invade, or are phagocytosed by the mosquito cells was still controversial. Would transmission electron microscopy help to clarify this issue?

3. The first thioester-containing protein in the mosquito serves as a complement-like opsonin and promotes phagocytosis of Gram-negative bacteria in the mosquito cell line (Levashina et al., 2001). Can we use a co-culture system as a tool for the functional analysis of TEP1 in the parasite-mosquito interactions?

4. During this project, the first generation of *A. gambiae* cDNA microarrays was developed by Drs. G. Dimopoulos and G. Christophides at EMBL (Dimopoulos et al., 2002). Can we characterize what type of immune responses is induced in the mosquito cells in an *in vitro* co-culture system by *Plasmodium* and how can these responses be compared with the immune responses to bacteria? Will genome-wide expressional analysis lead to identification of “parasite”-specific genes in *A. gambiae*?

# RESULTS

For the functional analysis of the parasite-mosquito interactions in the co-culture system I made use of three complementary approaches. I employed confocal microscopy to analyze binding of TEP1 to the parasites. The detailed cellular and ultrastructural interactions between mosquito cells and ookinetes were analyzed by transmission electron microscopy (TEM). Finally, genome-wide analysis of the co-culture system was performed by cDNA microarray.

## 1. Interactions between *P. berghei* ookinetes and the mosquito 5.1* cells in a co-culture system

*Plasmodium* ookinetes have been shown to invade epithelial cells of both vector and non vector insects (Sinden 1978, reviewed by Sinden 1999). Various models of invasion by ookinetes have been proposed, based on a range of observation methods and mosquito-parasite combinations. Most parasite-insect cells co-culture systems focus on establishment of conditions for completion of the sexual part of the *Plasmodium* life cycle *in vitro*. We exploited whether the co-culture system can be used to study host-parasite interactions.

Due to the absence of insect midgut epithelium-like cell lines, an immune-responsive mosquito hemocyte-like cell line Sua 5.1* was used in the experiments (Catteruccia et al., 2000). This line was established from trypsinized larvae of the Suakoko 2La strain of *A. gambiae* (Mueller et al., 1999), kindly supplied by Dr. Hans-Michael Mueller, Heidelberg. Cells are normally maintained in Schneider's medium supplemented with 10% FCS at 25˚C. The Sua 5.1* cells display a characteristic spindle shape and multiple developed lamellipodia stretching outside from the cell edges (Fig 1-1). The size of the Sua 5.1* cells varies from 3 to 10 μm in diameter. Transmission electron microscopy was used to observe basic cellular organelles such as nucleus, rough endoplasmic reticulum and mitochondria. We noted that the presence of lysosomes and autophagosomes varied from one cell to another in the same culture. These variations could arise from different cell types present in the Sua 5.1* line. However, we also observed a correlation between the age of the cell culture and the presence of autophagosomes, which could also indicate that the cells in the co-culture system are not synchronized.

For ookinete culture and purification, *P. berghei* parasite (clone 2.34) infected blood was collected from Balb/C mice. Parasitized blood drawn by cardiac puncture from infected mice was immediately mixed with pre-cooled RPMI-1640 medium (pH 7.4) containing 10% FCS, and passed through a column (Plasmodifur) to remove white blood cells. The blood was then transferred into a 75 ml culture flask and incubated at 20˚C for 24 h. Mature ookinetes were purified either using Nycodenz gradient (Carter et al., 1987) or by magnetic beads (Dynabead®) coated with 13.1 monoclonal antibody against P28, the ookinete surface protein.

To establish the *in vitro* co-culture system, a basement membrane-like Matrigel (Sigma) was used. Pre-cooled Matrigel was gently spread on the surface of sterile coverslips placed in a 24-well culture

plate. The mosquito cells were added into each well when the Matrigel was completely polymerized. When grown in the culture flask without the presence of Matrigel, Sua 5.1* cells were homogenously dispersed and attached to the bottom of the flask, whereas they appeared to aggregate in clusters when seeded on the surface of the Matrigel. After incubation for 24 h, cells spread over and attached to the Matrigel. The purified ookinetes were then directly placed on the cells at a ratio of 1 ookinete to 10 cultured cells (Figure 1-2).

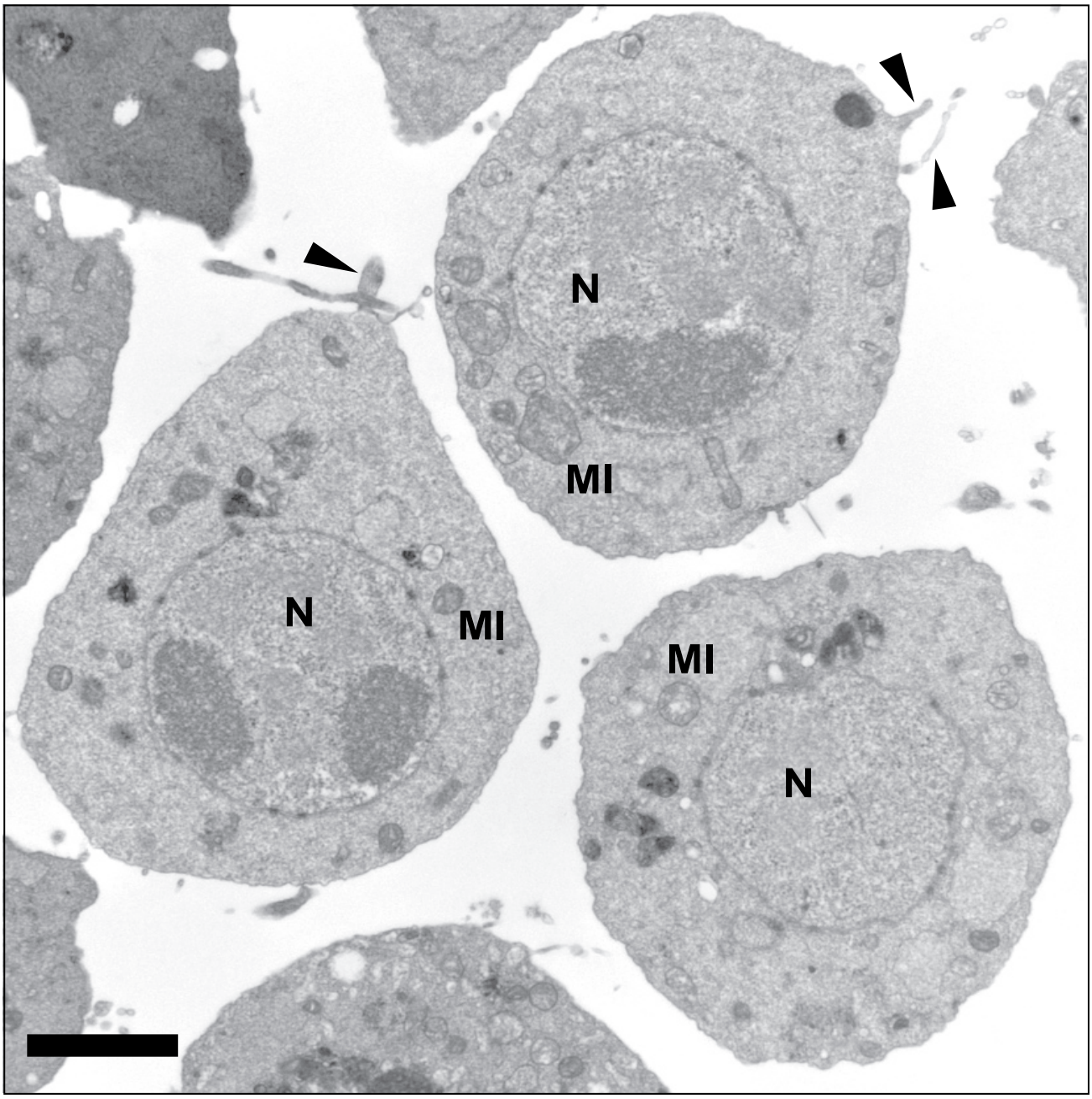


**Figure 1-1. Ultrastructure of thz mosquito Sua 5.1*cell line**.
The Sua 5.1* cells are presented as spindle-shaped, and normally with the lamellipodia (arrow heads) at the edge. The size of the Sua 5.1* cells varies from 3 μm to 10 μm in diameter. The cell organelles such as nucleus (N) and mitochondria (MI) are clearly visible. Scale bar = 1 μm.

We observed interactions between the mosquito cells and the ookinetes at 4, 16, 24 and 48 h of co-cul-

turing using confocal microscopy. As early as at 4 h of co-culture, ookinetes were detected inside the mosquito cells (Figure 1-8 A-D). When counted, the percentage of intracellular ookinetes increased with the co-culture time (Figure 1-3 A). At later time points, e.g. 6 d of co-culture, we also detected intracellular oocysts by staining with the antibody against circumsporozoite protein (CSP) (Nussenzweig et al., 1985) (Figure 1-8 E-G). However in our system, DAPI staining did not reveal any nuclear division neither for intracellular nor for extracellular oocysts.

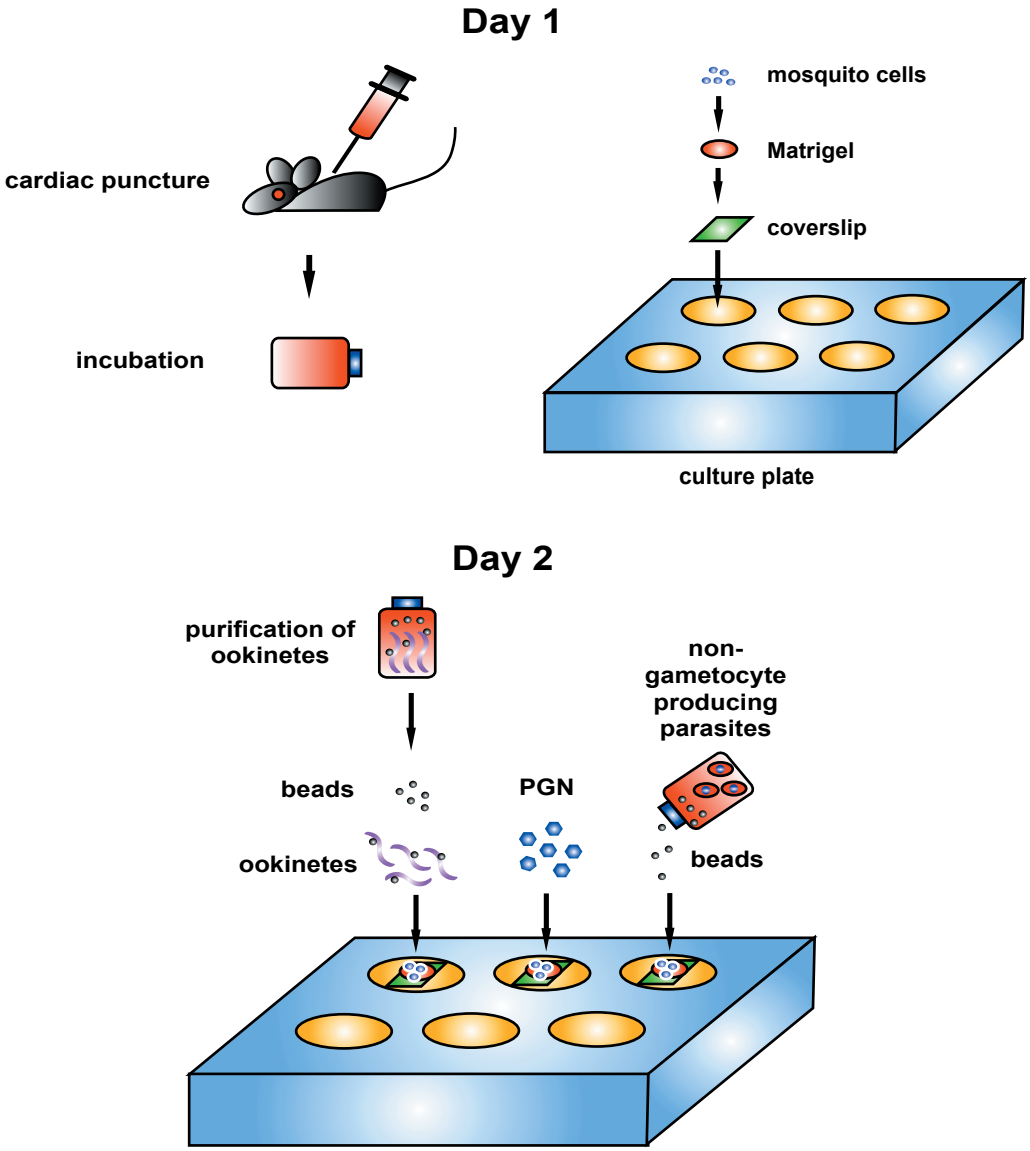


**Fig ure 1-2. Schematic representation of a protocol for the *in vitro* co-culture system**
The co-culture system is prepared in two days. At day 1, the parasitized blood is collected by cardiac puncture from a mouse infected with *P. berghei* (clone 2.34 or non-gametocyte producing clone 2.33) and incubated in RPMI-1640 medium at 20°C for 24 h. For the cell culture, a basement membrane-like pre-cooled Matrigel is gently spread on the coverslip in a culture plate. The mosquito Sua 5.1* cells are seeded on the surface of the polymerized Matrigel and incubated at 25°C for 24 h.
At day 2, mature ookinetes of *P.berghei* are purified on a column prepared from the magnetic beads coated with P28 antibody. The purified ookinetes and beads (2.34 clone of *P. berghei*) or beads (2.33 clone of *P. berghei*) are directly placed on the mosquito cells at 1 ookinete:10 mosquito cells ratio. Peptidoglycan (PGN) is directly added into the culture medium.

**A**

No. of intracellular beads or ookinetes / total beads or ookinetes recorded ( % )

| Hours of co-culture | Magnetic beads | Ookinetes |
|---|---|---|
| 4 | 67 / 252 (26.59) | 145 / 393 (36.90) |
| 16 | 93 / 310 (30.00) | 228 / 481 (47.40) |
| 24 | 74 / 253 (29.25) | 252 / 408 (61.76) |
| 48 | 98 / 282 (34.75) | 263 / 454 (57.93) |

**B**

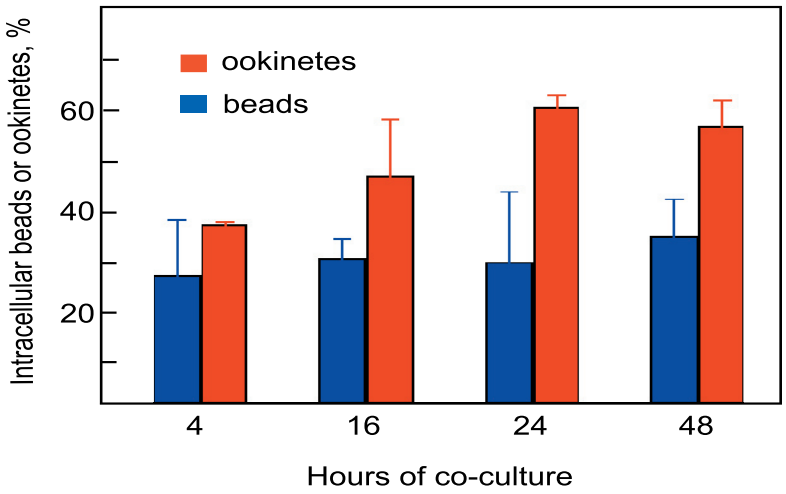


**Figure 1-3. Percentage of intracellular parasites and beads in the co-culture system.**
(A) The intra- and intercellular beads and ookinetes were counted from at least 10 microscope fields of 20x objective for each time point. The total numbers were recorded from three independent experiments.
(B) Percentage of intracellular beads (blue bars) and ookinetes (red bars) are shown at different time points of co-culture. Values are means + SD.

To determine whether parasites actively invade the mosquito cells or are phagocytosed by the cells, we first followed the number of intra- and extracellular ookinetes at different time points (4, 16, 24 and 48 h) of co-culture. As a control, we made use of magnetic beads that served to purify ookinetes from the red blood cell cultures and which were added to the co-culture together with the ookinetes. The experiments were performed using confocal microscopy and the resulting Z-series of optical sections are shown as 3-D reconstructions (Figure 1-8). The ookinetes and beads were counted from at least 10 microscope fields at 20-fold magnification for each time point and the results shown are from three independent experiments (Figure 1-3). The percentage of intracellular beads did not change with time and was around 30% already at the earliest observation point. This may indicate that the engulfment of the inert magnetic beads is rather a rapid process, which reached its plateau before the initiation of the analysis. Interestingly, the percentage of the intracellular ookinetes increased over time, peaking at 24 h of co-culture (61.76%) (Figure 1-3). We concluded that the cultured cell line reacts to the presence of ookinetes and beads by induction of phagocytosis, although with a different kinetics. The difference in the kinetics of engulfment between beads and live ookinetes could reflect either the preferential phagocytosis of beads by the cells at early stages of co-culture, or by an active evasion strategy of the ookinetes. Alternatively, it could also reflect the active invasion of the mosquito cells by the parasites. However, with the observations at hand we can not distinguish between these hypotheses. To confirm

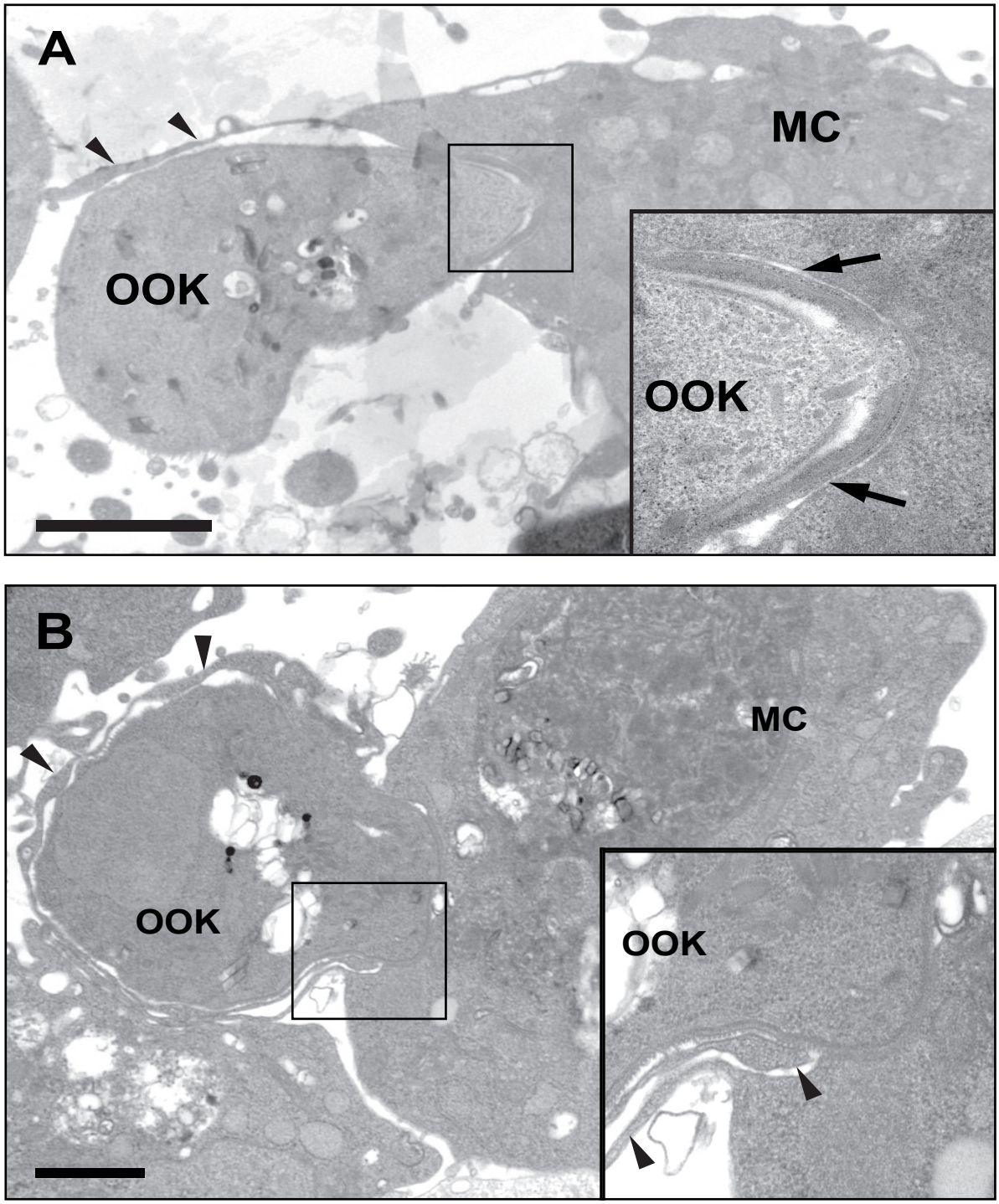


**Figure 1-4. Stages of ookinete engulfment by mosquito cells *in vitro*.**
Electron micrographs of the co-culture system demonstrating different stages of the phagocytosis of ookinetes by the mosquito cells. Samples were fixed at 48 h of co-culture. (A) In the early stage, the mosquito cell membrane is extended and forms a lamellipodium (arrow heads) toward the ookinete (OOK) whereas the ookinete orients toward the mosquito cell (MC) and pushing itself (arrows) to the cell membrane (inset, higher magnification of boxed region from A).(B) In the next step, the ookinete is totally surrounded by a thin layer of lamellipodium, which even folded into a two layered sheet (inset, detail of the boxed region from B). (C) When completely engulfed, the parasite is contained within a vacuole of the mosquito cell. Scale bar = 1 μm.

that the observed process of the ookinete engulfment is indeed phagocytosis, we analyzed the ultrastructural and morphological details of the parasites and the mosquito cells in the co-culture system by transmission electron microscopy.

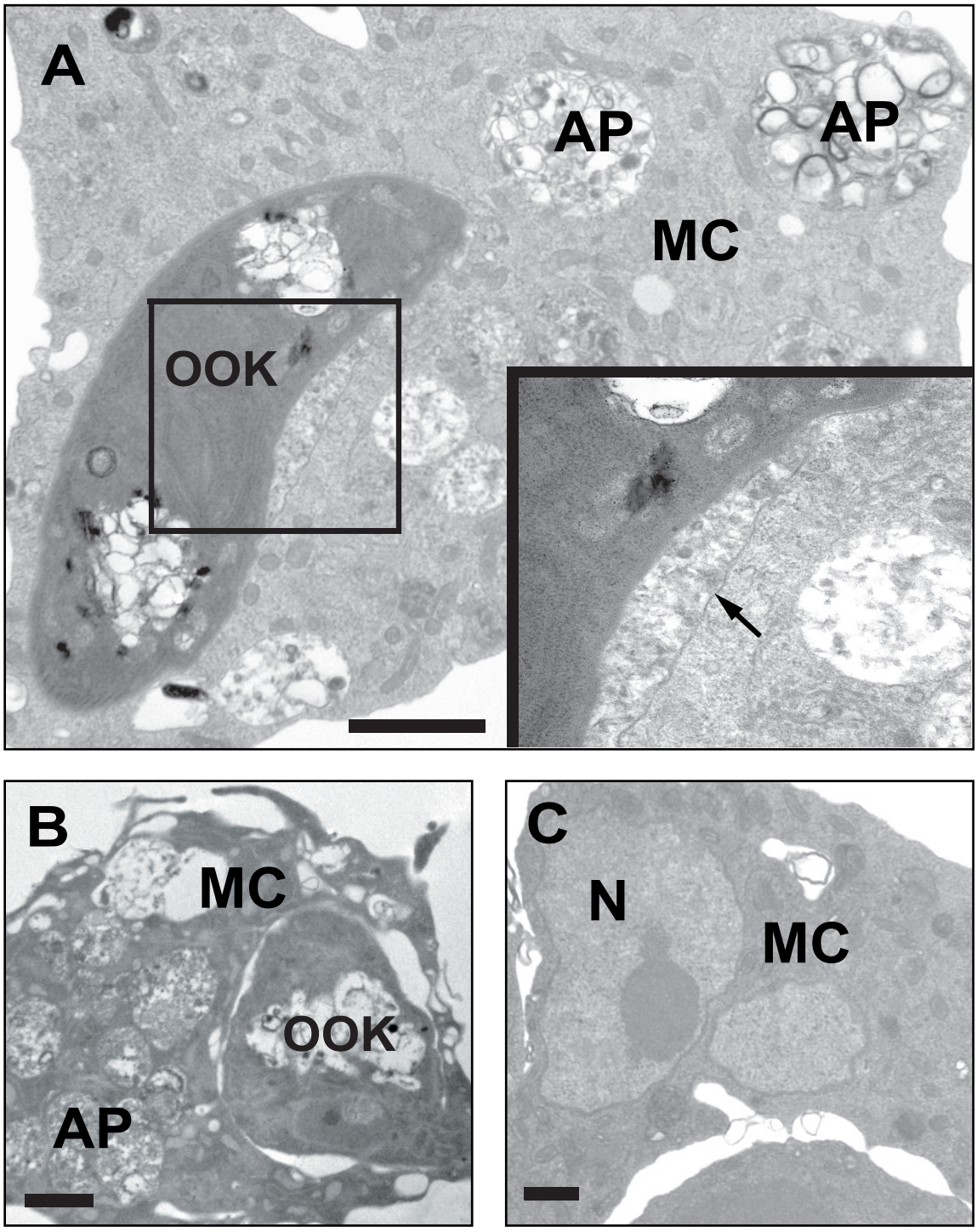


**Figure 1-5. Egulfment of ookinetes leads to the formation to a phagocytic vacuole and occasionaly correlates with the presence of autophagosomes**

(A) A phagocytosed ookinete surrounded by a membrane-bound vacuole (arrow) at 48 h of co-culture (inset, detail of the boxed region).

(B) Occasionally, a high number of autophagosomes is observed in the cells containing intracellular ookinetes (C) Such autophagosomes are mostly absent from the naive cells. Scale bar = 1 micron. MC: mosquito cell, OOK: ookinete, AP: autophagosome.

**2. Phagocytosis of ookinetes by the mosquito cells** *in vitro*

A previous report described several steps in the penetration of insect cells by ookinetes (Siden-Kiamos et al., 2000). The first step consisted of repeated reversible attachments of ookinetes to the cell surfaces, a process which the authors described as probing of the cell surface. By 24 h of co-culture, interactions between ookinetes and the cells became more intimate and massive cell penetration by

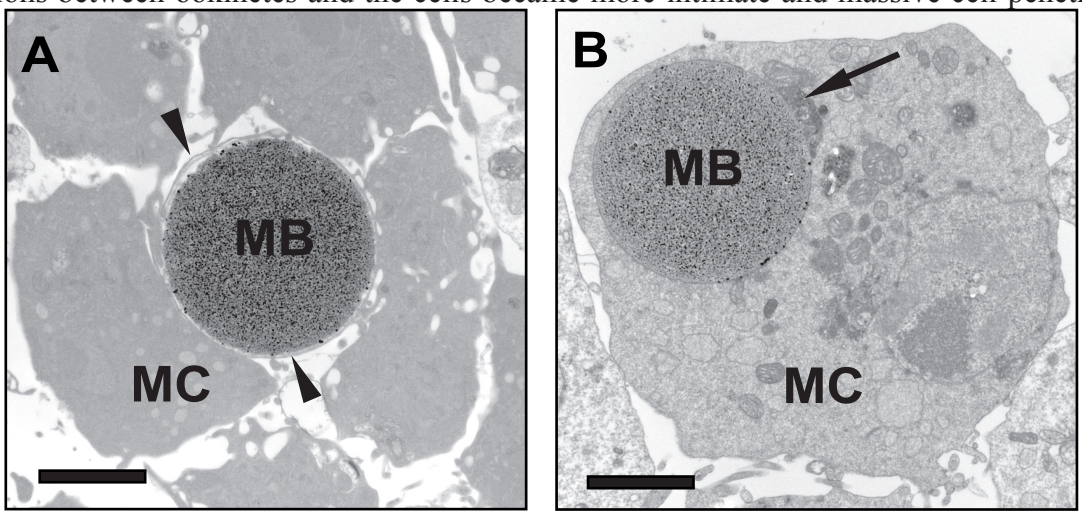


**Figure 1-6. Engulfment of magnetic beads by mosquito cells**
(A) Mosquito cells react to the contact with the magnetic bead by stretching lamellipodia (arrow heads) . (B) Mosquito cell engulfing a magnetic bead. Note a lysosome (arrow) in the close proximity to the bead surface. MB: magnetic bead, MC: mosquito cell. Scale bar = 1 μm.

ookinetes was observed. Nearly 50% of all counted ookinetes became intracellular at this time point (Siden-Kiamos et al., 2000). To provide a structural description of the process of cell penetration by ookinetes, we have used transmission electron microscopy and followed interactions between ookinetes and the mosquito cells at the same time points as described above for the confocal microscopy. In these experiments, a filter paper was used as a support for Matrigel instead of coverslips to facilitate the embedding of samples into the TEM-grade block.

As demonstrated in the Figure 1-3, the majority of the intracellular ookinetes which we have observed were phagocytosed by the mosquito cultured cells. Several stages of the process could be detected in the same specimen. We propose that in response to the ookinete probing of the cell surface, the mosquito cells protrudes several lamellipodium-like structures that make a first contact with the ookinete (Figure 1-4 A). The lamellipodia are specialized thin cytoplasmic projections powered by polymerized actin that extend from the front or leading edge of the cells. The formation of lamellipodia is known to depend on a signal-dependent reorganization of the actin filaments (Mejillano et al., 2004). In all cases, we observed that the apical pole of the ookinetes was pressed against the mosquito cell resulting in a slight (1-2 μm) invagination of the cell membrane. At the later time points, the ookinete became encircled by several layers of lamellipodia, and progressively moved further inside the mosquito cell (Figure 1-4 B). Abundant formation of lamellipodia observed at this stage is reminiscent of a zipper-

like mode of engulfment, which is characteristic of phagocytosis in macrophages (Allen and Aderem, 1996). The process terminated by the entire uptake of the ookinete by the mosquito cell (Figure 1-4 C). Once the ookinete is completely engulfed, it is surrounded by a membranous vacuole (Figure 1-5 A) further supporting the hypothesis that phagocytosis is involved in the parasite engulfment.

The same type of cellular reactions were detected for inert magnetic beads, which were also engulfed by the cells (Fig 1-6). Mosquito cells also reacted to the beads by protruding lamellipodia (Figure 1-6 A) and by induction of a zipper-like mode of phagocytosis (Figure 1-6 B).

Curiously, we observed that autophagosomes were abundant in the ookinete-engulfed mosquito cells (Figures 1-5 A and B), whereas only a few autophagosomes were detected in the mosquito cells in the absence of ookinetes (Figure 1-5 C). These observations suggest two possibilities: (1) autophagosomes are produced as a result of the phagocytosis of parasites; or (2) autophagosomes are accumulating in the cells independently of the phagocytosis of ookinetes. Further systematic electron microscopy analysis should clarify this issue.

Our observations indicate that the ookinetes are predominantly engulfed by the mosquito cells by phagocytosis. We conclude that the mosquito cells in culture are able to recognize ookinetes and beads and to react by activation of phagocytosis.

### 3. Binding of TEP1 to ookinetes in the co-culture system

Binding of TEP1 to the surface of parasites has been observed *in vivo* (Blandin et al., 2004). However, functional significance of TEP1 binding was unknown when we started this project. At that time, functional analysis of mosquito genes was developed only for *in vitro* cultures (Levashina et al., 2001). Therefore, we decided to use the adapted co-culture system for functional analysis of TEP1 binding to ookinetes.

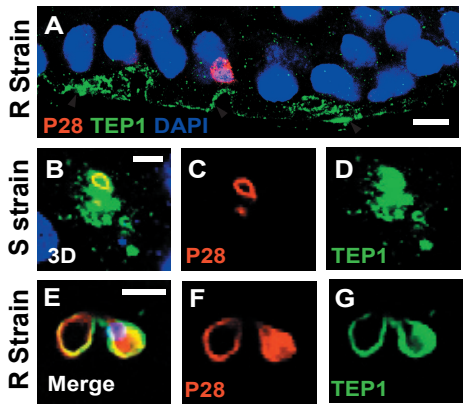


**Figure 1-7. Binding of TEP1 to ookinetes in the midgut**
(A) TEP1 (green) binds to the basal lamina (arrow head) of the mosquito midgut at 24 h post infection. Ookinetes are labeled with the antibody against parasite surface protein P28 (red), nucleus of the midgut cells are stained with DAPI (blue). Confocal sections (B-D, and E-G) were taken at 24 h post infection. TEP1 signal partially highly colocalizes with the signal for P28 in susceptible mosquitoes (S strain)(B-D), whereas this colocalization is more pronounced in refractory mosquito (R strain) (E-G). Scale bars are 10 μm in (A) and 5 μm in (B-G).

Previously it was shown by our group that Sua 5.1* cells produce TEP1 and secrete it into the culture medium (Levashina et al., 2001). Moreover, binding of TEP1 in the conditioned medium to the surface of bacteria was clearly demonstrated using immunostaining and immunoblotting techniques. This

binding, mediated by a covalent attachment of the C-terminal part of TEP1 to the bacterial surfaces, is absolutely required for optimal phagocytosis (Levashina et al., 2001). These results suggested that TEP1 produced by the Sua 5.1* cell line is functional when secreted into the cultural medium. To analyze binding of TEP1 to the surface of ookinetes in the co-culture system, we fixed samples at 4, 16, 24 and 48 h of co-culturing for confocal microscopy analysis.

We followed TEP1-ookinete interactions using anti-TEP1 polyclonal antibodies against the C-terminal moiety of the molecule. To our surprise, we could not detect TEP1 signal on the surface of the banana-shaped ookinetes at the first two days of co-culture. In contrast to *in vivo* observations (Figure 1-7), where TEP1 abundantly decorates ookinetes starting from 24 h post infection, the only stage which displayed some patchy TEP1 signal was the young oocyst. (Figure 1-8).

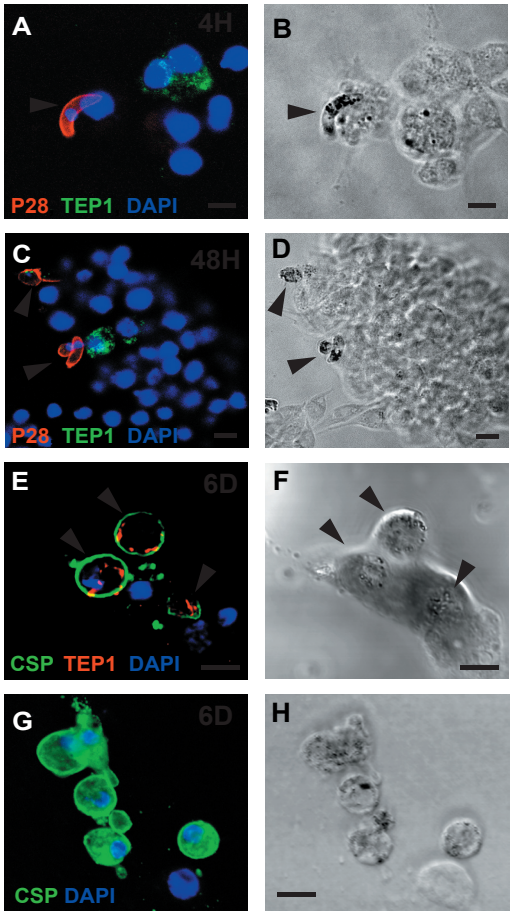


**Figure 1-8. Immunolocalization of TEP1 in a co-culture system**. Confocal images of the co-culture system showing engulfment of *P.berghei* ookinetes by the mosquito cells *in vitro*. The parasite surface protein P28 is used as the ookinete marker (A and C, red), TEP1 is detected by a polyclonal antibody (green, A and C) and (red, E). Early oocysts are labeled with the antibody against a circumsporozoite protein (CSP) (green, E and G). DAPI was used to stain nucleic acids (blue). Note that TEP1 is produced by some but not all mosquito cells (A and C). Banana-shaped ookinetes show no TEP1 binding, whereas a patchy TEP1 signal is detected on the round oocysts (green) at 48 h of co-culture (compare A and C). Young oocysts are engulfed by the mosquito cells at 6 days of co-culture (E and F). Some oocysts are detected extracellularly at 6 days of co-culture. Note that no nuclear division is observed at this time point of co-culture (G and H). (B), (D), (F) and (H) are DIC images of (A), (C), (E) and (G), repectively. Scale bar is 5 µm.

Our observations indicate that in contrast to the situation in the midgut, TEP1 does not recognize banana-shaped ookinetes when those are delivered directly to the co-culture system. Several possibilities could be considered to explain these observations. (1) In the mosquito midgut, ookinetes have first to traverse epithelial cells and only after that they make a first contact with TEP1 secreted by the hemocytes into the hemolymph and present in the lacunae of basal labyrinth. Whereas in our co-culture system, ookinetes are immediately exposed to the TEP1 which is secreted by the Sua 5.1* cells into the cultural medium. (2) It remains unclear whether TEP1 is fully proteolytically activated in our co-culture system. Although ookinetes are washed with PBS before being presented to the mosquito cells

in the Schneider culture medium, the medium might contain protease inhibitors or other components that prevent TEP1 cleavage. (3) Proteases (of mosquito or parasite origin) required for TEP1 activation might not be present or activated in this co-culture system. We could follow TEP1 activation/cleavage by immunoblotting. Our previous results show that TEP1 is continuously cleaved in the cultural medium of Sua 5.1* cells (Levashina et al., 2001), however, we did not analyze TEP1 cleavage in the co-culture system. New monoclonal antibodies directed against N-terminal part of TEP1 have been recently developed by S. Blandin at EMBL, and future studies might resolve this discrepancy between the two systems. However, absence of TEP1 on the surface of parasites prevented us from using the *in vitro* system for functional analysis of this molecule. Therefore, we turned out attention to the development of *in vivo* tools for functional gene analysis using dsRNA silencing technique (See Chapter 2).

**4. Transcriptional profiling of mosquito genes in the co-culture system**

Taken together, our microscopic observations indicate that distinct antiparasitic responses are induced by the parasites in the mosquito midgut and in the developed co-culture system. Absence of TEP1 binding to the ookinetes in the co-culture system impeded further development of this system for functional analysis of this particular type of host-parasite interactions. To provide more complete characterization of the responses of the mosquito hemocyte-like cells *in vitro* to the parasites, we performed transcriptional profiling using cDNA-based 4000 microarrays established by G. Dimopoulos and G. Christophides. These experiments were perfromed in the laboratory of Prof. F.C. Kafatos in collaboration with G. Christophides, EMBL, Heidelberg.

Total RNAs were isolated from the samples of a co-culture of *P.berghei* ookinetes with *A. gambiae* Sua 5.1* cells after different periods of incubation. Four time points were chosen that corresponded to the previous confocal and transmission electron microscopy analysis (4, 16, 24 and 48 h of co-culturing). As a positive control for immune gene induction, we treated the mosquito cells with peptidoglycan (PGN), the major constituent of the bacterial cell walls and a potent inducer of immune responses in the mosquito cells *in vitro* (Dimopoulos et al., 2002). To distinguish between specific and non-specific responses to ookinetes, we then incubated the *P. berghei* ANKA 2.33 non-gametocyte producing strain with the mosquito cells as a negative control. As no gametocytes were produced by these parasites, the negative control contained mostly magnetic beads which were used for ookinete purification. As a reference probe for the microarray analysis, we used unchallenged (naïve) cells. Clustering analysis and graphic presentations were performed by using the CLUSTER and TREEVIEW software (see Materials and Methods). To ensure reproducible expressional profiles, genes were only selected for cluster analysis if regulated above a 2-fold threshold in at least two out of three experiments. Genes were divided into 5 clusters based on distinguishable expression profiles (Fig 1-7). The detailed data on the gene expression are summarized in the Table 1-2.

**Cluster 1** is characterized by consistent down regulation of gene expression upon both ookinete and PGN challenge. The genes in this group have diverse potential roles in the mosquito: regulation of

transcription, nucleic acid metabolism and regulation of lipid metabolism. Some other genes encoded nucleic acid binding proteins, trans-actin transcription factor and a fatty acid binding protein. Two genes that encode a putative eukaryotic translation initiation factor 1A and a proton-coupled amino acid transporter are up-regulated at 4 h of co-culture by both ookinete and PGN challenge and down-regulated at the later time points. Interestingly, an immune gene, prophenoloxidase 3 (PPO3) is down-regulated by ookinetes and by PGN at all time points.

**Cluster 2** regroups genes that are up-regulated by both ookinetes and PGN. This group also contains *Plasmodium* genes which were spotted on the chips as a positive control for the ookinete presence. These genes encode a *P. berghei* myosin, P28(Pbs21) (an ookinete surface protein), a *P. berghei* tubulin, a von Willebrand factor A domain-related protein (WARP), a secreted ookinete adhesive protein (SOAP) and a circumsporozoite and thrombospondin related anonymous protein-related protein (CTRP). These genes indeed are present in the samples from the ookinete co-cultures and absent from PGN-treated samples. An immune gene encoding PeptidoGlycan Recognition Protein LC (PGRP-LC) appears in this cluster and is up-regulated by both ookinete and PGN challenge. Other genes in this cluster are mostly involved in metabolic processes such as glycolysis (e.g. a lactate dehydrogenase), carbohydrate or lipid metabolism.

**Cluster 3** assembl genes that are predominantly down-regulated by PGN. These genes are mostly involved in protein metabolism and transcription: an enzyme essential for the anaplerotic reactions (phosphoenolpyruvate carboxykinase), two laminin alpha chain precursors and two genes containing laminin-type EGF-like domain. Intriguingly, some immune genes are also down-regulated by both ookinete and PGN challenge. Two *A. gambiae* serine proteases (Ser1 and Ser2), a gene containing leucine-rich repeats (LRR) that shows homology to the *Drosophila* Toll receptor, and a serine protease inhibitor (SRPN10). Interestingly in contrast to the expressional profile in the co-culture system, *SRPN10* was previously shown to be strongly induced during early stages of midgut invasion (Danieli et al., 2003).

**Cluster 4** is dominated by the potential immune-responsive genes. The genes in this cluster are strongly up-regulated by PGN challenge, whereas only slight up-regulation is detected after the ookinete challenge. They encode a homologue of the *Drosophila* PeptidoGlycan Recognition Protein LB (PGRP-LB) (Werner et al., 2000), a dopa decarboxylase which is involved in prophenoloxidase-activation cascade, two clones encoding the Leucine-Rich repeat Immune Protein 1 (LRIM1) (Osta et al., 2004), three different fibrinogen domain lectins that might be involved in aggregation of bacteria (Gokudan et al., 1999), two Gram-Negative bacteria Binding Proteins (GNBPs) (Tamayo et al., 1999 and Lee et al., 2000), and a homologue of the *Caenorhabditis elegans* adaptor protein CED-6, which is implicated in the phagocytosis of apoptotic corpses (Zhou et al., 2001). Interestingly, three mosquito antimicrobial peptide genes (*Defensin1*, *Cecropin 1* and *Gambicin*) (Vizioli et al., 2001a and 2001b) are up-regulated by PGN challenge. Importantly, two genes encoding thioester-containing proteins (*TEP1* and *TEP2*) (Levashina et al., 2001, Christophides et al., 2002, Blandin et al., 2004) are also

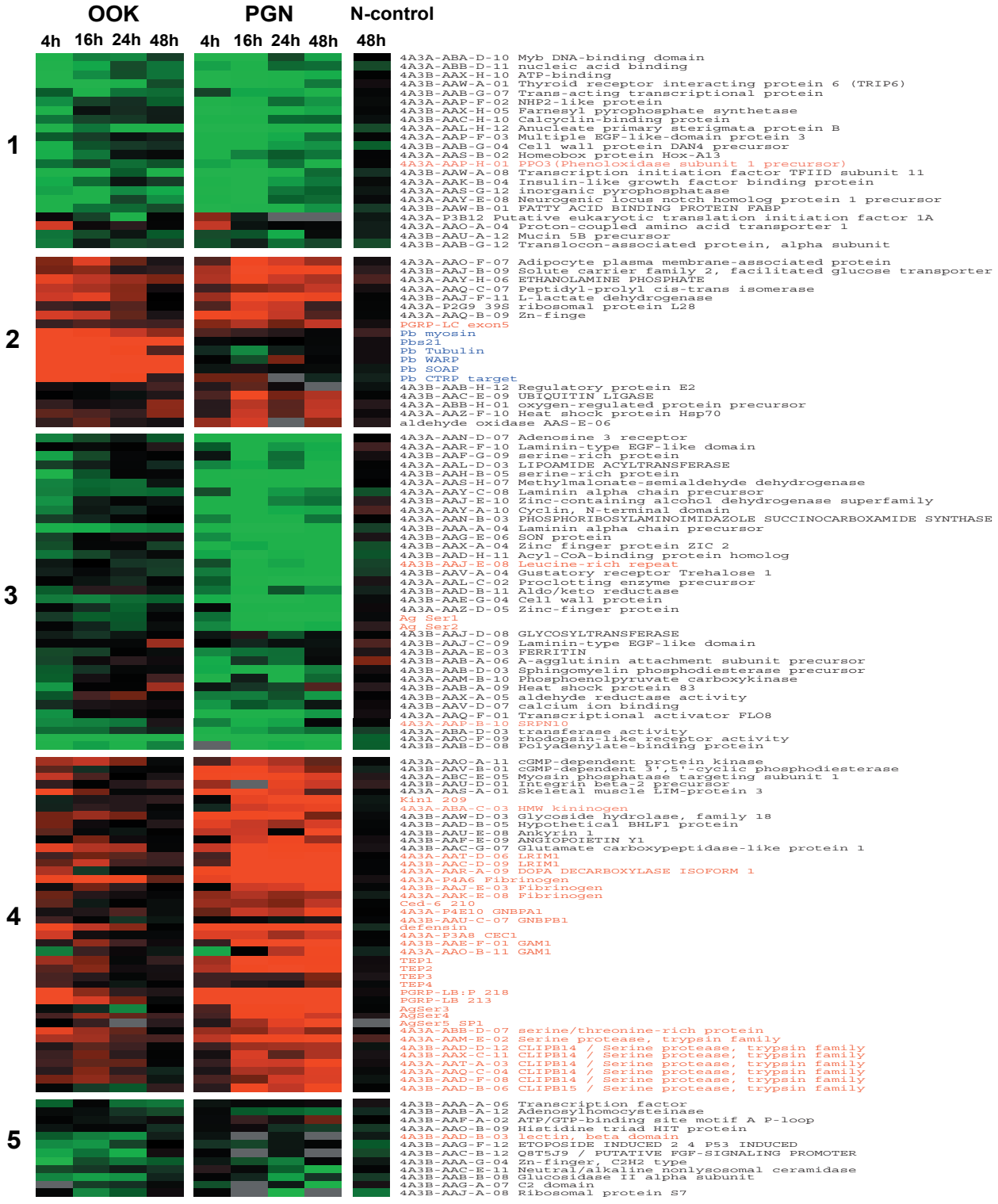


Figure 1-9. Transcriptional profiling analysis of co-culture system. Differential expression profiles of *in vitro* co-culture system challenged by ookinetes (OOK), peptidoglycan (PGN) and a non-gametocyte producing *P. berghei* ANKA 233 strain parasite as the negative control (N-control) and assayed in 4 time-course experiments (4, 16, 24 and 48h of co-culture). The reference probe was from unchallenged (naive) cells. The cluster matrix was divided into 5 clusters based on transition between distinguishable expression profiles. The *Plasmodium* genes (blue) were positive controls for ookinete challenge. With our special interest, the immune genes were labelled in red.

strongly up-regulated by PGN challenge. Finally, four serine protease encoding genes (*Ser3*, *Ser4*, *Ser5* and *SP14D*) (Christophides et al., 2002) are also predominantly up-regulated by PGN. We note that these genes are only modestly up-regulated by the ookinete challenge.

**Cluster 5** represents genes that are down-regulated specifically by the ookinete challenge. The genes in this group are annotated for diverse functions: a transcription factor, a glucosidase II alpha subunit and a ribosomal protein S7. It is important to note here that a gene encoding the ribosomal protein S7 (Blandin et al., 2004) is used for normalization of RNA samples in Northern blotting and in semi-quantitative and in real time PCR experiments. However, it is becoming clear that the expression levels of this house-keeping gene are affected by some immune stimuli and care should be taken when using this gene for data normalization.

Expressional analysis of the co-culture system by cDNA microarrays confirmed previous reports that PGN treatment is a strong inducer of cell responses evidenced by a clear up- or down-regulation of gene expression. In contrast, using this method we were unable to identify ookinete-specific responses in the mosquito cultured cells. Genes induced by ookinetes were also or even more responsive to the PGN treatment. We conclude that Sua 5.1* cells in co-culture system do not distinguish between two different stimuli and mount a “general” type of immune responses, including induction of antimicrobial peptide genes. It is important to note, that some markers characteristic of parasite invasion in the midgut, e.g. SRPN10 (Danielli et al., 2004), are controversially regulated in our co-culture model.

Table 1-2 Profiles of gene expression in co-culture system

| EST number and gene function | Average ratio | | | | | | | | |
|---|---|---|---|---|---|---|---|---|---|
| | OOK | | | | PGN | | | | N-control |
| | 4 h | 16 h | 24 h | 48 h | 4 h | 16 h | 24 h | 48 h | 48 h |
| **Imuunity** | | | | | | | | | |
| 4A3A-AAP-H-01 PPO3(Phenoloxidase subunit 1 precursor) | -0.2312 | -0.3654 | -0.3665 | -0.2439 | -0.5786 | -0.5989 | -0.4765 | -0.7122 | 0.0245 |
| PGRP-LC exon5 | 0.9845 | 1.0023 | 0.8459 | 0.7945 | 1.3302 | 1.9872 | 1.6435 | 1.8932 | 0.1002 |
| 4A3B-AAJ-E-08 Leucine-rich repeat | -0.3145 | 0.0765 | -0.125 | -0.1452 | -0.5122 | -0.7845 | -0.5145 | -0.8145 | 0.0712 |
| Ag Ser1 | -0.2912 | -0.2844 | -0.1997 | 0.0638 | -0.2632 | -0.4342 | -0.3831 | -0.5424 | 0.0065 |
| Ag Ser2 | -0.0565 | -0.1876 | -0.2654 | -0.0765 | -0.4587 | -0.8543 | -0.6878 | -0.6677 | 0.0112 |
| 4A3A-AAP-B-10 SRPN10 | -0.4432 | -0.4565 | -0.567 | -0.0398 | -0.4788 | -0.6098 | -0.7322 | -0.0323 | 0.0466 |
| Kin1 209 | -0.1777 | 0.2034 | 0.3198 | 0.3778 | 0.0887 | 1.3345 | 1.9865 | 1.8765 | 0.0345 |
| 4A3A-ABA-C-03 HMW kininogen | -0.1586 | 0.4855 | 0.2234 | 0.1654 | -0.3435 | 1.3349 | 1.8833 | 1.9943 | 0.5443 |
| 4A3A-AAT-D-06 LRIM1 | 0.9876 | 0.9433 | 0.2351 | 0.3987 | 0.8452 | 2.1512 | 2.8845 | 2.6545 | 0.0654 |
| 4A3B-AAC-D-09 LRIM1 | 0.8844 | 1.3212 | 0.2654 | 0.5125 | 0.7458 | 2.1784 | 2.5654 | 2.9554 | 0.0455 |
| 4A3A-AAR-A-09 DOPA DECARBOXYLASE ISOFORM 1 | 0.3224 | -0.4565 | 0.1343 | 0.0965 | 2.3345 | 2.9877 | 3.2225 | 2.9841 | 0.0077 |
| 4A3A-P4A6 Fibrinogen | 1.2256 | 1.9875 | 2.0565 | 1.0225 | 1.2223 | 1.6555 | 1.4654 | 2.4485 | 0.0551 |
| 4A3B-AAJ-E-03 Fibrinogen | 0.7877 | 0.8865 | 0.4515 | 0.1255 | 0.0551 | 1.9774 | 1.9845 | 2.9845 | 0.0088 |
| 4A3A-AAK-E-08 Fibrinogen | 0.6548 | 0.4515 | 0.3889 | 0.2489 | 1.0987 | 2.0198 | 2.0458 | 0.9851 | 0.0144 |
| Ced-6 210 | 0.1522 | -0.1291 | -0.2955 | -0.1066 | 1.2203 | 1.9855 | 1.7815 | 1.9952 | 0.0995 |
| 4A3A-P4E10 GNBPA1 | 0.0151 | 0.0916 | 0.6948 | -0.2954 | 0.5209 | 1.7848 | 1.6945 | 2.0145 | 0.0077 |
| 4A3B-AAU-C-07 GNBPB1 | 0.5584 | -0.0984 | -0.2484 | -0.1066 | 0.0552 | 0.0985 | -0.1152 | 0.8799 | 0.0445 |
| defensin | 2.012 | 1.9856 | 1.6512 | 0.5512 | 2.4897 | 2.8455 | 2.9856 | 3.0415 | 0.0415 |
| 4A3A-P3A8 CEC1 | 1.0514 | 0.9845 | 0.4851 | 0.1251 | 2.0115 | 2.4329 | 1.5545 | 2.0155 | 0.0338 |
| 4A3B-AAE-F-01 GAM1 | 0.8878 | 1.0245 | 0.9815 | 0.1255 | 0.9981 | 1.9152 | 2.154 | 2.4451 | 0.5122 |
| 4A3A-AAO-B-11 GAM1 | -0.2215 | 0.7815 | 0.1522 | -0.5321 | -0.3315 | 0.0981 | 1.5125 | 1.9845 | 0.0152 |
| TEP1 | 0.7782 | 0.6987 | 0.1221 | 0.5123 | 0.8723 | 2.5672 | 2.887 | 3.127 | 0.0753 |
| TEP2 | 0.6123 | 0.8873 | 0.0231 | 0.0118 | 0.9531 | 2.4538 | 2.6712 | 3.1231 | 0.0811 |
| TEP3 | 0.5721 | 0.5151 | -0.2515 | 0.1151 | 0.3945 | 0.2953 | 0.3485 | 0.4198 | 0.0815 |
| TEP4 | 0.5273 | 0.1845 | -0.2545 | -0.2811 | 0.3481 | 0.2152 | 0.2958 | 0.3816 | 0.0522 |
| PGRP-LB:P 218 | 2.1043 | 1.2313 | 0.1882 | 0.1212 | 3.1265 | 3.2012 | 3.6788 | 3.8801 | 0.0782 |
| PGRP-LB 213 | 2.2245 | 1.5955 | 1.266 | -0.1308 | 3.3696 | 3.1621 | 3.8976 | 3.315 | 0.0826 |
| AgSer3 | 0.1565 | -0.2152 | -0.3552 | 0.0981 | 0.9151 | 2.5125 | 2.8455 | 2.6512 | 0.0441 |
| AgSer4 | 0.8155 | 0.4811 | 0.8565 | 0.9978 | 0.9151 | 2.4515 | 2.6154 | 2.0154 | 0.7845 |
| AgSer5 | 0.1152 | 0.2512 | N | 0.1784 | 0.9915 | 1.4512 | 2.9815 | 2.6651 | N |
| 4A3A-ABB-D-07 serine/threonine-rich protein | 1.2032 | 0.9415 | 0.8154 | 0.0415 | 1.0225 | 1.3516 | 1.5021 | 1.6512 | 0.0415 |
| 4A3A-AAM-E-02 Serine protease, trypsin family | 0.9815 | 0.8154 | 0.6451 | 0.7154 | 1.0415 | 1.5415 | 1.6684 | 2.0415 | 0.0894 |

| | | | | | | | | | |
|---|---|---|---|---|---|---|---|---|---|
| 4A3B-AAD-D-12 CLIPB14 / Serine protease, trypsin family | 0.2156 | 0.4915 | 0.5154 | -0.4156 | 0.9845 | 1.9984 | 2.1415 | 2.3345 | -0.014 |
| 4A3B-AAX-C-11 CLIPB14 / Serine protease, trypsin family | 0.2194 | 0.4845 | 0.3741 | -0.3215 | 0.0815 | 1.1542 | 0.9215 | 1.2032 | 0.0152 |
| 4A3A-AAT-A-03 CLIPB14 / Serine protease, trypsin family | 0.3515 | 0.5845 | 0.4145 | -0.1201 | 0.5815 | 1.2415 | 1.2815 | 1.6984 | 0.0784 |
| 4A3A-AAQ-C-04 CLIPB14 / Serine protease, trypsin family | 0.2154 | 0.3752 | 0.2415 | -0.3152 | 0.0984 | 0.9451 | 1.2245 | 1.6985 | 0.0154 |
| 4A3B-AAD-F-08 CLIPB14 / Serine protease, trypsin family | 0.3715 | 0.4145 | 0.3851 | -0.4516 | 0.2874 | 0.4265 | 1.4512 | 1.9845 | 0.0138 |
| 4A3B-AAD-B-06 CLIPB14 / Serine protease, trypsin family | -0.1526 | -0.3215 | -0.4512 | 0.7812 | 0.3815 | 1.2415 | 1.1415 | 1.8894 | 0.0455 |
| 4A3B-AAD-B-03 lectin, beta domain | -0.2203 | -0.2522 | -0.3615 | -0.1251 | -0.1522 | N | -0.1655 | N | 0.0815 |
| **Stress response** | | | | | | | | | |
| 4A3A-ABB-H-01 oxygen-regulated protein precursor | 0.1245 | 0.0988 | 0.0712 | 0.5415 | 0.2254 | 0.8458 | 0.6514 | 0.7715 | 0.1002 |
| 4A3A-AAZ-F-10 Heat shock protein Hsp70 | 0.2232 | 0.1987 | 0.1025 | 0.2354 | 0.1178 | 0.5415 | 0.3451 | 0.4873 | 0.0984 |
| aldehyde oxidase AAS-E-06 | 0.1021 | 0.2012 | 0.0984 | 0.1145 | 0.4512 | 0.7745 | N | 0.6512 | 0.0985 |
| 4A3A-AAL-C-02 Proclotting enzyme precursor | -0.1145 | -0.1452 | -0.1985 | -0.0987 | -0.2784 | -0.3845 | -0.3415 | -0.3784 | 0.0045 |
| 4A3B-AAA-E-03 FERRITIN | -0.1885 | -0.2154 | -0.0952 | -0.1078 | -0.3078 | -0.2819 | -0.2451 | -0.1083 | 0.1008 |
| 4A3B-AAB-A-09 Heat shock protein 83 | -0.3894 | 0.0085 | 0.0152 | 0.9845 | -0.0145 | -0.1054 | -0.1925 | 0.3487 | 0.1058 |
| 4A3B-AAX-A-05 aldehyde reductase activity | -0.2044 | 0.4512 | 0.7891 | 0.0145 | -0.3378 | -0.3258 | -0.2893 | -0.3178 | 0.0985 |
| **Carbohydrate / lipid metabolism** | | | | | | | | | |
| 4A3B-AAX-H-05 Farnesyl pyrophosphate synthetase | -0.3154 | -0.0112 | -0.2105 | -0.0845 | -0.4875 | -0.6849 | -0.598 | -0.8451 | 0.0155 |
| 4A3A-AAS-G-12 inorganic pyrophosphatase | -0.3845 | -0.4122 | -0.3987 | -0.512 | -0.3945 | -0.4815 | -0.4152 | -0.1545 | -0.0254 |
| 4A3A-AAO-F-07 Adipocyte plasma membrane-associated protein | 0.3515 | 0.3984 | 0.2945 | 0.1209 | 0.3455 | 0.1265 | 0.1022 | 0.9845 | 0.0384 |
| 4A3B-AAJ-B-09 Solute carrier family, glucose transporter | 0.3151 | 0.3284 | 0.0985 | 0.1251 | 0.3415 | 0.5152 | 0.4851 | 0.5362 | 0.1526 |
| 4A3A-AAL-D-03 LIPOAMIDE ACYLTRANSFERASE | -0.2984 | -0.3014 | -0.0012 | -0.2546 | -0.2545 | -0.3512 | -0.2958 | -0.4152 | 0.0415 |
| 4A3A-AAN-B-03 PHOSPHORIBOSYLAMINOIMIDAZOLE | -0.0145 | -0.2102 | -0.0144 | -0.0048 | -0.2451 | -0.3516 | -0.4152 | -0.3215 | 0.0395 |
| 4A3B-AAD-H-11 Acyl-CoA-binding protein homolog | -0.3215 | -0.2984 | -0.4152 | -0.1205 | -0.3519 | -0.4156 | -0.5126 | -0.4895 | -0.1205 |
| 4A3B-AAJ-D-08 GLYCOSYLTRANSFERASE | -0.2152 | -0.3152 | -0.2984 | -0.1292 | -0.2548 | 0.2145 | -0.3185 | 0.1058 | 0.0325 |
| 4A3B-AAB-D-03 Sphingomyelin phosphodiesterase precursor | -0.3849 | -0.2548 | -0.1548 | 0.0985 | -0.9845 | -0.8154 | -0.4512 | -0.4512 | 0.0012 |
| 4A3A-AAM-B-10 Phosphoenolpyruvate carboxykinase | -0.3845 | 0.1548 | -0.2516 | 0.2415 | -0.548 | -0.0388 | -0.4152 | -0.3512 | 0.0154 |
| 4A3B-AAV-A-04 Gustatory receptor Trehalose 1 | -0.2105 | -0.0152 | -0.3152 | -0.1254 | -0.3985 | -0.4152 | -0.5126 | -0.4981 | -0.1021 |
| 4A3B-AAW-D-03 Glycoside hydrolase, family 18 | 0.351 | 0.3845 | 0.2985 | 0.0845 | 1.512 | 1.4882 | 1.7845 | 0.985 | 0.0451 |
| 4A3B-AAC-G-07 Glutamate carboxypeptidase-like protein 1 | 0.7845 | 0.5481 | 0.4115 | 0.0951 | 0.845 | 1.4512 | 1.5488 | 1.7845 | 0.0512 |
| 4A3B-AAB-B-08 Glucosidase II alpha subunit | -0.3845 | -0.4022 | -0.3984 | -0.2845 | -0.0145 | -0.1524 | -0.3985 | -0.2154 | -0.2415 |
| 4A3B-AAW-B-01 FATTY ACID BINDING PROTEIN FABP | -0.3512 | -0.2514 | -0.3517 | -0.2985 | -0.4589 | -0.4015 | -0.3985 | -0.3645 | -0.1205 |
| 4A3B-AAJ-F-11 L-lactate dehydrogenase | 0.7845 | 1.2542 | 0.9874 | 0.0952 | 0.452 | 1.5245 | 1.4988 | 1.3845 | 0.0855 |
| **Protein metabolism** | | | | | | | | | |
| 4A3B-AAW-A-01 Thyroid receptor interacting protein 6 (TRIP6) | -0.3845 | -0.3451 | -0.4152 | -0.2985 | -0.3845 | -0.3478 | -0.4152 | -0.4895 | 0.0422 |
| 4A3B-AAC-H-10 Calcyclin-binding protein | -0.221 | -0.1025 | -0.1695 | -0.0984 | -0.3845 | -0.3512 | -0.7845 | -0.1542 | 0.0415 |
| 4A3A-AAK-B-04 Insulin-like growth factor binding protein | -0.3125 | -0.2845 | -0.0845 | -0.2154 | -0.3845 | -0.3056 | -0.2845 | -0.2877 | 0.0384 |

| | | | | | | | | | |
|---|---|---|---|---|---|---|---|---|---|
| 4A3A-AAO-A-04 Proton-coupled amino acid transporter 1 | 1.2055 | 0.0415 | 0.4315 | 0.1022 | 1.2107 | -0.1215 | 0.0845 | 0.0365 | -0.1021 |
| 4A3B-AAC-E-09 UBIQUITIN LIGASE | -0.1021 | 0.2102 | -0.1845 | 0.2164 | 0.4512 | 1.4152 | 0.9854 | 1.0254 | 0.0385 |
| 4A3A-AAP-F-03 Multiple EGF-like-domain protein 3 | -0.2451 | -0.3012 | -0.0144 | -0.1235 | -0.3985 | -0.4087 | -0.3581 | -0.2154 | -0.0338 |
| 4A3A-AAR-F-10 Laminin-type EGF-like domain | 0.0845 | -0.0984 | 0.0035 | 0.1845 | -0.2485 | -0.3598 | -0.2987 | -0.3415 | 0.1526 |
| 4A3B-AAF-G-09 serine-rich protein | -0.3258 | -0.2485 | 0.0985 | 0.0354 | 0.0415 | -0.3378 | -0.2451 | -0.3985 | 0.1099 |
| 4A3B-AAH-B-05 serine-rich protein | -0.3152 | -0.298 | 0.0845 | 0.0745 | -0.3895 | -0.3458 | -0.2485 | -0.3784 | 0.0845 |
| 4A3A-AAY-C-08 Laminin alpha chain precursor | -0.2487 | -0.1985 | -0.2485 | -0.2784 | -0.1865 | -0.3859 | -0.3856 | -0.3715 | -0.2481 |
| 4A3A-AAY-A-10 Cyclin, N-terminal domain | -0.1902 | -0.0945 | -0.1088 | 0.0844 | -0.3874 | -0.2854 | -0.5216 | -0.4785 | 0.1254 |
| 4A3B-AAA-A-04 Laminin alpha chain precursor | -0.3215 | -0.3351 | -0.3459 | -0.3485 | -0.4152 | -0.3845 | -0.4152 | -0.3548 | -0.2845 |
| 4A3B-AAJ-C-09 Laminin-type EGF-like domain | 0.0984 | 0.0855 | 0.0769 | 0.7154 | 0.0145 | -0.1254 | -0.0054 | -0.0849 | 0.2412 |
| 4A3B-AAB-A-06 A-agglutinin attachment subunit precursor | -0.385 | 0.1025 | 0.2215 | 0.1548 | -0.3845 | -0.2548 | -0.2555 | 0.0945 | 0.425 |
| 4A3A-ABA-D-03 transferase activity | -0.2889 | -0.2684 | -0.1936 | -0.1452 | -0.3887 | -0.3952 | -0.3478 | -0.2855 | -0.1548 |
| 4A3A-AAO-A-11 cGMP-dependent protein kinase | 0.3512 | 0.3998 | 0.2845 | 0.0125 | 0.1088 | 0.2985 | 0.3154 | 0.4152 | 0.0215 |
| 4A3B-AAV-B-01 cGMP-dependent 3',5'-cyclic phosphodiesterase | 0.2985 | -0.5145 | -0.1254 | 0.0985 | 1.0855 | 1.2542 | 1.0995 | 0.8945 | -0.4152 |
| 4A3B-AAF-E-09 ANGIOPOIETIN Y1 | 0.0985 | 0.5412 | 0.3512 | 0.0845 | 0.0215 | 0.6845 | 1.2545 | 1.0054 | 0.0377 |
| 4A3B-AAC-E-11 Neutral/alkaline nonlysosomal ceramidase | -0.2485 | -0.2855 | -0.0845 | -0.2589 | 0.1542 | 0.0485 | -0.2885 | -0.3966 | 0.0977 |
| **Transcription / nucleic acid metabolism** | | | | | | | | | |
| 4A3A-ABA-D-10 Myb DNA-binding domain | -0.3389 | -0.2885 | -0.3012 | -0.2844 | -0.3541 | -0.3895 | -0.2845 | -0.3995 | -0.0144 |
| 4A3A-ABB-D-11 nucleic acid binding | -0.3485 | -0.3511 | -0.2411 | -0.2844 | -0.3855 | -0.2748 | -0.2845 | -0.2448 | -0.1988 |
| 4A3B-AAX-H-10 ATP-binding | -0.3351 | -0.3845 | -0.2845 | -0.3011 | -0.3748 | -0.4122 | -0.3845 | -0.3845 | 0.0325 |
| 4A3B-AAW-A-08 Transcription initiation factor TFIID subunit 11 | -0.3115 | -0.3844 | -0.2995 | -0.3415 | -0.3251 | -0.3749 | -0.3771 | -0.2745 | -0.1877 |
| 4A3A-AAY-E-08 Neurogenic locus notch homolog protein 1 | -0.3755 | -0.3174 | -0.2956 | -0.3277 | -0.4077 | -0.3976 | -0.2799 | -0.2855 | -0.0045 |
| 4A3A-P3B12 Putative eukaryotic translation initiation factor 1A | 0.0877 | -0.1998 | -0.3744 | -0.0112 | 0.5411 | -0.2871 | N | N | -0.1247 |
| 4A3B-AAB-G-12 Translocon-associated protein, alpha subunit | -0.3215 | -0.0514 | -0.2487 | -0.2985 | -0.2115 | -0.0744 | -0.3114 | -0.2998 | -0.2748 |
| 4A3A-AAY-H-06 ETHANOLAMINE PHOSPHATE | 1.065 | 0.985 | 0.7784 | 0.7115 | 0.6548 | 1.2055 | 0.9852 | 0.7152 | 0.1542 |
| 4A3A-AAQ-C-07 Peptidyl-prolyl cis-trans isomerase | 0.8845 | 0.648 | 0.5784 | 0.0956 | 0.1022 | 0.2551 | 0.3002 | 0.4125 | 0.0511 |
| 4A3A-AAQ-B-09 Zn-finge | 0.784 | 0.7715 | 0.5123 | 0.122 | 0.9852 | 0.8848 | 0.7485 | 0.3152 | 0.0988 |
| 4A3B-AAB-H-12 Regulatory protein E2 | 0.0552 | 0.0745 | 0.0985 | 0.1028 | 0.0855 | 0.1187 | 0.0856 | N | -0.1142 |
| 4A3A-AAN-D-07 Adenosine 3 receptor | -0.3335 | -0.2789 | -0.1025 | -0.2245 | -0.3384 | -0.3784 | -0.4189 | -0.5478 | 0.0251 |
| 4A3A-AAS-H-07 Methylmalonate-semialdehyde dehydrogenase | -0.3145 | -0.2984 | -0.3215 | -0.0845 | -0.3541 | -0.3552 | -0.1478 | -0.4513 | 0.0798 |
| 4A3B-AAJ-E-10 Zinc-containing alcohol dehydrogenase | -0.3351 | -0.1485 | -0.0919 | -0.0893 | -0.3719 | -0.3895 | -0.2985 | -0.2774 | 0.0887 |
| 4A3B-AAX-A-04 Zinc finger protein ZIC 2 | -0.2441 | -0.0888 | -0.8911 | -0.2983 | -0.3478 | -0.389 | -0.4088 | -0.3187 | -0.2784 |
| 4A3A-AAZ-D-05 Zinc-finger protein | -0.0788 | -0.2784 | -0.3105 | -0.2105 | -0.0444 | -0.3784 | -0.4152 | -0.3789 | 0.0781 |
| 4A3B-AAD-B-11 Aldo/keto reductase | -0.1022 | 0.1005 | 0.1088 | -0.1245 | -0.2445 | -0.3215 | -0.198 | -0.2781 | -0.1245 |
| 4A3A-AAQ-F-01 Transcriptional activator FLO8 | -0.3012 | -0.0998 | -0.0451 | -0.1078 | -0.3874 | -0.4011 | -0.3487 | -0.298 | -0.0049 |
| 4A3A-AAO-F-09 rhodopsin-like receptor activity | -0.3331 | -0.3315 | -0.3784 | -0.2984 | -0.3379 | -0.3915 | -0.3718 | -0.3078 | -0.1845 |
| 4A3B-AAB-D-08 Polyadenylate-binding protein | -0.3148 | -0.4298 | -0.3154 | -0.3874 | N | -0.3718 | -0.3815 | -0.3982 | -0.2145 |
| 4A3B-AAA-A-06 Transcription factor | -0.2015 | -0.0981 | -0.1452 | -0.1874 | -0.0781 | -0.0415 | -0.0985 | -0.0802 | -0.0035 |

| | | | | | | | | | |
|---|---|---|---|---|---|---|---|---|---|
| 4A3B-AAB-A-12 Adenosylhomocysteinase | -0.0788 | -0.0998 | -0.2014 | -0.2781 | -0.0985 | -0.2014 | -0.2873 | -0.3301 | -0.2784 |
| 4A3B-AAF-A-02 ATP/GTP-binding site motif A P-loop | 0.0845 | -0.0145 | -0.0854 | 0.0054 | -0.0415 | 0.0782 | 0.0451 | 0.4152 | 0.0038 |
| 4A3A-AAO-B-09 Histidine triad HIT protein | -0.1205 | -0.0458 | -0.0982 | -0.2485 | -0.1078 | -0.0985 | -0.2987 | -0.3852 | -0.0825 |
| 4A3B-AAA-G-04 Zn-finger, C2H2 type | -0.3328 | -0.2784 | -0.1785 | -0.3852 | -0.1087 | -0.2874 | -0.3782 | -0.0985 | 0.0778 |
| 4A3B-AAC-B-12 PUTATIVE FGF-SIGNALING PROMOTER | -0.3385 | -0.285 | -0.3988 | -0.0991 | -0.0047 | N | -0.1055 | N | -0.2078 |
| 4A3B-AAG-F-12 ETOPOSIDE INDUCED 2 4 P53 INDUCED | -0.3877 | -0.2985 | -0.1729 | -0.0415 | -0.1785 | -0.1902 | -0.0892 | 0.0349 | -0.214 |
| **Cell organization and biogenesis** | | | | | | | | | |
| 4A3B-AAB-G-07 Trans-acting transcriptional protein | -0.2145 | -0.3587 | -0.2987 | -0.2981 | -0.1874 | -0.2888 | -0.3789 | -0.3784 | 0.0778 |
| 4A3A-AAS-A-01 Skeletal muscle LIM-protein 3 | 1.781 | 0.452 | 0.0154 | 0.0544 | 1.6845 | 1.8895 | 1.7159 | 1.014 | 0.0483 |
| 4A3B-AAB-G-04 Cell wall protein DAN4 precursor | -0.3032 | -0.2781 | -0.2985 | -0.2748 | -0.3378 | -0.3984 | -0.3415 | -0.3882 | -0.1982 |
| 4A3A-AAS-B-02 Homeobox protein Hox-A13 | -0.3154 | -0.2145 | 0.0145 | 0.0982 | -0.3874 | -0.2214 | -0.1845 | -0.1885 | 0.0984 |
| 4A3B-AAU-A-12 Mucin 5B precursor | -0.2225 | -0.1922 | -0.1783 | -0.2188 | -0.1568 | -0.1773 | -0.3845 | 0.0841 | 0.0385 |
| 4A3B-AAE-G-04 Cell wall protein | -0.3387 | -0.3152 | -0.2874 | -0.1784 | -0.2145 | -0.3088 | -0.1545 | -0.2189 | -0.0841 |
| 4A3A-ABC-E-05 Myosin phosphatase targeting subunit 1 | 0.4541 | 0.2258 | 0.0458 | 0.9852 | 1.7685 | 1.9952 | 1.8402 | 1.4512 | 0.0985 |
| 4A3B-AAU-D-01 Integrin beta-2 precursor | 0.0445 | -0.1025 | 0.1545 | 0.2087 | 0.3325 | N | 0.4512 | 0.3389 | 0.0365 |
| 4A3B-AAU-E-08 Ankyrin 1 | 0.1453 | -0.1125 | -0.1055 | -0.211 | 1.0222 | 1.5201 | 0.415 | 1.5426 | 0.0012 |
| 4A3B-AAV-D-07 calcium ion binding | -0.1102 | 0.0512 | 0.0784 | 0.0145 | -0.3152 | -0.1225 | -0.3215 | -0.2114 | 0.0125 |
| **Ribosomal protein** | | | | | | | | | |
| 4A3A-P2G9 39S ribosomal protein L28 | 0.1102 | 0.0985 | 0.2044 | 0.0781 | 0.1852 | 0.4489 | 0.3981 | 0.2078 | 0.0489 |
| 4A3B-AAJ-A-08 Ribosomal protein S7 | 0.0855 | -0.3145 | -0.2982 | 0.0145 | 0.1125 | N | -0.3245 | N | -0.3152 |
| **others** | | | | | | | | | |
| 4A3A-AAP-F-02 NHP2-like protein | -0.3014 | -0.2215 | -0.1985 | -0.2014 | -0.3896 | -0.2984 | -0.1078 | -0.3152 | -0.0785 |
| 4A3A-AAL-H-12 Anucleate primary sterigmata protein B | -0.3145 | -0.2415 | -0.3352 | -0.3145 | -0.3784 | -0.3451 | -0.2879 | -0.4185 | -0.1452 |
| 4A3B-AAG-E-06 SON protein | -0.2201 | -0.0417 | -0.0572 | -0.0144 | -0.2548 | -0.3815 | -0.3455 | -0.3998 | 0.0952 |
| 4A3B-AAD-B-05 Hypothetical BHLF1 protein | 0.2895 | 0.0854 | -0.1022 | 0.1452 | 0.9855 | 0.8815 | 0.7815 | 0.8023 | 0.0859 |
| 4A3B-AAG-A-07 C2 domain | N | -0.2014 | -0.1782 | -0.0448 | -0.0852 | N | -0.3258 | N | -0.3157 |
| ***Plasmodium* genes** | | | | | | | | | |
| Pb myosin | 1.8057 | 1.7395 | 1.2992 | 0.5162 | 0.2474 | 0.2941 | 0.2485 | 0.3753 | 0.0408 |
| Pbs21 | 2.8036 | 2.0465 | 2.0322 | 2.4599 | 0.1301 | 0.2681 | 0.2826 | 0.0813 | 0.0184 |
| Pb Tubulin | 2.9504 | 2.5642 | 2.6623 | 0.5017 | -0.1114 | -0.3861 | -0.1038 | 0.2221 | 0.0569 |
| Pb WARP | 4.4139 | 3.7327 | 3.1259 | 4.0579 | 0.2749 | -0.2197 | 0.1219 | 0.0961 | 0.0806 |
| Pb SOAP | 6.4311 | 5.8142 | 4.7932 | 5.9791 | -0.1472 | 0.0685 | 0.227 | 0.1399 | 0.0202 |
| Pb CTRP target | 4.1223 | 3.8891 | 2.9873 | 0.7621 | 1.0123 | 0.923 | N | -0.1289 | 0.1409 |

# CONCLUSIONS

In this project, we established an *in vitro* co-culture system using a mosquito hemocyte-like cell line to study mosquito-parasite interactions. We demonstrate by transmission electron microscopy that ookinete probing of the cell surface by the apical end results in a slight invagination of the cell membrane. Mosquito cells respond to the ookinetes by stretching lamellipodium-like structures, which at the later time points completely encircle parasites leading to their engulfment. Intracellular ookinetes are surrounded by a membranous vacuole, which resembles a phagosome. The observed reactions are strikingly similar to the zipper-like mode of phagocytosis and we propose that in our co-culture system phagocytosis is responsible for the engulfment of ookinetes.

It has been reported that the *in vitro* development of *P. berghei* early oocysts occurs predominantly intracellular (Syafruddin et al., 1992 and Siden-Kiamos et a., 2000), however in both reports, the intracellular oocysts failed to further develop into sporozoites. Recently, Al-Olayan and colleagues (Al-Olayan et al., 2002) reported the successful development of infective sporozoites in an *in vitro* co-culture of *P. berghei* parasites with a *Drosophila* S2 cell line. In this model, parasite development was achieved extracellularly in the presence of Matrigel. In our co-culture system, we observed development of ookinetes into early oocysts both intra- and extracellularly but no further development evidenced by nuclear division was detected. This might indicate that some crucial components required for the sporogonic parasite development *in vitro* were lacking in our co-culture system.

TEP1 is functional and promotes phagocytosis of Gram-negative bacteria in the same mosquito cell line that we use in our co-culture system (Levashina et al., 2001). Our observations indicate that in contrast to midgut invasion, TEP1 does not bind to the banana-shaped ookinetes *in vitro*. Patchy, inconspicuous TEP1-reactive signals were detected on the surface of rounded young oocysts. We speculate the differences in the ability of TEP1 to bind ookinetes are due to the different cellular environments between the *in vivo* and *in vitro* systems. *In vivo*, ookinetes are facing epithelial cells, which differ from the hemocyte-like cells used for co-culture by a number of characteristics, including strong polarization, absence of phagocytotic capabilities, expression of specific markers, just to mention a few. In addition, these differences could be extended to distinct temporal interactions: during the midgut invasion, ookinetes have first to cross epithelial cells and then come in contact with TEP1 in the basal labyrinth. This is in contrast with the co-culture system, where ookinetes are immediately exposed to TEP1 that is present in the culture medium. Finally, although the mechanism(s) of TEP1 activation remain(s) unknown, TEP1 might not be properly activated in our co-culture system. Therefore, we conclude that the *in vitro* co-culture system is unsuitable for TEP1 functional analysis.

The cDNA microarray analysis of the co-culture system did not detect genes that would be regulated specifically in response to the ookinete presence. Most of the regulated genes, which we have divided into five pattern-specific clusters, are regulated in response to both, the ookinete presence and the PGN treatment. Surprisingly to us, some genes known to be induced during the parasite invasion of the

midgut, were down-regulated by the ookinete presence in our co-culture system.

Our detailed characterization of the *in vitro* system highlights several important differences with the *in vivo* midgut invasion process, and raises a note of caution for future studies relying solely on the co-culture system for analyses of host-parasite interactions.

# CHAPTER 2

## The complement-like protein TEP1 is a determinant of vectorial capacity in the malaria vector *Anopheles gambiae*

# Introduction

Double stranded RNA (dsRNA) gene silencing in adult mosquitoes and assays to analyze knockdown phenotypes allowed us to address the role of thioester-containing protein 1 in mosquito antiparasitic defense, and especially, in the recognition of parasites and the activation of effector responses. A family of TEP genes has been identified in the genome of *A. gambiae* (Christophides et al., 2002) and one of these, *TEP1*, was studied in more detail (Levashina et al., 2001). TEP1 resembles its vertebrate complement homologues and plays a role in opsonozation of bacteria for phagocytosis.

As discussed in Chapter 1, the *in vitro* co-culture system did not allow us to perform functional analysis of TEP1. S. Blandin and collaborators succeeded in adapting the double stranded RNA interference for functional gene analysis in mosquito adults (Blandin et al., 2002). We, therefore, made use of the dsRNA knockdown of *TEP1* to study the mosquito-parasite interactions *in vivo*. Our study of parasite development in the mosquitoes was greatly facilitated by the use of a GFP-expressing parasite provided by B. Frankle-Fayard (LUMC, Leiden) (Franke-Fayard et al., 2004). This was not only instrumental for counting of surviving oocysts, but also provided a tool to distinguish between live and dead parasites.

I was specifically involved in the studies which demonstrated TEP1 binding to the parasite surface. Using my experience with the electron microscopy, I have adapted immunohistochemical analysis to detect TEP1 protein in the mosquito midgut using a polyclonal antibody against TEP1.

In addition, we examined the biological diversity of two strains of *A. gambiae*: the susceptible G3 strain which allows a fraction of parasite to develop into sporozoite and the refractory L3-5 strain, which kills and melanizes a number of parasite species, including *P. berghei*, after they have traversed the midgut epithelium (Collins et al., 1986).

Here I summarize our results which are published in Cell (Blandin et al., 2004).

# Results

1. Parasites suffer significant losses during midgut invasion, not only in refractory (R) mosquitoes, but also in susceptible (S) mosquitoes. The kinetics of parasite killing and the observation of moribund ookinetes led us to propose (i) that ookinetes are lyzed in the basal labyrinth of the midgut epithelium, and that this accounts for major parasite losses associated with midgut invasion in both strains, and (ii) that contrary to general belief, melanization in R mosquitoes does not kill parasites, but occurs after parasite death, most likely serves to isolate dead parasites from surrounding live mosquito tissues.

2. TEP1 binds to the surface of ookinetes, after they have crossed the midgut epithelium. The electron microscopical studies further confirmed that TEP1 binds to the surface of bacteria and ookinetes in the mosquito midgut (Figure 2-1). Interestingly, we observed that TEP1 binding is temporally correlated with the appearance of morphologically degenerate ookinetes. Moreover, the vast majority of TEP1-labelled ookinetes were dead. We also detected TEP1 on the surface of oocysts, however, at this stage binding of TEP1 does not affect parasite development. The same is true for later parasite stages, sporozoites, which have to cross the hemocoel and migrate through the hemolymph to the salivary glands. We could not detect TEP1 signal on the sporozoite surface, suggesting that sporozoites are not recognized by TEP1. This finding is intriguing, as TEP1 is mostly present in the hemolymph. How sporozoites avoid the recognition by TEP1 remains to be clarified but we can expect to discover strategies employed by parasites to escape from the mosquito immune surveillance.

3. The binding of TEP1 to ookinetes and oocysts is associated with two peaks of transcriptional up-regulation at 24 h and 4 days post infection. It is possible to suggest that transcriptional regulation provides a mechanism to replenish the level of TEP1 circulating in the hemolymph. However, the molecular mechanisms of this signaling back-loop are not understood.

4. Silencing of TEP1 by dsRNA results in a five-fold increase in parasite (oocyst) survival in S mosquitoes. In R mosquitoes, TEP1 knockdown both increases parasite numbers and completely abolishes their melanization, thus converting refractory mosquitoes into susceptible ones. Our results clearly demonstrate that TEP1 is an essential mosquito factor implicated in parasite killing.

5. We observe faster and more efficient parasite killing in R mosquitoes than in S mosquitoes. In addition, the disposal mode of dead parasites differs between two strains: lysis in S mosquitoes and lysis and melanization in R mosquitoes. We correlate the observed differences between two strains with the ability of TEP1 to bind parasites, which is also faster and more efficient in R than in S mosquitoes.

6. To explain differences in TEP1 functioning between the two strains, we demonstarte that TEP1 is encoded by two distinct allels in R and S mosquitoes: *TEP1s* is specially associated with S strain, whereas *TEP1r* is present only in R mosquitoes. The comparative sequence analysis of the two alleles reveals that most of the substitutions are clustered in the C3d-like region, which contains the thioester

site and directly binds to substrates. We speculate that the polymorphism detected between *TEP1s* and *TEP1r* might account for the more efficient parasite killing in R mosquitoes.

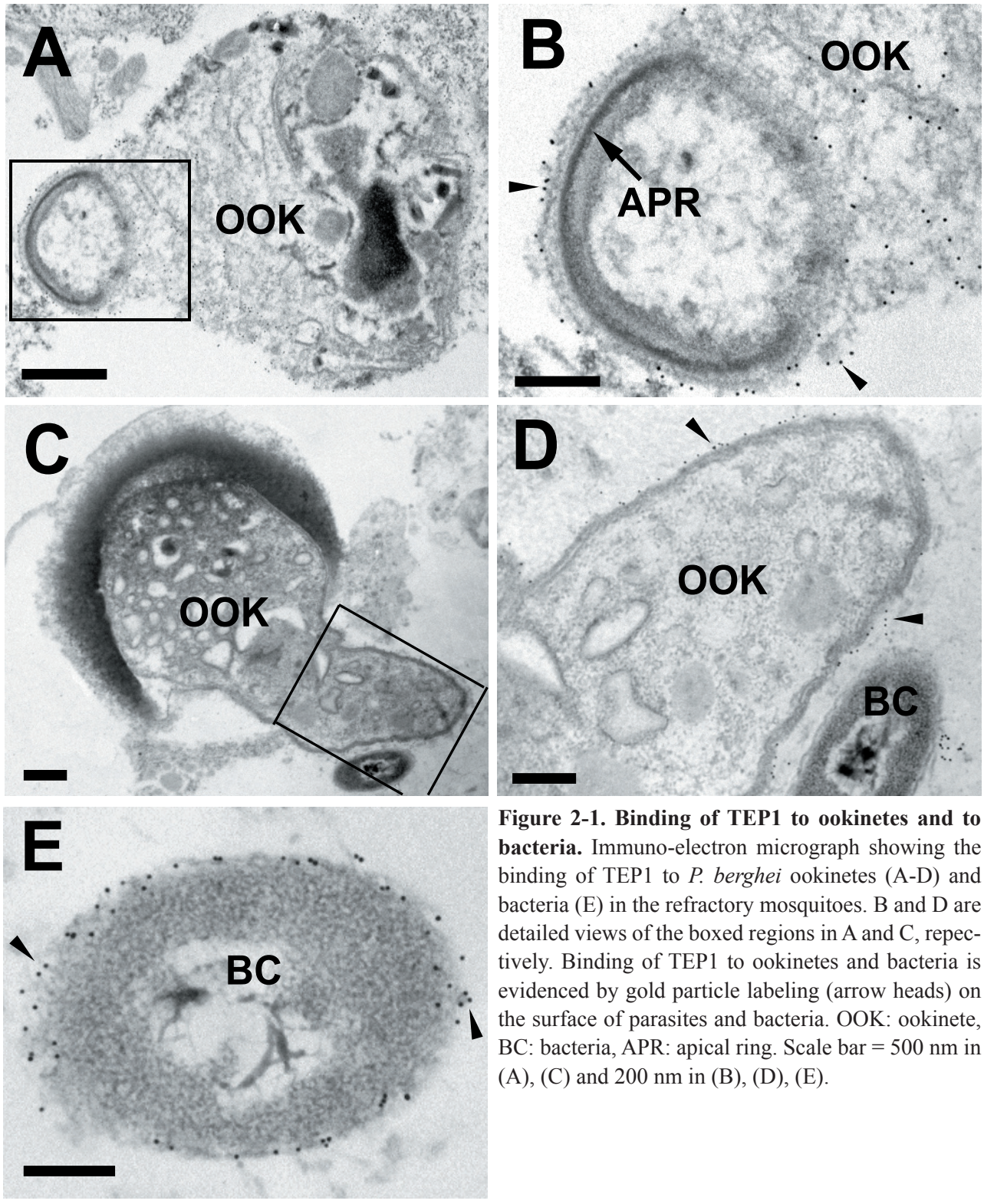


**Figure 2-1. Binding of TEP1 to ookinetes and to bacteria.** Immuno-electron micrograph showing the binding of TEP1 to *P. berghei* ookinetes (A-D) and bacteria (E) in the refractory mosquitoes. B and D are detailed views of the boxed regions in A and C, repectively. Binding of TEP1 to ookinetes and bacteria is evidenced by gold particle labeling (arrow heads) on the surface of parasites and bacteria. OOK: ookinete, BC: bacteria, APR: apical ring. Scale bar = 500 nm in (A), (C) and 200 nm in (B), (D), (E).

# Conclusions

Functional analysis of TEP1 allowed us to demonstrate that TEP1 binds to and mediates killing of midgut stages of *P. berghei*. TEP1 binding to different types of pathogens and the consequent promotion of phagocytosis of bacteria in the mosquito hemocoel or parasite killing in the midgut, are reminiscent of functions of the complement factors in mammals.

Our studies on the role of TEP1 in the antiparasite defence demonstrate (i) that mosquitoes actively defend themselves against *Plasmodium* parasites, (ii) that the dramatic losses undergone by parasites in the first day after infection are essentially due to the mosquito immune responses and (iii) identify TEP1 as an important actor in these immune responses.

Taken together, our results led us to propose the following two-step model for immune responses of *A. gambiae* to *P. berghei.* In the first step, after crossing the midgut epithelium, parasites come in contact (within the basal labyrinth) with soluble hemolymph components, but not with hemocytes. One of the hemolymph components, TEP1, recognizes and binds to the ookinetes, causing their death by an as yet unknown mechanism. The second step is the disposal of dead parasites by either lysis or, in the case of refractory mosquitoes, lysis and melanization. The model predicts that the processes of disposal of dead parasites (i.e. melanotic encapsulation and lysis) are controlled by genes other than *TEP1*. It is notable that TEP1 binding to and killing of parasites occurs in both R and S mosquitoes, albeit more slowly in the latter. We have observed that the two *TEP1* alleles, *TEP1s* and *TEP1r,* were specifically associated with the S and R strains, respectively. We speculate that the polymorphism of the *TEP1* locus could account, at least partially, for the more efficient killing of parasites in R mosquitoes.

Noteworthy, in TEP1-deficient mosquitoes we detected a small number of dead ookinetes that were not labeled with TEP1 suggesting that TEP1 is not the only mosquito gene that controls parasite development and that other genes and gene cascades act in concert to keep the parasite load low during infection. In keeping with this, a Leucine-Rich repeat Immune Protein 1, LRIM1, was recently shown to be implicated in the mosquito antiparasitic responses (Osta et al., 2004).

**Complement-Like Protein TEP1 Is a Determinant of Vectorial Capacity in the Malaria Vector *Anopheles gambiae***

Stephanie Blandin, **Shin-Hong Shiao**, Luis F. Moita, Chris J. Janse, Andrew P. Waters, Fotis C. Kafatos and Elena A. Levashina

**Cell, 2004, Vol. 116, Pages 661–670**

# CHAPTER 3

## Ultrastructural study of the sporogonic development of *Plasmodium berghei* in *Anopheles gambiae*

# INTRODUCTION

The ultrastructure of the sporogonic stages of *Plasmodium* parasites in its vector mosquitoes has been extensively studied (see below). However, the description of the parasite-mosquito interactions remains global and, hence, quite schematic, especially when the development of the precise parasite species within the precise mosquito host is sought. Previous ultrastructural studies based on different parasite-mosquito combinations have finely described ultrastructural details of organization of asexual and sexual parasite stages, pointing out the structural conservation between all invasive or all sporogonic forms throughout the parasite life cycle (reviewed by Aikawa, 1971).

The ultrastructure of *P. berghei* ookinete during its development in *A. stephensi* was studied Sinden and Canning (Sinden and Canning, 1972; Canning and Sinden, 1973). The authors paid special attention to the resorption of the apical complex organelles and some pellicular components in the oocyst cytoplasm during the ookinete/oocyst transformation. They suggested that differentiation begins immediately as the ookinete reaches the basal lamina. The fine structure of the sporogonic development of *P. falciparum* in *A. gambiae* has also been carefully described and suggests that there are greater structural similarities between *P. falciparum* and the avian malaria parasites than between *P. falciparum* and those species infecting rodents (Sinden et al., 1978). Subsequently, the interaction of *P. falciparum* ookinetes with the midgut epithelium of *A. stephensi* was reported, and the observations suggested that the ookinetes take an intercellular route when traversing the epithelial monolayer (Meis et al., 1987; Meis et al., 1989).

In addition, the ookinetes of *P. cynomolgi* were found melanotically encapsulated beneath the basal lamina in a refractory strain of *A. gambiae*. Completely encapsulated parasites were found as early as 16 h after the blood meal, suggesting the melanization is a rapid response (Paskewitz et al., 1988). The ookinetes of the avian malaria parasite *P. gallinaceum* were observed in both intracellular and intercellular position in the midgut of *A. aegypti*. The midgut epithelial cytoplasm around the apical end of invading ookinetes was replaced by fine granular material (Torii et al., 1992). A membranous structure was observed within this fine granular area. Most ookinetes were seen intracellularly on the luminal side and intercellularly on the hemocoel side of the midgut epithelium (Torii et al., 1992). Ultrastructural studies showed that the death of *P. gallinaeceum* ookinetes occurs while the ookinete lies free in the midgut epithelial cell cytosol, usually surrounded by an organelle-free zone that consists of a fine fibrillar material (Vernick et al., 1995). Interestingly, no vacuole was found surrounding the intracellular ookinetes in these studies.

It was proposed that the ookinetes of *P. gallinaceum* preferentially invade a special type of midgut cells in *A. aegypti*, the Ross cell. Ross cells do not stain with a basophilic dye (toluidine blue), and are less osmiophilic. In addition, these cells are highly vacuolated and express large amounts of vesicular ATPase. The enzyme is associated with the apical plasma membrane, cytoplasmic vesicles, and tubular extensions (Shahabuddin et al., 1998). However, Han et al., (2000) and Zieler et al., (2000a) could

not detect structurally distinct cell types in *A. stephensi* and *Ae. aegypti* mosquitoes before parasite invasion.

Using an *ex vivo* system, Zieler and colleagues described a gliding motion of the *P. gallinaceum* ookinete migration through the cells of the *A. aegypti* mosquito midgut (Zieler et al., 2000a). The authors found no evidence to support the existence of a morphologically distinct midgut cell type preferentially invaded by ookinetes. The invaded cells in their study appear indistinguishable from other midgut cells. Invasion of a midgut cell always occurs at its lateral apical surface and the invasion process is very rapid and is often followed by invasion of a neighboring midgut cell by the same ookinete. Brightfield microscopy observations suggested that parasite intrusion changes dramatically the morphology of the invaded cells and causes cell death (Zieler et al., 2000a).

Similar observations were reported for *P. berghei* and *A. stephensi* by Han and colleagues (Han et al., 2000). Ookinetes invaded mosquito cells that did not express high levels of vesicular ATPase. As a result of invasion, midgut cells appear damaged and protrude towards the midgut lumen. In addition, invaded cells produce high levels of nitric oxide synthase. These data indicated that the parasite inflicts extensive damage leading to the subsequent death of invaded cells. To escape from the dying cell, parasite is capable of extensive movement and invades up to 6 midgut cells. The epithelial cell damage is repaired efficiently by an actin purse-string mediated restitution mechanism, which allows the damaged epithelial cell to bud off the midgut (Han et al., 2000). An independent study demonstrated the dynamics of ookinete motility in living mosquitoes, and showed that the ookinetes use a combination of three distinct modes of motility to traverse the midgut wall: stationary rotation, translocational spiraling and straight-segment motility (Vlachou et al., 2004). During midgut invasion, the ookinetes display a highly constricted structure and could sequentially traverse several neighboring epithelial cells before reaching the basal lamina. *P. berghei* crossed midguts of both *A. stephensi* and *A. gambiae* by an intracellular route . The authors also speculated that the invaded midgut cells undergo apoptosis and are expelled from the epithelium.

It was reported that the sporozoites of *P. berghei* migrated in the salivary gland of *A. stephensi* by a gliding motility, a type of motility associated with their capacity to invade host cells. Large numbers of sporozoites are found in the cavities of secretory cells at the distal end of the salivary glands and only a few sporozoites reached the wide open salivary duct. Only the sporozoites that locate within the ducts can be ejected when mosquito salivates. The authors indicated that sporozoites need to migrate from cavities into ducts to be ejected and their progression inside ducts favors their early ejection. They suggested that the gliding motility appeared to be used not only for host cell invasion but also for locomotion *in vivo* (Frischknecht et al., 2004).

As discussed in the General Introduction, parasites suffer dramatic losses during their development in a mosquito. One proposed mechanism of host refractoriness is by prevention of certain *Plasmodium* species from crossing the peritrophic matrix (PM) in the midgut of an incompatible mosquito vector

(Tellam et al., 1999; Ghosh et al., 2000). The PM crosslinks glycoproteins and chitin microfibrils into a proteoglycan matrix that in most insects separates the food from the midgut epithelium (reviewed by Lehane 1997). The insect PM could be of two types. A type I PM is delaminated from the entire midgut epithelium and, in some cases, may only be formed in response to feeding and the type of meal ingested. A type II PM is produced by a specialized region of the anterior midgut and forms a continuous sleeve that is always present (reviewed by Lehane 1997). For example, mosquito larvae produce type I PM and adult females produce type II PM after a blood meal (reviewed by Lehane 1997). As it is positioned between the food bolus and the midgut epithelium, the PM plays key roles in the intestinal biology of the insect. The PM protects the midgut epithelium from mechanical damage and insult from pathogens (reviewed by Abraham et al., 2004). It acts as a semi-permeable membrane regulating passage of molecules between the different midgut compartments. Finally, it helps to separate the midgut lumen into different, physiologically significant compartments (Devenport et al., 2004).

Shahabuddin et al., (1995) have tested the role of PM in refractoriness of several mosquito species by studying sporogonic development of *P. gallinaceum* in susceptible and refractory mosquito species in the presence and absence of the PM. The disruption of PM was performed by a treatment of the midgut with polyoxin D, a potent inhibitor of chitin synthase. The absence of the PM did not increase the susceptibility of *A. aegypti* and *A. gambiae*, nor did it make *A. stephensi* more susceptible to *P. gallinaceum* infection. These results indicated that the PM does not restrict compatibility of *P. gallinaceum* to certain mosquito species and suggested that determinants of refractoriness come into play after the entrance of the parasite into the mosquito midgut cells (Shahabuddin et al., 1995). Even though, the question of whether the PM serves as a physical barrier to prevent the mosquito midgut from the parasite invasion remains unsolved.

Here, we followed *P. berghei* development in the *A. gambiae* midgut by transmission electron microscopy to provide more detailed characterization of the parasite development within this mosquito species. The following issues were addressed:

1. Mosquito midgut provides an environment for the digestion of blood meal and development of parasites. What ultrastructural changes are induced by a blood feeding in the mosquito midgut ?

2. Two types of peritrophic matrix (PM) have been reported in insects and one of them (type II PM) is thought to play role of a physical barrier against parasite invasion (reviewed by Lehane 1997). Would PM provide a physical barrier for *P. berghei* invasion in *A. gambiae*?

3. Recent *ex vivo* observations of live parasites indicate that ookinetes preferentially enter midgut cells through their apical lateral membranes immediately adjacent to the site of intercellular junctions (Zieler et al., 2000). How and where do parasites enter the mosquito epithelial cells *in vivo*?

4. Numerous studies using light or electron microscopy have investigated ookinete migration across

the midgut epithelium for various malaria species in diverse mosquito hosts (see above and reviewed by Baton et al., 2005). Some claimed ookinete migration is intercellular, whereas others argued that it is intracellular. How do *P. berghei* ookinetes travel through the midgut epithelium in *A. gambiae*?

5. Immune responses to the parasites in refractory strains of mosquitoes may result in the parasite mysis or melanization (reviewd by Sinden 1999). Our results suggest that the parasite are not killed by melanotic encapsulation and that the parasite killing in the *A. gambiae* midgut is mediated by the binding of the thioester-containing protein 1 to the surface of ookinetes (Blandin et al., 2004). What are TEP1-dependent mechanisms of the parasite killing?

# RESULTS

## 1. The ultrastructure of *A. gambiae* midgut epithelial cells and *P. berghei* ookinete

The mosquito midgut occupies the obvious space in the abdominal cavity. It is composed of a single layer of epithelial cells, which play a crucial role in the bloodmeal digestion and, most importantly, are the site of the parasite sporogonic development within the mosquito (Billingsley et al., 1996). Based on outward appearance, the mosquito midgut is divided into two parts, anterior (AMG) and posterior midgut (PMG) (Fig 3-1 A). The anterior midgut is a narrow tube of about 50 μm in diameter

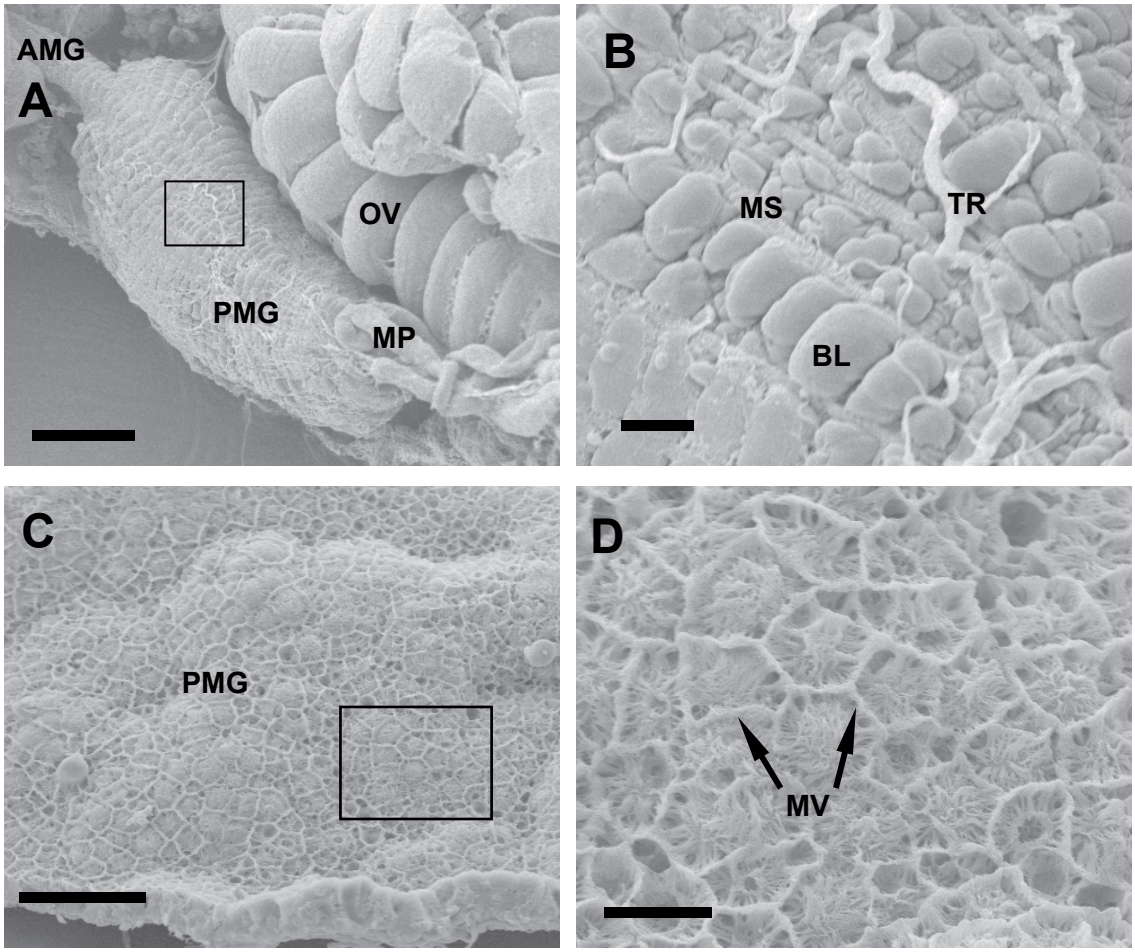


**Figure 3-1. Scanning electron micrographs showing the female *A. gambiae* midgut epithelium viewed from the basal (A, B) and the apical side (C, D).** The entire midgut contains anterior and posterior parts (AMG and PMG, respectively), with connections to Malpighian tubules (MP) at the end of the posterior part (A). The anterior midgut is a thin pipe of about 50 microns in diameter. The posterior midgut is specialized for nutrient absorption and is also the site of parasite invasion. It is normally between 100 to 200 μm in diameter before blood feeding. However, after blood ingestion it stretches up to 1 mm in diameter. The basal surface of the midgut is always tightly covered with longitudinal and transversal muscles (MS). In addition, tracheas (TR) are also seen above the muscle (B, higher magnification of the boxed region in A). The apical part of the posterior midgut is covered with microvilli (MV), which are formed by foldings of the cell membrane(C and D). Polygon-shaped midgut cells are linked to each other by junctional complexes. The microvilli seem to be more condensed at the junctional complexes (D, higher magnification of the boxed region in C). Scale bars in μm: (A), 200; (B), 20; (C), 20; (D), 10. BL: basal lamina, OV: ovaries.

and 200-300 μm in length. It is linked to the foregut by the proventriculus forming a U-shaped region (Billingsley et al., 1996). The anterior midgut does not dramatically distend in length or diameter after blood-feeding, nor does it provide a site for parasite development (Billingsley et al., 1996). The posterior midgut is a thin tube of around 700 μm in length and 100 to 200 μm in diameter before blood-feeding. The diameter of the PMG can be enlarged up to 1 mm immediately after the blood meal. The terminal end of PMG is connected to the hindgut and has links to the Malpighian tubules (MP). The MP is known to function as a filter chamber. Water is moved from the midgut lumen across the epithelium to the lumen of the MP for subsequent excretion (Billingsley et al., 1996).

Midgut epithelium is a single layer of columnar, polarized cells, contacting the basal lamina and having an apical surface exposed to the midgut lumen (Billingsley et al., 1990)(Figure 3-4). On one side, the midgut cells are bound to a basal lamina, which faces the body cavity filled with the hemolymph (Figure 3-1 B). On the other side, the apical part faces the midgut lumen (Figure 3-1 C). The two sides of the epithelium are thus referred to as basal and apical sides. The basal side is intensely covered by a network of longitudinal and transversal muscles (MS). The muscle cells are tightly attached to the basal lamina (BL) of the midgut and serve as the scaffolding of the midgut (Figure 3-1 B). The trachea (TR) and hemocytes, insect blood cells, are dispersed on the surface of the basal lamina. The apical side consists heavily of microvilli (MV). The cells are arranged closely together and appear as polygonal in surface view (Figure 3-1 C). The microvilli are abundant but not homogenously dispersed. It seems that the microvilli are more concentrated close to the junctional complexes (Figure 3-1 D).

The basolateral plasma membrane is usually highly and irregularly convoluted, forming the basal labyrinth, and this folding sometimes extends into the apical third of the cells (Figure 3-2 and 3-3 B). The basal labyrinth appears to function in ion and water transport out of the lumen, and provides spaces for exchanges of molecules (Billingsley 1990). The apical third of the basolateral plasma membrane is usually involved in adhesion to neighboring cells (Figure 3-2), and contains junctional complexes (Figure 3-3 A). A large part of the central portion of the cell is occupied by a prominent, often lobed, nucleus (Figure 3-2). The nucleolus and chromatin are often observed by electron microscopy. The other major structures in epithelial cells are usually those associated with the endoplasmic reticulum. The rough endoplasmic reticulum (RER) is often highly organized into elaborate stacks or concentric whorls. These whorls are common in the midgut of blood-sucking insects (Billingsley 1990). Additionally, lipid droplets (Figure 3-2), glycogen clusters (Figure 3-3 B) and lysosomes are abundantly dispersed in the cell cytoplasm, indicating that the midgut cell has associated roles in storage and lysosomal activity. The mitochondria are normally accumulated at the apical and basal part of the cell.

Insect midgut cells are joined to each other at their lateral borders by junctional complexes (JN) whose function is a mechanical linkage of the adjacent cell (i.e. smooth septate junctions) and intercellular communication (i.e. gap junction) (Lane et al., 1996). The most prominent intercellular associations are the apical smooth septate junctions. Beneath septate junctions, gap junctions are most commonly observed (Figure 3-3 A).

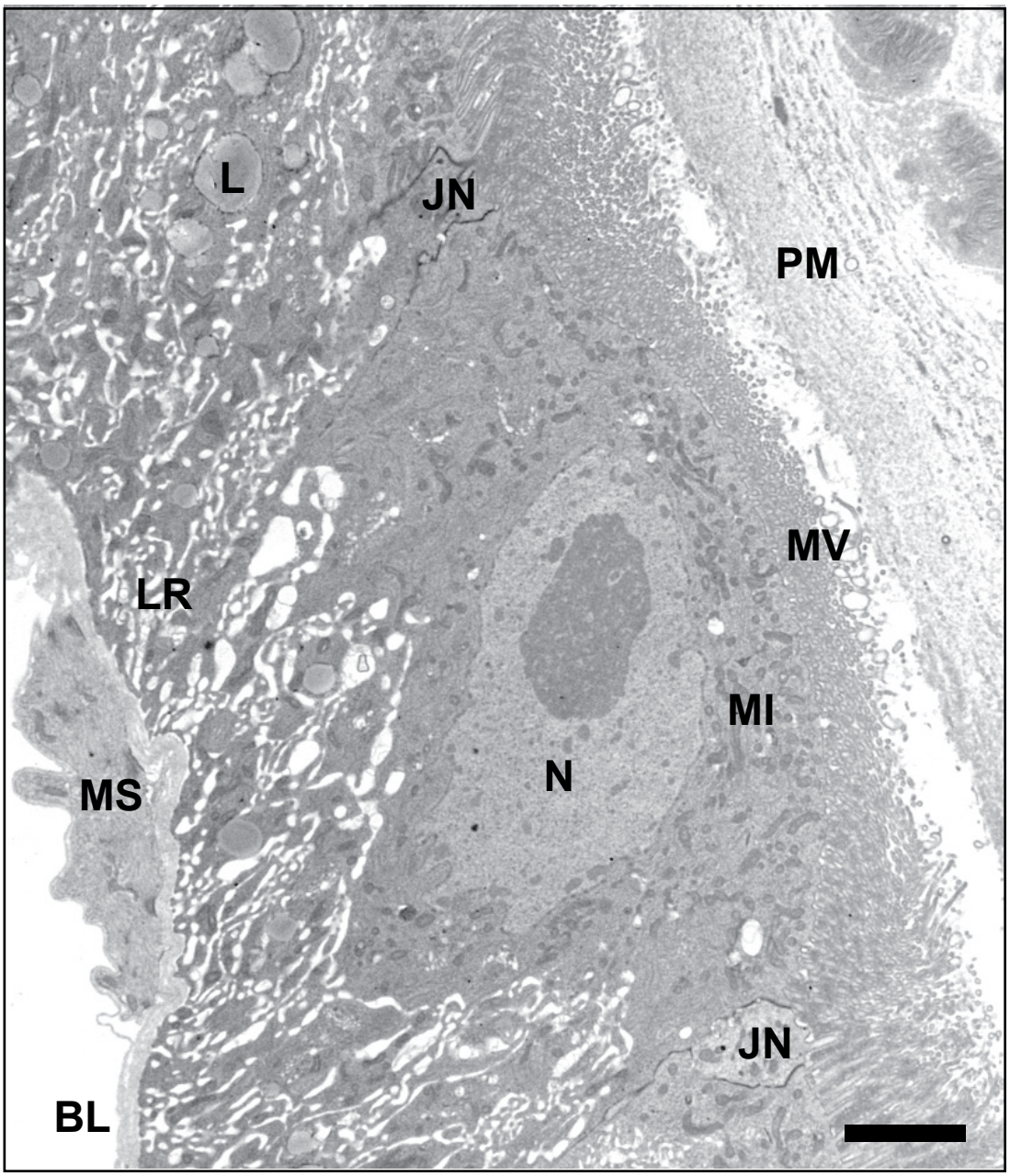


**Figure 3-2. Transmission electron micrograph representing typical *A. gambiae* epithelial cells.** A brush border of microvilli (MV) lines the lumen, and a continous peritrophic matrix (PM) is formed above the microvilli after blood-feeding. Mitochondria (MI) are concentrated in the apical part of the cells. The nucleus (N) is located centrally, and the cytoplasm is rich in rough endoplasmic reticulum. Lipid droplets (L) are widely located in the entire cell. Junctional complexes (JN) are present at the lateral borders of cells. The basolateral plasma membrane is thrown into convoluted folds to form the basal labyrinth (LR) and the whole epithelium rests on a continuous basal lamina (BL). Muscles (MS) are often tightly adhered to the basal lamina. Scale bar = 2 μm. Note: although, this section is free of parasites, it was prepared from a mosquito 33 h after *P. berghei* infection.

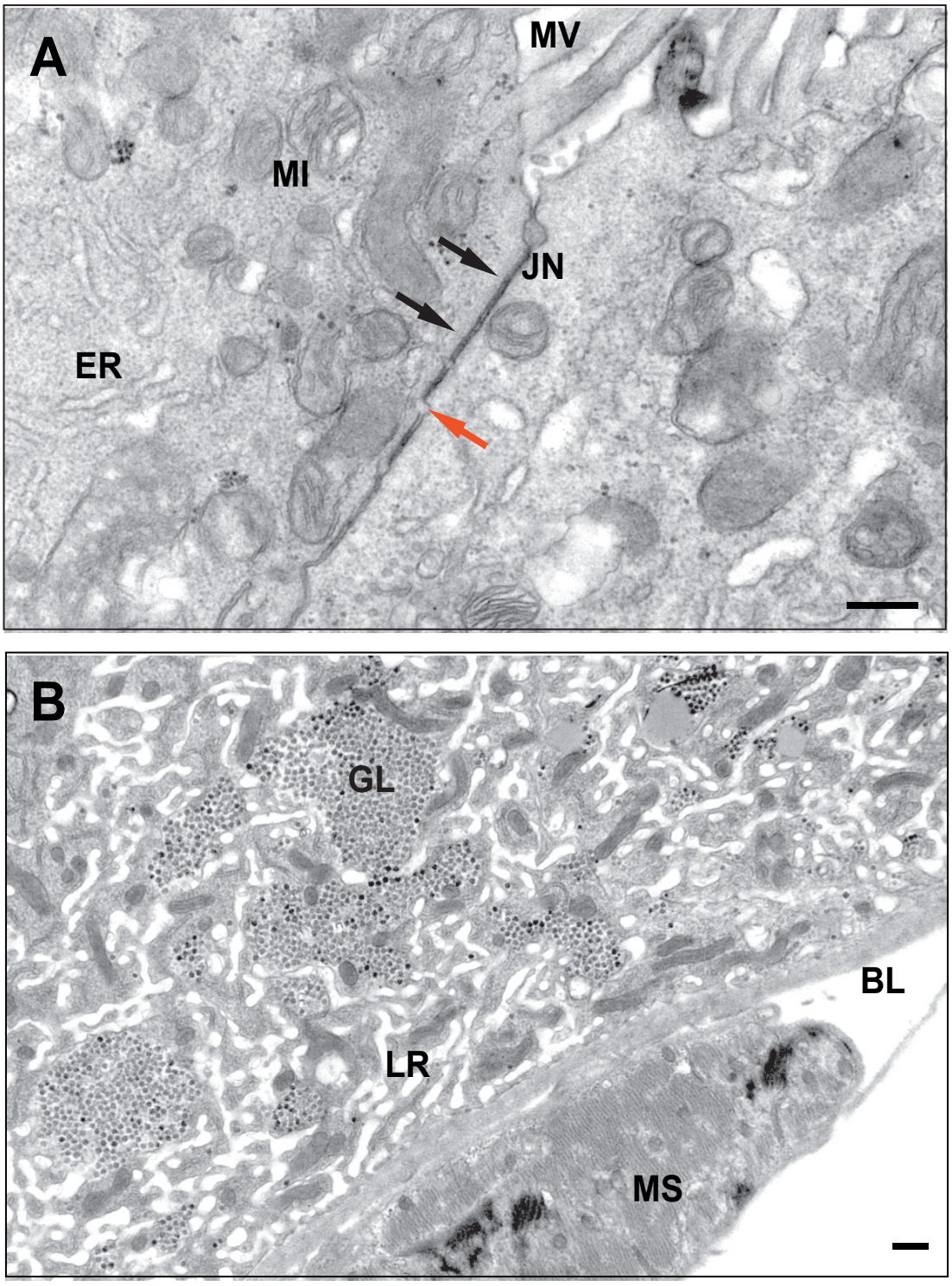


**Figure 3-3 The apical (A) and basal (B) part of epithelium.** The mosquito midgut cells are joined to each other on their lateral borders by junctional complexes (JN). The most prominent intercellular associations are the apical smooth septate junctions (black arrows), which form a circumferential belt around the luminal border of the midgut cell. Gap junctions are commonly observed beneath septate junctions (red arrow). The basal labyrinths (LR) are folds of the basolateral plasma membrane that provide extensive extracellular spaces. Glycogen clusters (GL) are often observed spread all over the epithelium. MV: microvilli, MI: mitochondria; ER: endoplasmic reticulum, BL: basal lamina, MS: muscle. Scale bars = 500 nm.

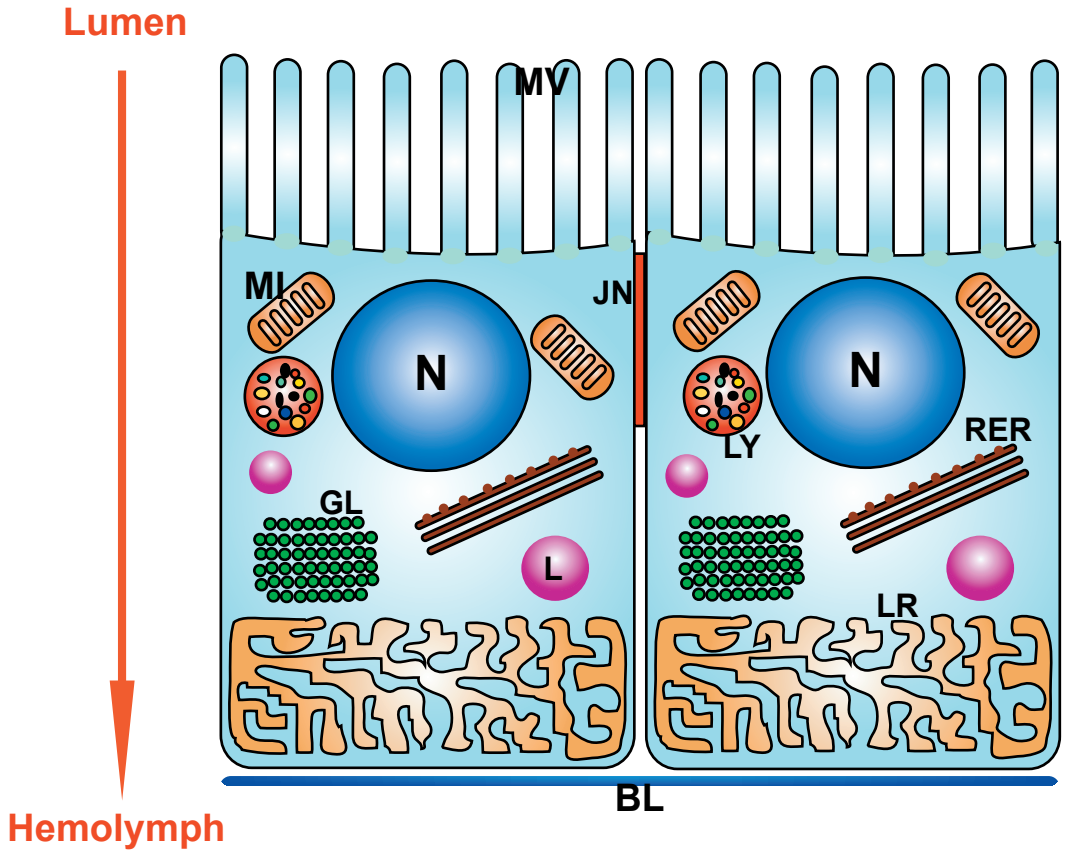


**Figure 3-4 Diagram illustrating simplified organization of the midgut cells.** The membrane at the apical part is folded into microvilli (MV), whereas the basolateral plasma mambrane forms basal labyrinth (LR). A regular basal lamina (BL) is situated at the basal end of the cell. The cells are linked by junctional complex (JN) that is situated at the apical side. Nucleus (N), mitichondria (MI), rough endoplasmic reticulum (RER) and lysosomes (LY) are always present. Lipid droplets (L) and glycogen (GL) clusters are often observed. Arrow indicates the direction of parasite migration.

The *P. berghei* ookinete has a characteristic banana shape and is 7 to 10 μm in length. The anterior end bearing the apical complex is tapered from the rest of the body and the whole body is covered by two parasite pellicle membranes (Fig 3-5). The apical complex is the most dynamic part of the ookinete, which serves as a locomotion organ to penetrate the midgut wall and migrate through the epithelium. An electron-dense collar is situated at the tip of the apical complex. This collar (C) covers the anterior projecting tapered end, and extends a short distance over the shoulder but does not extend over the entire ookinete body. A polar ring (PR) lays concentrically with the collar. Beneath the anterior part of the collar is an electron-dense lower ring (LR) which encloses an opening of similar diameter to the orifice of the collar. Microtubules extend posteriorly beneath the parasite pellicle membrane. Several electron-dense organelles lie in the anterior part of the ookinete. The rough endoplasmic reticulum (RER) that fills a large portion of the body is often highly organized into elaborate stacks. The Golgi apparatus (G) is observed. The nucleus is often located at the posterior side of the ookinete. Double membrane-bound bodies, which are mitochondria (MI), are present as irregular tubes or elongated vesicles. Hemozoin appears at the anterior end of the ookinete (Canning et al., 1973).

**2. The utlrastructure of the mosquito midgut after blood-feeding**

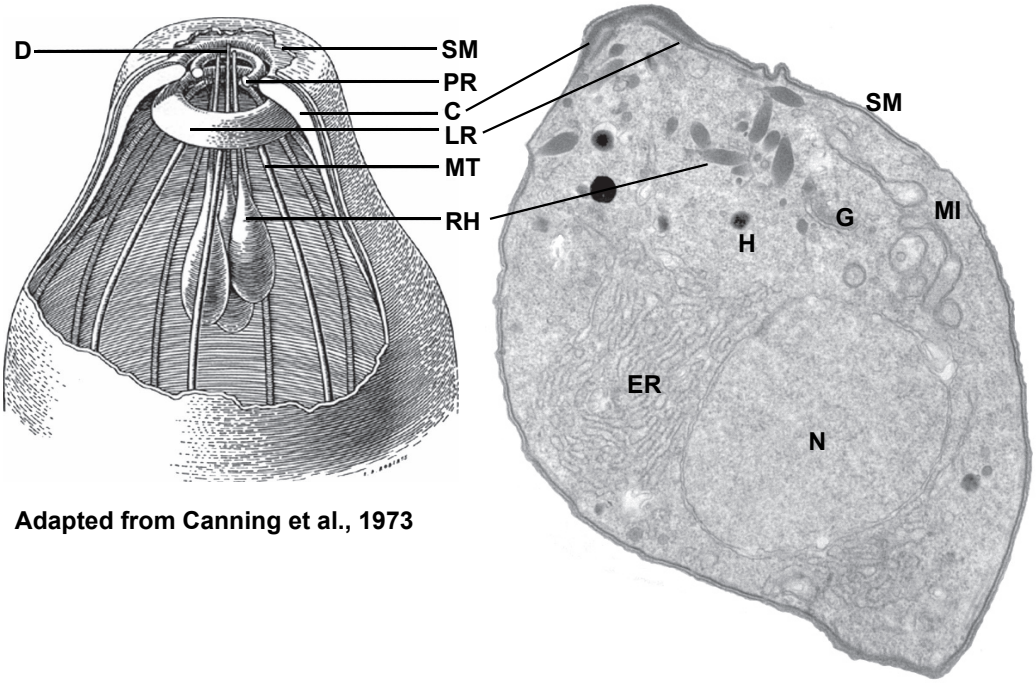


**Figure 3-5 Ultrastructure of a *Plasmodium* parasite**. C: collar, D: rhoptry duct, ER: endoplasmic reticulum, G: Golgi apparatus, H: hemozoin, LR: lower ring, MI: mitochondria, MT: microtubule, N: nucleus, PR: polar ring, RH: rhoptries, SM: parasite surface membrane.

As mentioned above, the mosquito midgut is around 100 to 200 µm in diameter before a blood meal and can be stretched up to 1 mm after blood-feeding. The thickness of the single layered epithelial cell can be stretched two-fold, from around 20 µm to as thin as 10 or even 5 µm in some parts of the fed midgut (not shown). The outward appearance of mosquito midgut, observed by light microscopy does not seem to change dramatically except for its size. Using TEM, we observed dense aggregates of secretory vesicles at the apical side of cells before the blood feeding. These aggregates were no longer visible after the blood meal (Figure 3-6). In order to digest the meal, insects must secrete enzymes from the midgut cells into the lumen. The perceived primary role of the digestive epithelial cells is indeed synthesis and secretion of digestive enzymes (Billingsley et al., 1996). Our observations indicate that the observed secretory vesicles might be involved in the blood digestion by the mosquito and release digestive enzymes near the base of the microvilli shortly after the blood meal.

Ookinete invasion of the mosquito midgut cells causes severe cell damage, induces expression of nitric oxide synthase (NOS) and leads to apoptosis of host cells (Han et al., 2000 and 2002, Kumar et al., 2004). We examined the mosquito midguts after non-infectious and infectious blood meal. The apoptotic cells are characterized by a reproducible pattern of structural alterations in the nucleus and cytoplasm (Pollard et al., 2002). These include (i) loss of microvilli and of intercellular junctions; (ii) shrinkage of the cytoplasm; (iii) changes in the organization of the cell nucleus, typically hyper-

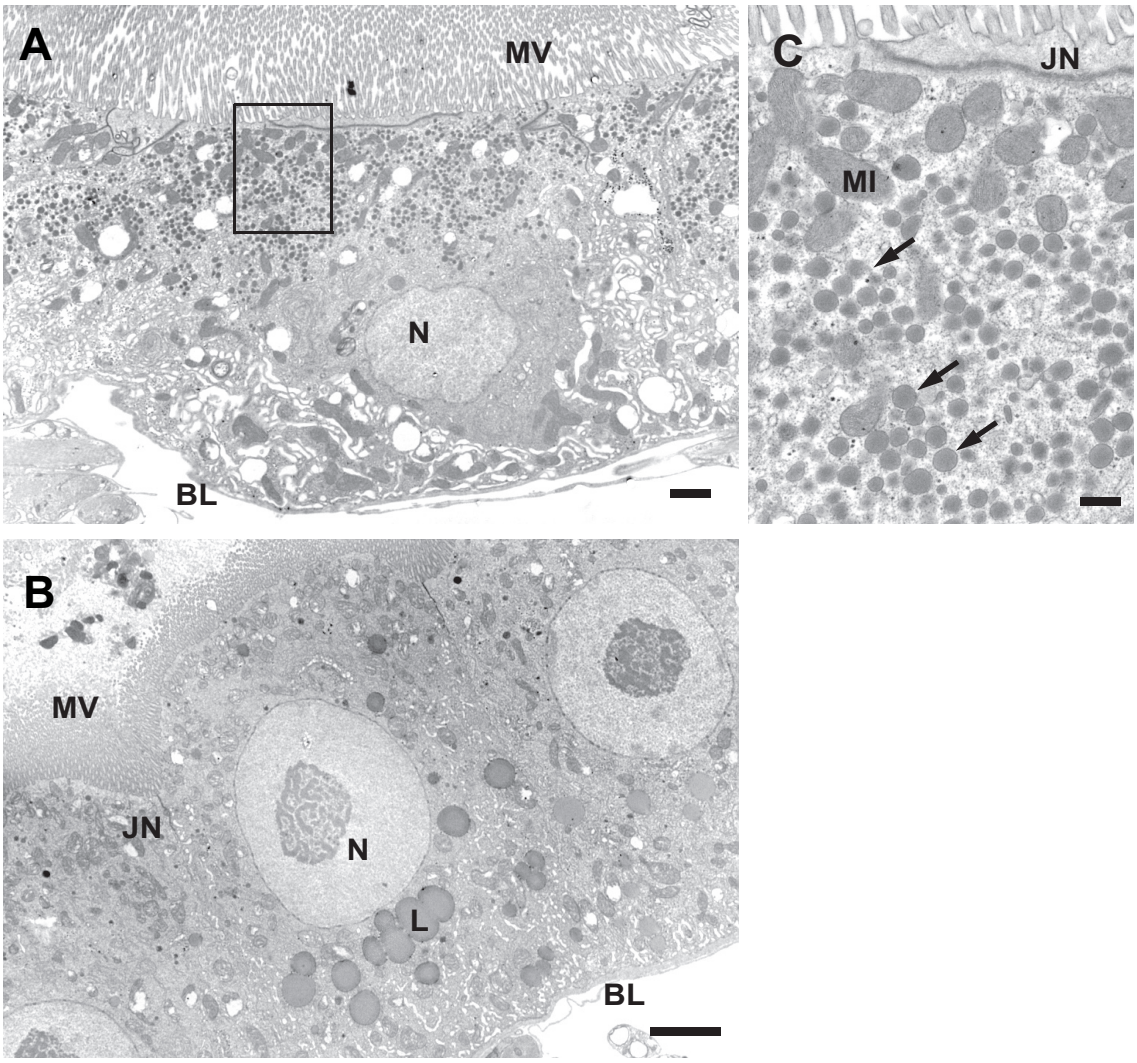


**Figure 3-6 The ultrastructural alteration after blood feeding in the mosquito midgut cell.** The epithelial cell of the naive mosquito exhibits basic cell organelles such as nucleus, mitochondria, endoplasmic reticulum (A, and close up of the boxed region in A is at C). A large amount of secretory vesicles (arrow) is accumulated at the apical part of the midgut. The secretory vesicles disappear 24 h after blood-feeding, (B). BL: basal lamina, JN: junctional complex, L: lipid, MI, mitochondria, MV: microvilli, N: nucleus. Scale bars in μm: (A), 2; (B), 2; (C), 0.5.

condensation of the chromatin; (iv) increased electron-density of the entire cytoplasm (Figure 3-7). Surprisingly, our preliminary observations of semi-thin sections reveal presence of apoptotic cells in both non-infected and infected mosquito midguts, suggesting that apoptosis might not be restricted to the ookinete invasion (Figure 3-7, insets). Careful quantification of the apoptotic cells in infected and non-infected midgut tissues is needed to clarify this issue.

In addition to columnar epithelial cells, the midgut epithelium of *A. stephensi* contains triangular cells that do not extend to the apical midgut surface (Baton et al., 2004). We also observed this type of cells in the *A. gambiae* midgut. These cells are relatively small in size compared with the mature epithelial cells, and posses a huge nucleus which occupies almost the entire electron lucent cell. The overall morphology suggests that these cells are blastocells or embryonic midgut cells (Figure 3-8). Blasto-

cells are normally located at the basal side of the midgut, and are the source of regenerative cells that participate in the rapid turnover of the epithelial cells.

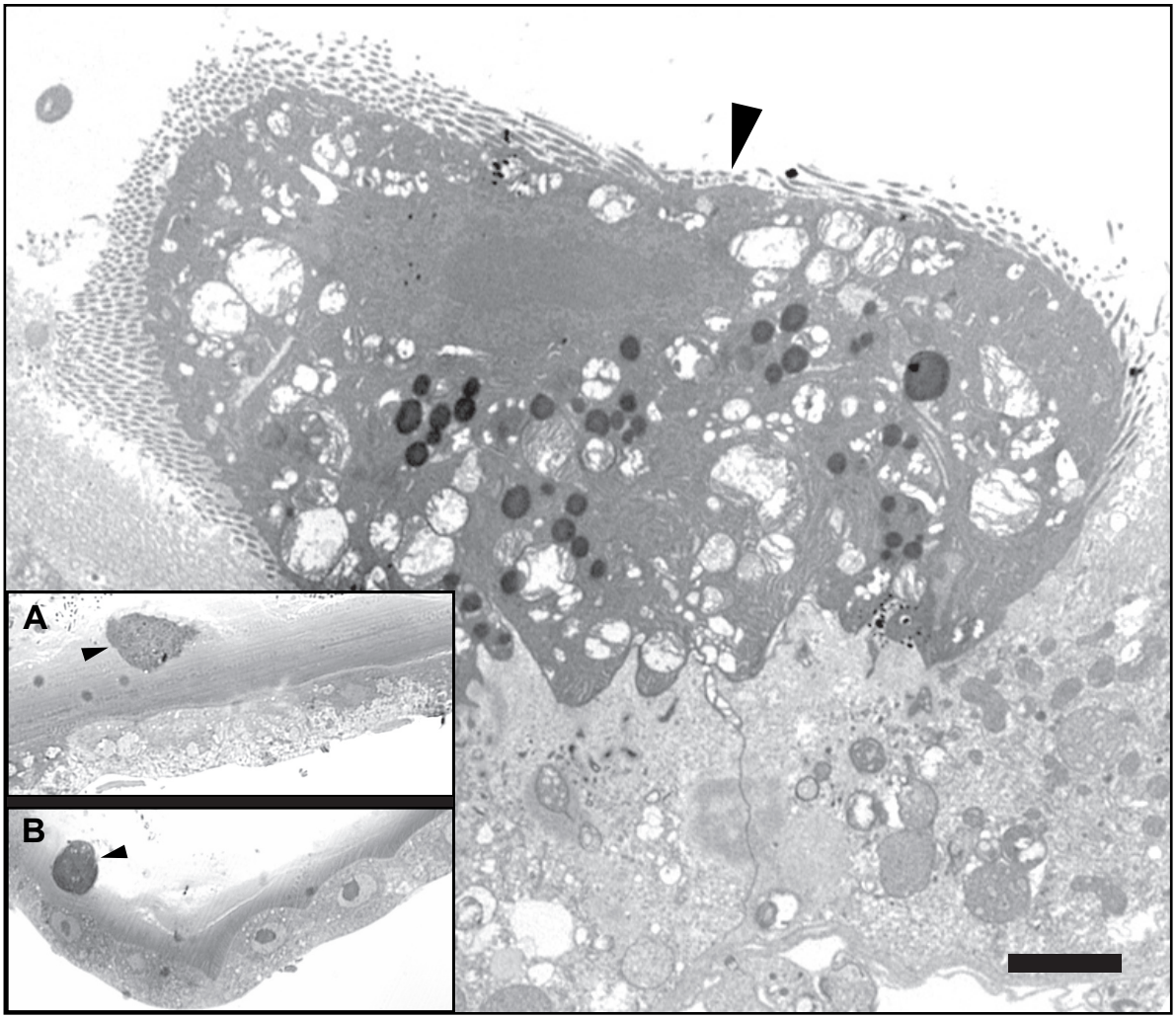


**Figure 3-7 Apoptotic epithelial cells are expelled into the lumen.** Apoptotic cells are characterized by electron dense, vacuolated cytoplasm and loss of microvilli. Insets are semi-thin sections of normal blood-fed (A) and infectious blood-fed (B) mosquito midguts. Both of them show apoptotic cells (arrow) that are protruding towards the lumen, suggesting that apoptosis appears to be a general programmed cell death mechanism in mosquito. Scale bar = 2 μm.

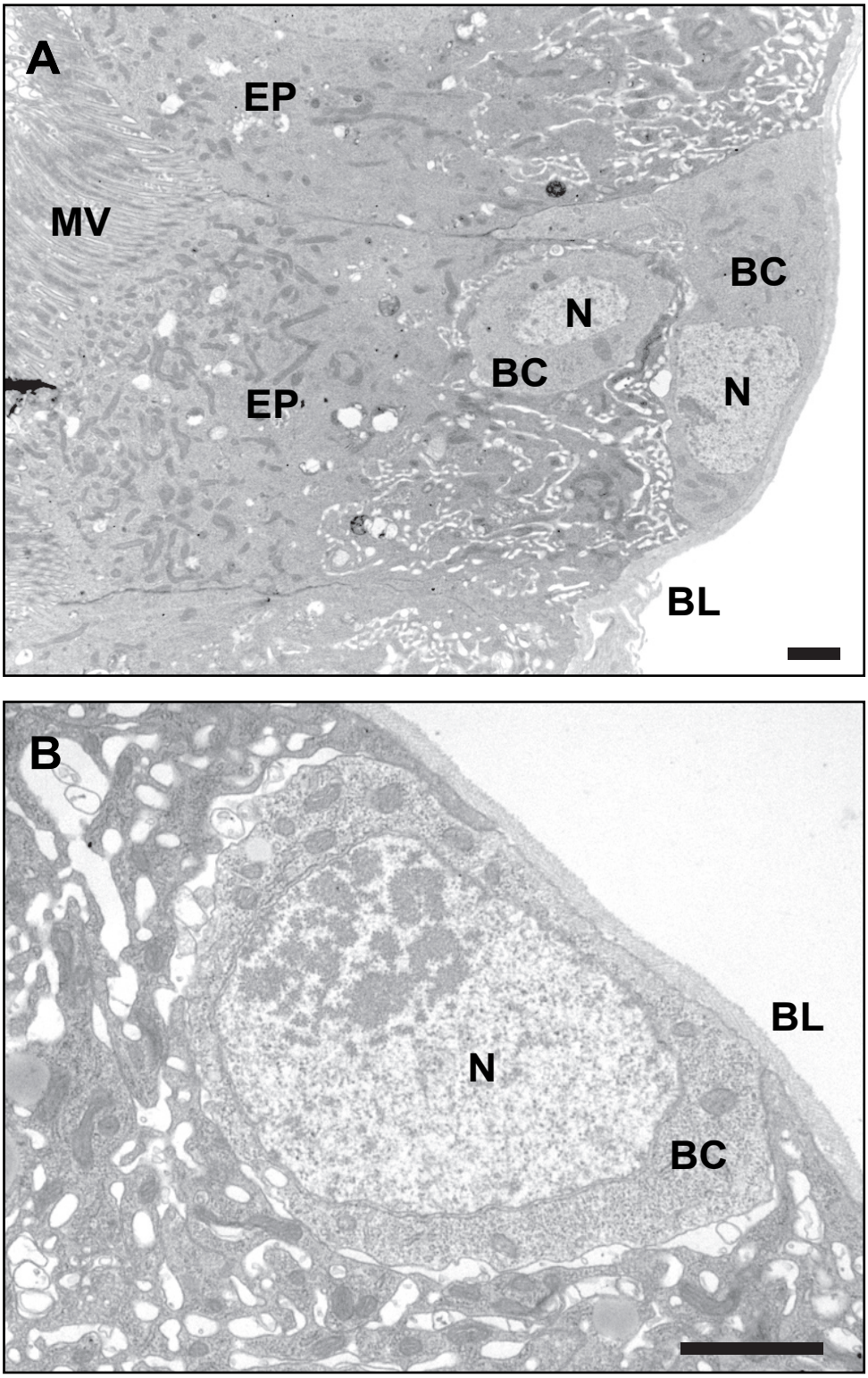


**Figure 3-8 Blastocells are often observed at the basal part of the midgut epithelium.** Blastocells are embryonic epithelial cells which will replace the apoptotic cells as a general metabolistic mechanism. Blastocells are normally located at the basal part of the epithelium, beneath the basal lamina (A) and are characterized by a relatively large nucleus and fewer cell organelles (A and B). BC: blastocells, BL: basal lamina, EP: epithelial cell, JN: junctional complex, MV: microvilli. Scale bars = 1 μm.

**3. The polymerization of the peritrophic matrix in *A. gambiae* occurs after the entry of *P. berghei* into the migdut**

It has been proposed that the PM serves as a major physical barrier against parasites in the mosquito midgut (reviewed by Lehane, 1997). The PM is a thick (1–20 μm) chitin-containing net secreted by the midgut epithelium, which is polymerized by the ingested blood meal (Tellam et al., 1999; Shao et al., 2001). The PM is thought to be a physical barrier because it is thick and surrounds the entire blood bolus (Figure 3-9). Indeed, some bacteria clusters, which we observed in the blood bolus 33 h after blood meal, were securely separated from the epithelium by the PM and stayed in the lumen (Figure 3-9 A and B).

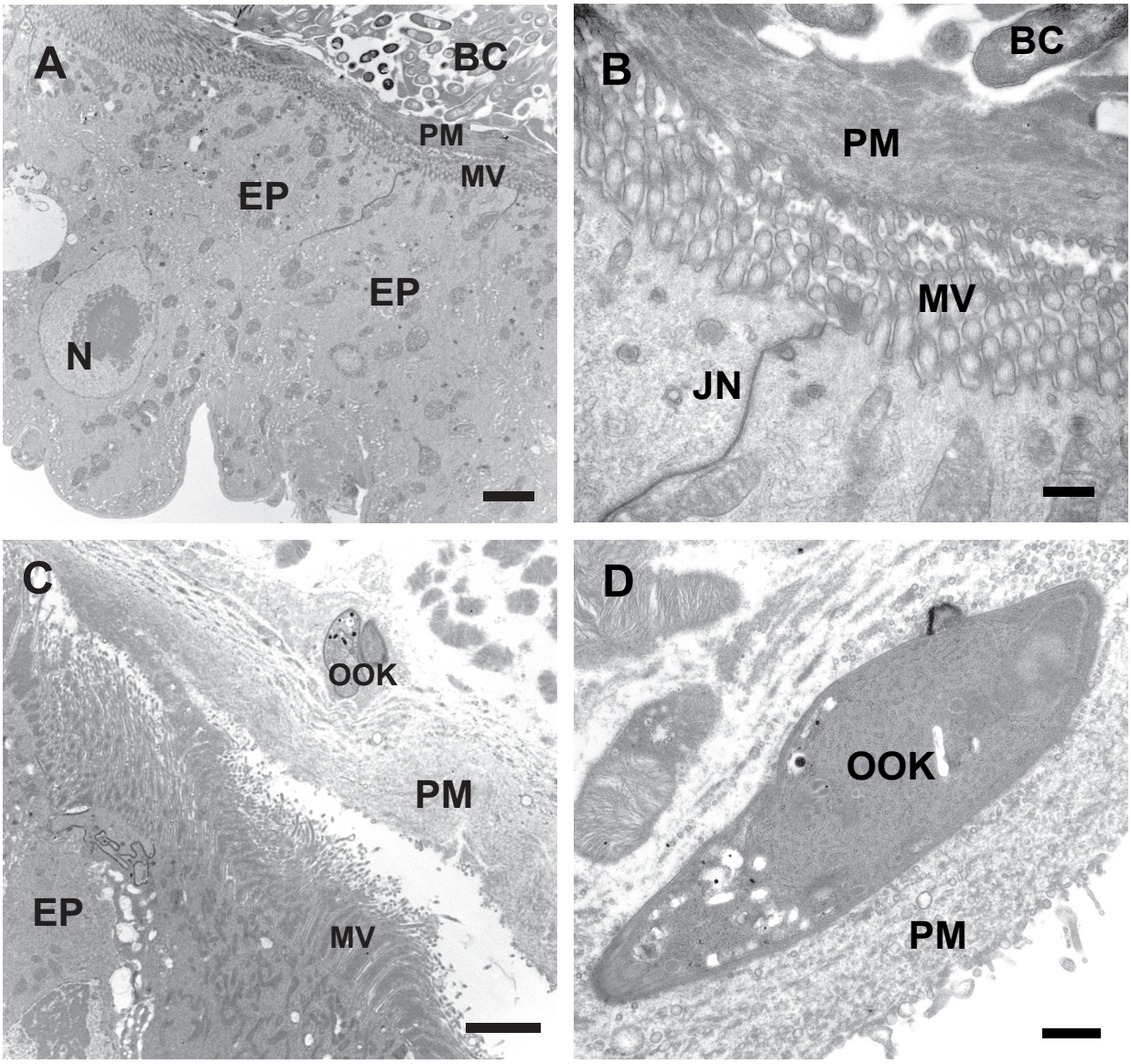


**Figure 3-9. The peritrophic matrix (PM) is a thick chitin-containing layer synthesized after the ingestion of blood meal by the midgut epithelium.** (A). The PM is thought to be a physical barrier to pathogens, such as bacteria and parasites (B, enlarged from the boxed region of A). The complete polymerization of PM is observed at 28 h after blood feeding. However, the majority of the parasites are already detected at the basal side of the midgut at 24 h post infection. Some delayed ookinetes are observed in the PM (C and D). BC: bacteria, EP: epithelial cell, MV: microvilli, JN: junctional complex, OOK: ookinete, N: nucleus. The mosquitoes were dissected and fixed at 28 h post infection. Scale bars in μm: (A), 2; (B), 0.5; (C), 2; (D), 0.5.

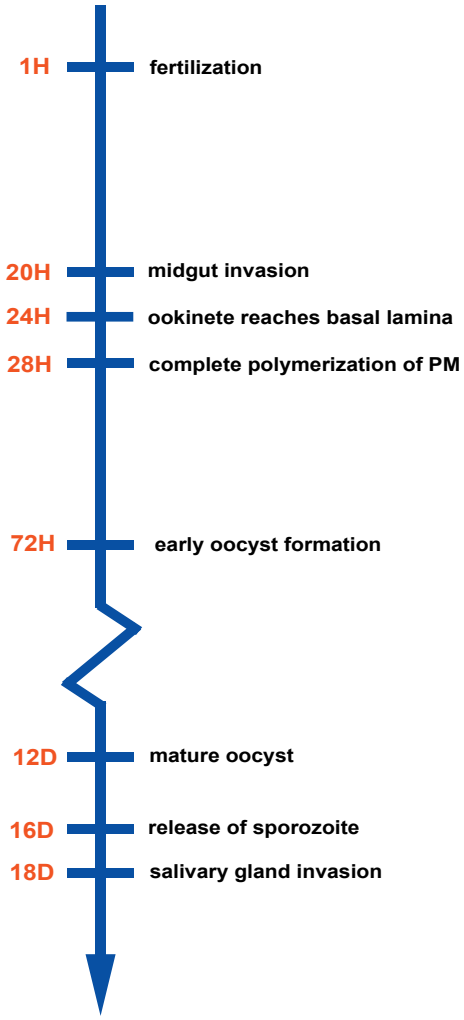


**Figure 3-10. Time line of *P. berghei* development in the *A. gambiae* midgut at 20˚C.** Blue arrow inducates time post infection. H: hour, D: day, PM: peritrophic matrix.

We could never detect polymerization of PM before 24 h post infection. We and others observed that the majority of *P. berghei* ookinetes (85%) completed the invasion of the *A. stephensi* midgut epithelium by 22 h after infection (Shiao et al, unpublished data, Kadota et al., 2004). These observations suggest that by the time that the PM is completely polymerized, the majority of the ookinetes have already entered the midgut. Only a few delayed ookinetes that migrate from the lumen to the midgut at 28 h post infection are sequestered by the PM (Figure 3-9 C and D). Our observations indicate that in *A. gambiae,* the complete polymerization of the PM happens later than the invasion of the majority of the parasites. We conclude that while the PM may play a role as a barrier to protect the midgut from bacteria, it does not play a major role in the prevention of parasite invasion in *A. gambiae*. A summary of the time scale of the sporogonic development of *P. berghei* observed in *A. gambiae* is presented in Figure 3-10.

**4. The mechanism of parasite entry into the midgut cell**

The exact place where *Plasmodium* parasites enter the mosquito midgut cells has been controversial for a long time. As described in the introduction, several studies performed by light microscopy or electron microscopy have investigated this phenomenon. However, bias from small sample sizes characteristic of previous electron microscopy studies (typically fewer than 20 parasites were observed) has probably given rise to the conflicting results. Current theory suggests that parasites enter the midgut cell at the place where three epithelial cells converge (Zieler et al., 2000). We initiated systematic fine structural studies to clarify this question. 124 ookinetes were followed within 21 individual susceptible mosquitoes at different time points (21, 22, 23, 24, 28, 32, 44 and 48 h) after infection. To our disappointment, we were unable to catch ookinetes at the early stages of entry. The ookinetes were found either in the lumen (Figure 3-11) or already inside the midgut cells. Before invasion, mature ookinetes pass through a homogenous electron-dense region between midgut and the blood bolus. This region might be composed of digestive enzymes that are secreted by the midgut or/and by the nutrients extracted from the blood meal. The ookinetes first attach to the actin-based microvilli and a network of branching fibers called the microvilli-associated network as reported previuosly (Zieler et al., 2000b), and then appear to migrate towards the midgut intercellular junctions (Figure 3-11).

Similar results were obtained in a recent study of the membrane-attack ookinete protein (MAOP) that is involved in the parasite invasion (Kadota et al., 2004). In this report, 80 ookinetes were observed by transmission electron microscopy at 22 h after the blood meal. However, the authors failed to detect ookinetes in the process of penetration of the apical membrane of the midgut. The intimate contact between the midgut cells and the parasites is described only for MAOP-disrupted ookinetes (Kadota et al., 2004). Disruptant ookinetes migrate to the midgut epithelium and attach to the cell surface at the apical tip (in a process resembling that of the ookinete attachment to the mosquito cells in the co-culture system, see Chapter 1), but were unable to enter the cytoplasm by rupturing the cell membrane. Interestingly, a related protein was previously shown to be necessary for the invasion of the liver sinusoidal cells, suggesting that malaria parasites use conserved mechanisms for membrane rupture in different host invasive stages (Kadota et al., 2004). Taken together, these results prompt us to speculate that the penetration course of ookinetes into the mosquito epithelium is an obviously rapid and elusive process for such a tool as transmission electron microscopy.

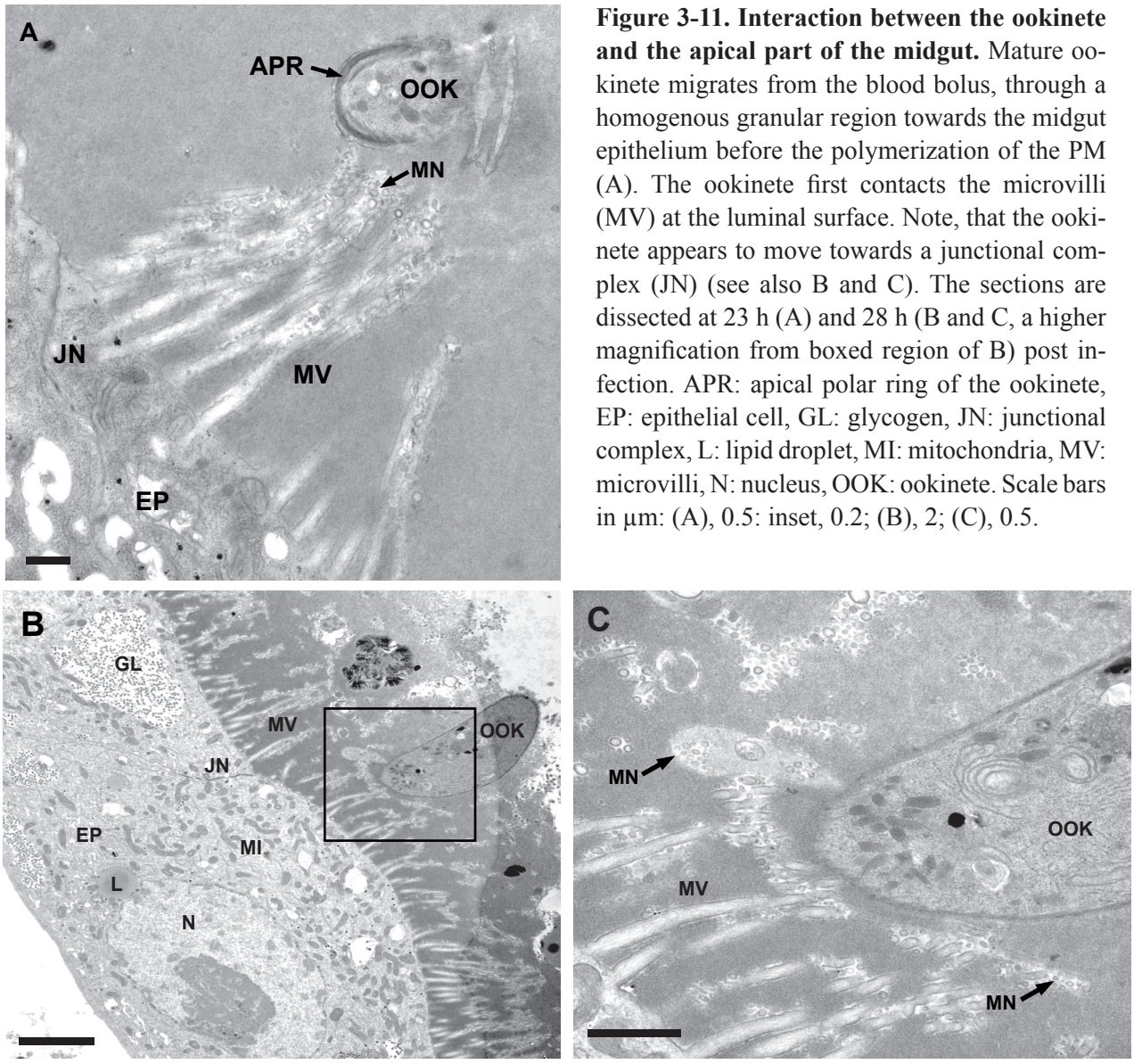


**Figure 3-11. Interaction between the ookinete and the apical part of the midgut.** Mature ookinete migrates from the blood bolus, through a homogenous granular region towards the midgut epithelium before the polymerization of the PM (A). The ookinete first contacts the microvilli (MV) at the luminal surface. Note, that the ookinete appears to move towards a junctional complex (JN) (see also B and C). The sections are dissected at 23 h (A) and 28 h (B and C, a higher magnification from boxed region of B) post infection. APR: apical polar ring of the ookinete, EP: epithelial cell, GL: glycogen, JN: junctional complex, L: lipid droplet, MI: mitochondria, MV: microvilli, N: nucleus, OOK: ookinete. Scale bars in µm: (A), 0.5: inset, 0.2; (B), 2; (C), 0.5.

**5. *P. berghei* ookinetes preferably take an extracellular route to cross the *A. gambiae* midgut cells**

The route taken by malaria ookinetes to cross the midgut epithelium of the mosquito vector has been (and continues to be) controversial. Various models of invasion by the ookinete have been proposed, based on a range of observation methods and mosquito-parasite combinations (described in the Introduction). To date, general consensus postulates that the route of ookinete migration depends on the parasite-vector combination.

Extracellular parasites are characterized by the presence of the epithelial cell membrane situated on the exterior of the parasite pellicle membrane (Figure 3-12), thus separating the ookinete from the midgut cell. Ookinetes situated in the space between epithelial cells appear to migrate through the intercellular space from the apical to the basal side of the midgut (Figure 3-12 A and B). Once the ookinetes reach the basal labyrinth with the apical complex end pointing toward the basal lamina, they remain in the extracellular space and develop into oocysts (Figure 3-12 C). In our study, within a total of 124 ookinetes observed from 21 different mosquito midguts dissected and fixed between 21 to 48 hours after infection, the majority (n = 113) were observed to be separated from the cytoplasm of the midgut cell by a membrane.

Only in a few cases (11 of total 124 parasites), the ookinetes appeared to be intracellular. Intracellular parasites are characterized by the absence of the epithelial membrane covering the parasite surface (Figure 13-3), indicating that the ookinetes are in direct contact with the cytoplasm of epithelial cells. However, absence of the cellular membrane may also result from an artefact during sample preparation. Interestingly, the intracellular ookinetes were mostly located near the apical side of the midgut, just beneath the microvilli and close to the junctional complex. These observations suggest that intracellular parasites might represent ookinetes at the early stages of penetration of the midgut epithelium, visualized by the close proximity to the apical junctional complex and, possibly, to the entry site itself. However, the small sample size of the intracellular parasites limits further conclusions and more observations will be needed to investigate this possibility.

Based on our study, we propose that the *P. berghei* ookinetes preferably take an extracellular route to cross the *A. gambiae* midgut.

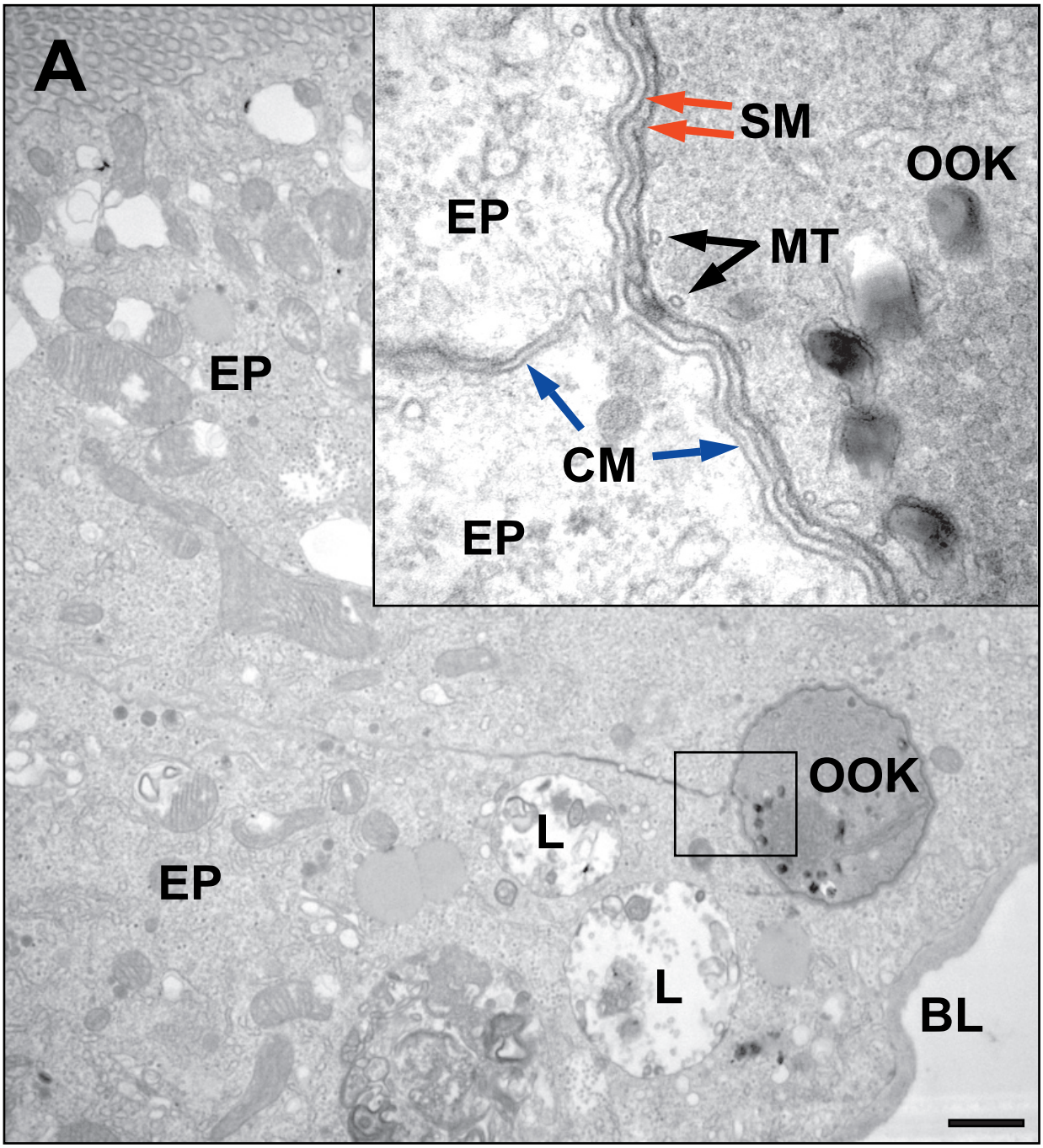


**Figure 3-12. *P. berghei* ookinetes preferably take an extracellular route to migrate through the *A. gambiae* midgut epithelium.** Transmission electron micrographs (A, B and C) show intercellular localization of the parasites between two neighboring cells separated by lateral cellular membranes (CM). The parasite double membranes are indicated by red arrows, and cell membranes are indicated by blue arrows (insets are higher magnifications of the boxed regions). When the parasite reaches the basal lamina, it always stays extracellularly in the basal labyrinth (C, and inset). EP: epithelial cell, SM: parasite surface membrane, OOK: ookinete, BL: basal lamina, L: lysosome, LR: basal labyrinth, MT: microtubule. Scale bars = 2 μm.

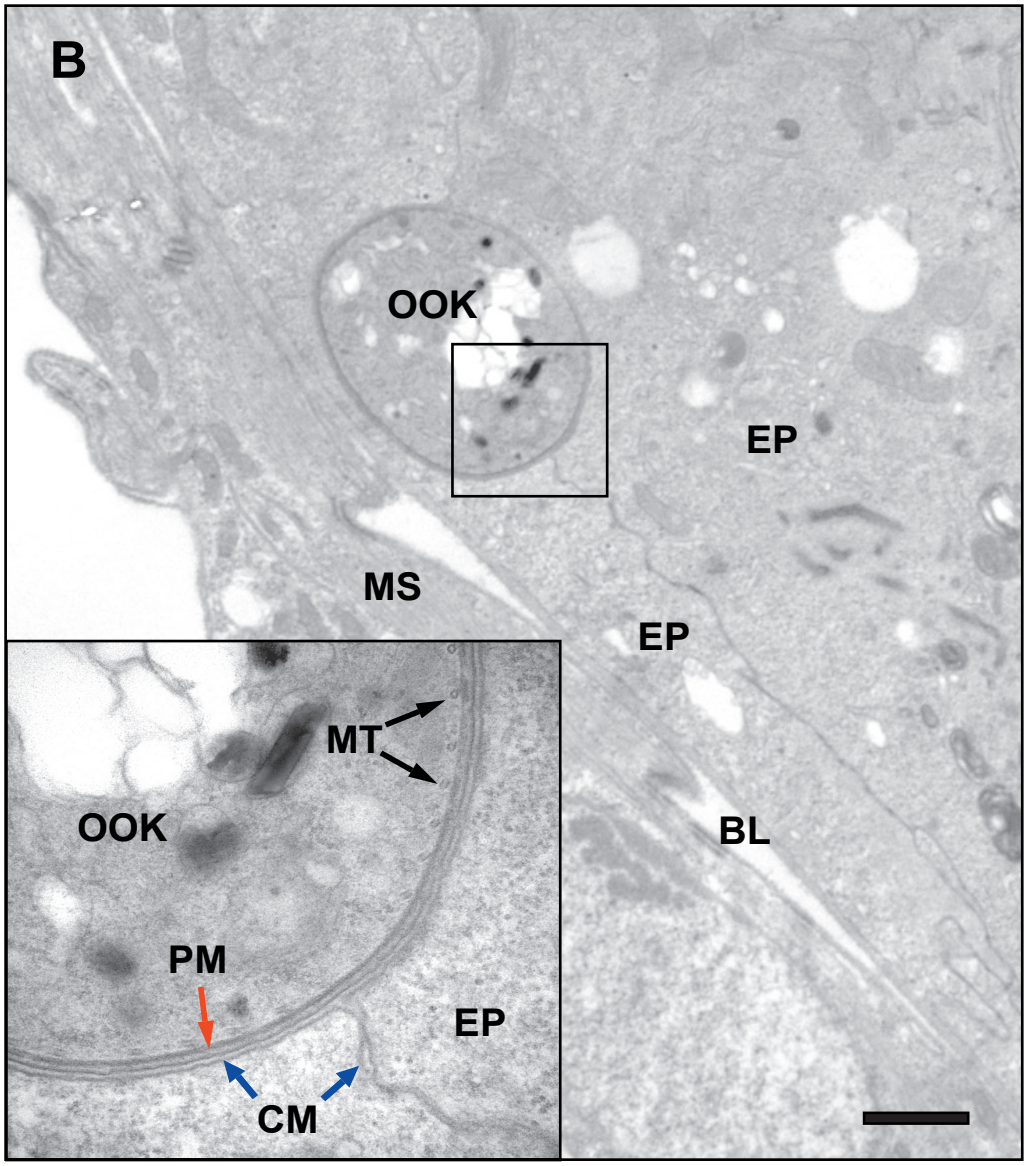


**Figure 3-12 B**. Legend as above.

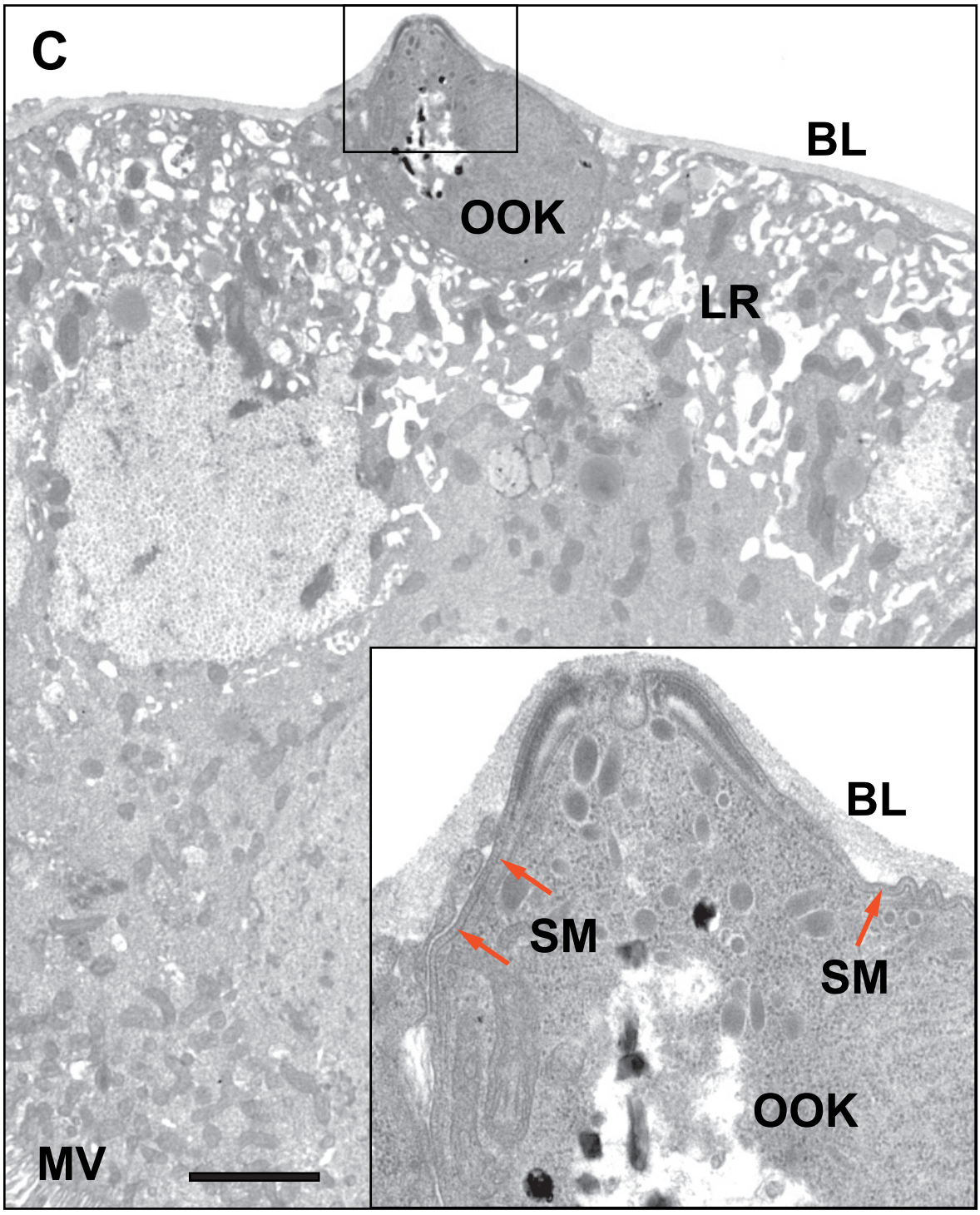


**Figure 3-12 C**. Legend as above.

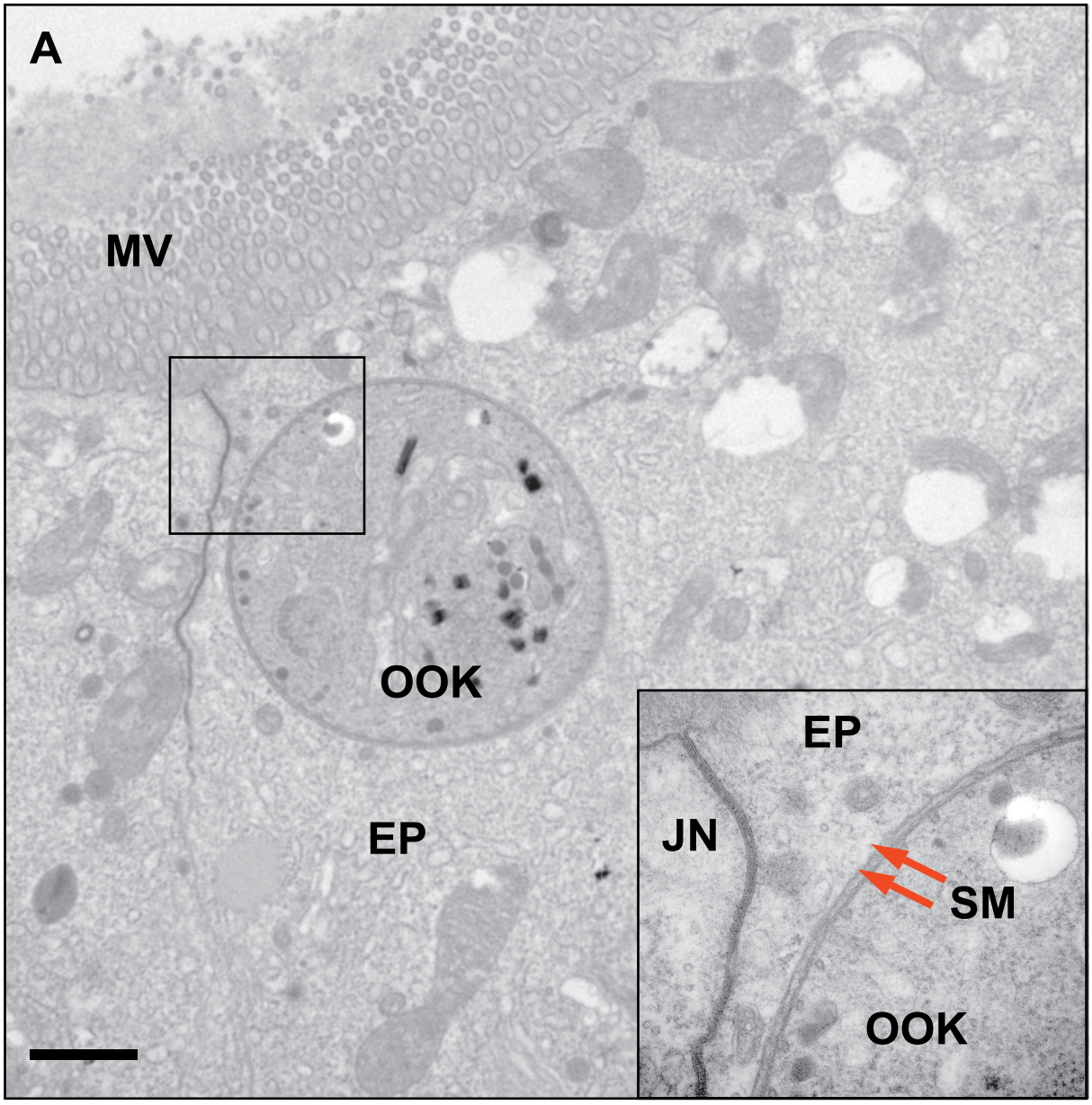


**Figure 3-13. Rare case of the intracellular ookinete localization (A and B).** The ookinete is considered to be intracellular if no cellular membranes that separate the parasite from the epithelium could be detected. In our experiments, all the intracellular ookinetes observed were located close to the apical part of the midgut. Insets are higher magnification view from boxed region. EP: epithelial cell, JN: junctional complex, MV: microvilli, SM: parasite surface membrane, OOK; ookinete. The samples are taken at 24 h post infection. Scale bar = 2 µm.

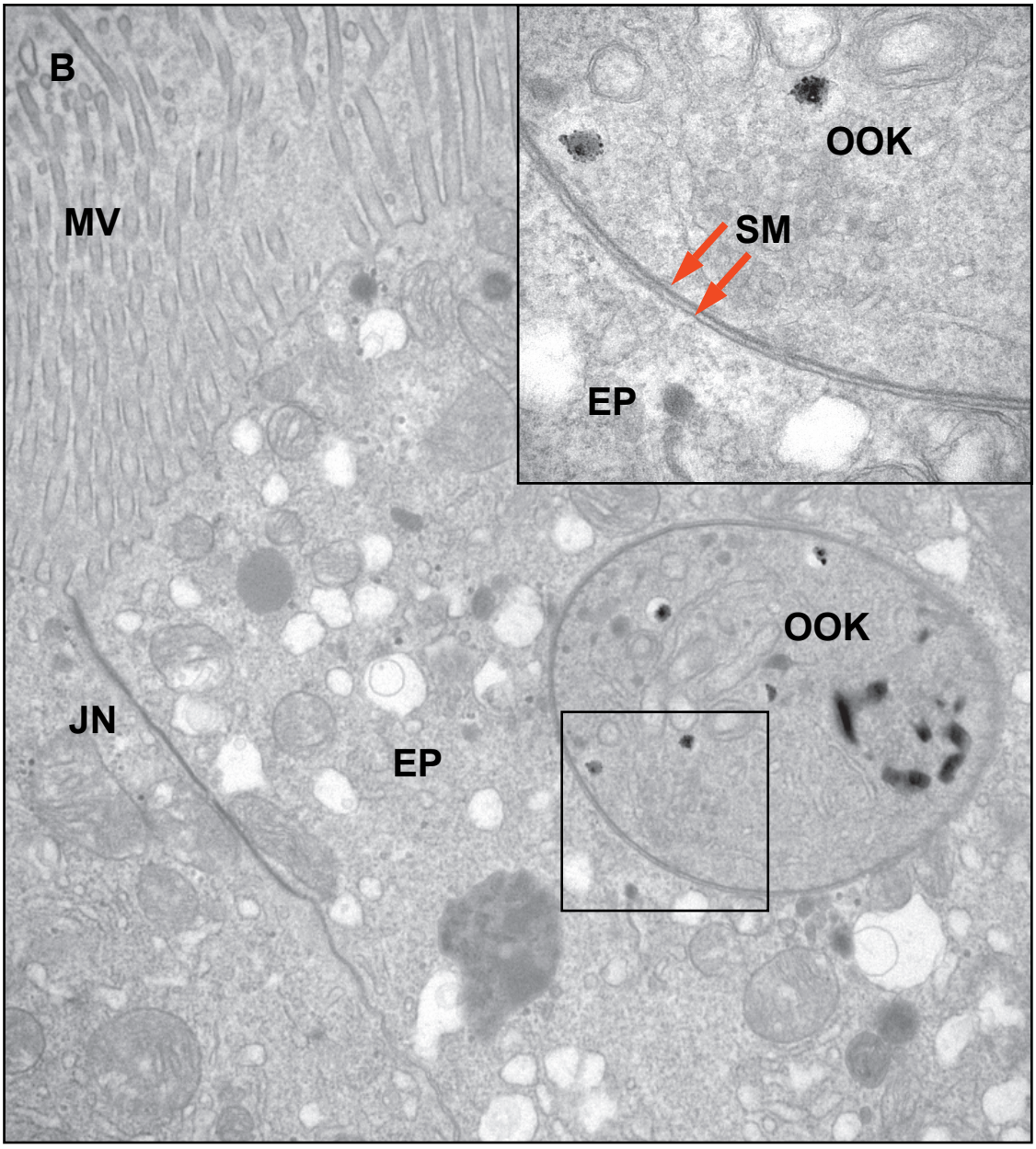


**Figure 3-13 B**. Legend as above.

### 6. *P. berghei* ookinetes are killed by a lytic mechanism in *A. gambiae*

We proposed that ookinete lysis in the basal labyrinth is one of the mechanisms that account for major parasite losses, and that it represents a general mechanism of parasite destruction (Blandin et al., 2004). Indeed using TEM, we observed ookinetes that were lysed in the mosquito midgut (Figure 3-14). The lysed ookinetes were situated extracellularly in the midgut and were characterized by the complete disorganisation of the entire body and nucleus or by vacuolisation of the entire ookinete. The pellicle membrane of the lysed ookinete was normally intact thus preserving the banana-like shape of the parasite. However, molecular mechanisms that trigger the lytic destruction are still unknown.

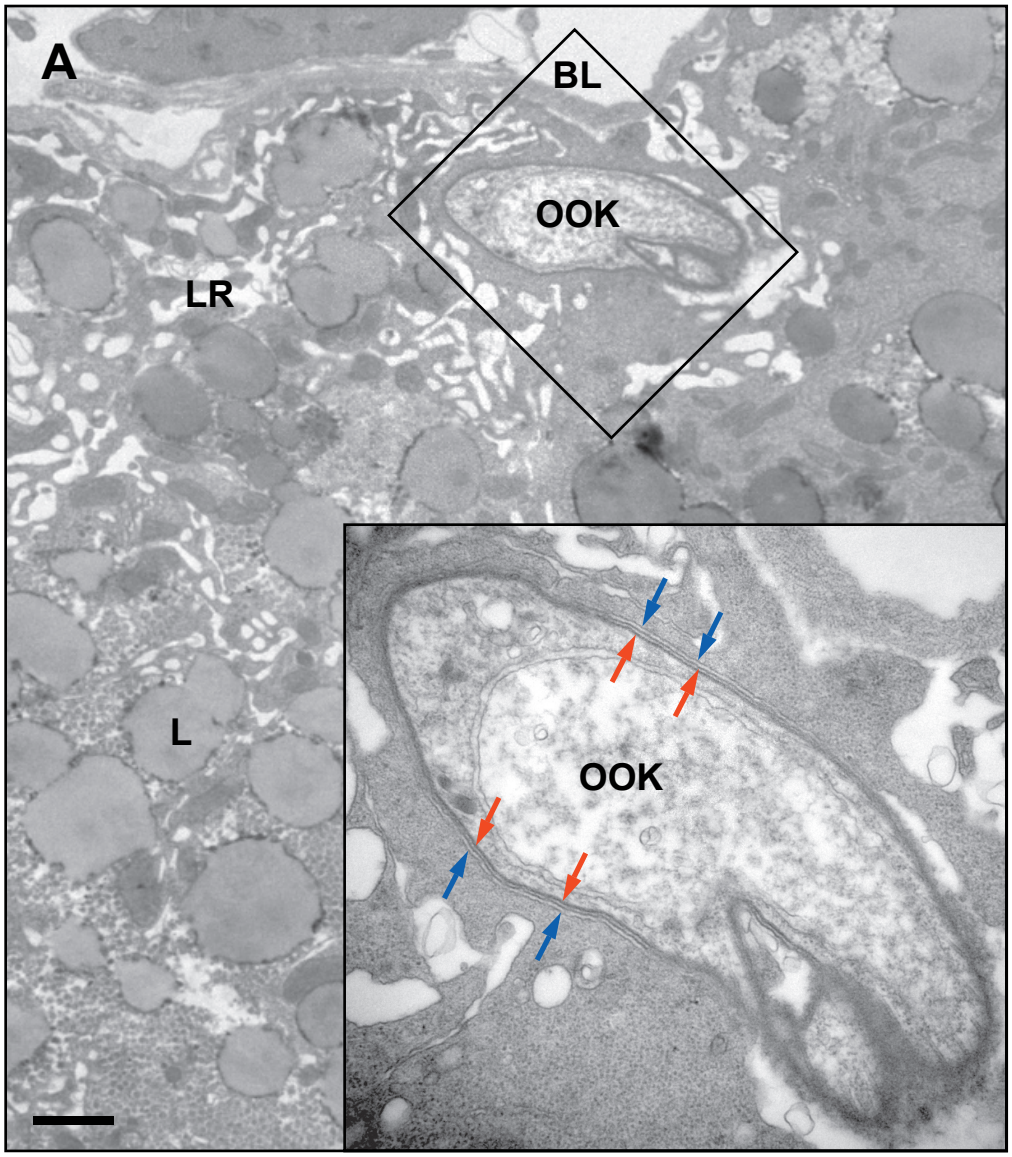


**Figure 3-14 A and B. Ookinete lysis in susceptible and refractory mosquitoes.** Lysed ookinete in the basal labyrinth (A, front page, and B). Note the parasite surface membrane (red arrows) is still intact even though the organelles of ookinete appear lysed. The ookinete is separated from the mosquito epithelium by a cellular membrane (blue arrows). The samples were taken at 33 h post infection in R mosquito (A) and S mosquito (B). BL: basal lamina, OOK: ookinete, MV: microvilli. Insets are higher magifications of boxed region. Scale bars = 1 μm.

**Figure 3-14 A**. Legend as above.

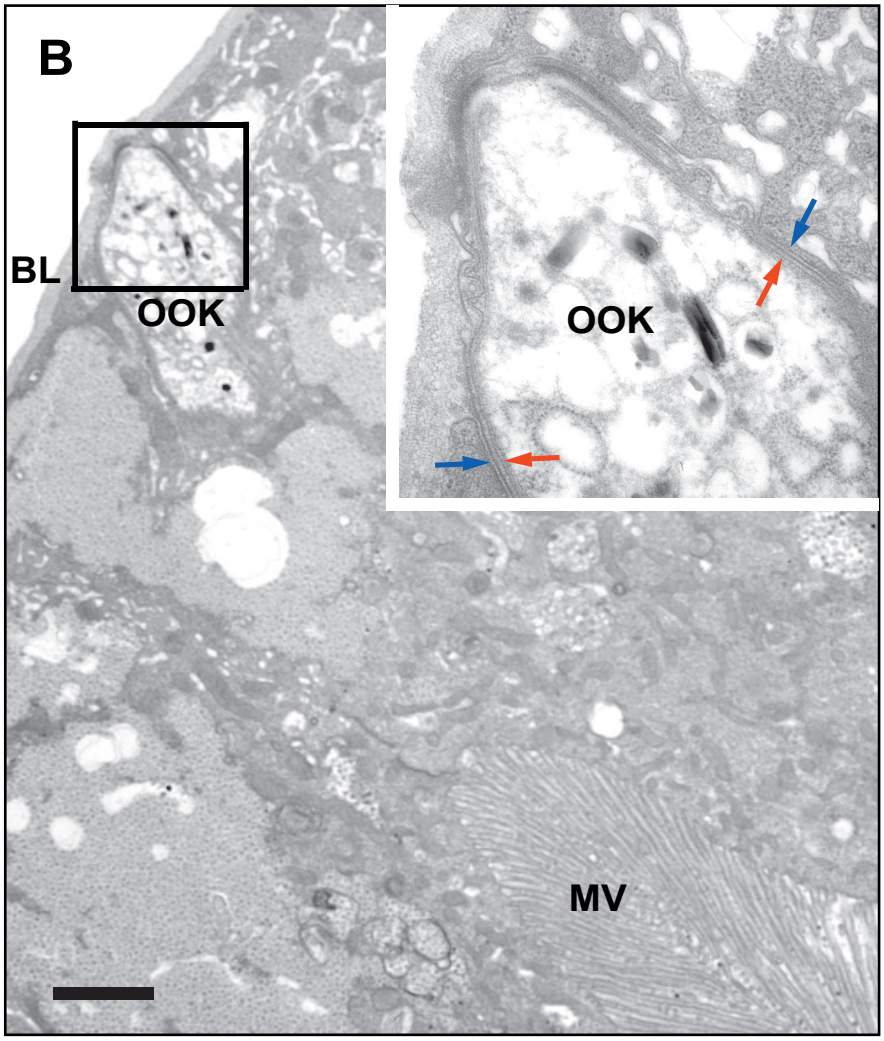


## 7. Sporogonic development of *P. berghei* in the *A. gambiae* midgut

After ookinetes reach the extracellular space of the basal labyrinth beneath the basal lamina, they round up and transform into oocysts. The oocyst capsule is in contact with the basal lamina of the mosquito epithelium. The epithelial basal lamina can be distinguished from the relatively electron-dense oocyst capsule (Figure 3-16). Both the epithelial basal lamina and the early oocyst capsule are composed of finely granular material. The oocyst capsule is a hollow sphere of approximately 1 μm thickness that is directly attached to the oocyst. In sections of oocyst cytoplasm, ribosomes are present in great numbers, usually randomly dispersed. Rod-shaped mitochondria are also randomly dispersed throughout the oocyst cytoplasm. In the oocyst, the nucleus goes through several rounds of division and the newly formed nuclei are randomly dispersed (Canning et al., 1973). The nucleus shape is roughly oval or that of an irregular polygon. A definite nuclear envelope is present, composed of two dense membranes (Figure 3-15).

Sporoblast segregation begins with the appearance of vacuoles located just beneath the oocyst capsule (Figure 3-15). The vacuoles coalesce and eventually form large clefts subdividing the oocyst cytoplasm into sporoblasts (Figure 3-16). At this stage, the oocyst capsule becomes electron-dense and is

clearly distinguishable from the basal lamina (Figure 3-16). Of interest at this stage is the change in the position of the multinuclei, previously randomly distributed, which now come to lie just below the sporoblast plasma membrane (Figure 3-16 and 3-17).

The sporozoite pellicular complex comprises an outer plasma membrane and an inner membrane that appears as a linear electron dense area (Figure 3-18). Further sporozoite budding is accompanied by an orderly ingress of sporoblast organelles and some inclusions. The paired organelle precursors lead this procession and undergo further development characterized by a condensation granular network into a dense, compact, pear-shaped inclusion. The mature sporozoites share similar structures to ookinetes: two pellicular membrane complexes, microtubules lying beneath the pellicular membrane, several rhoptries at the apical part. The mature sporozoites are released from the oocyst into the hemocoele and migrate toward the salivary gland. Thus, the sporogonic development of *P. berghei* parasites in *A. gambiae* is complete (reviewed by Fujioka et al., 2002).

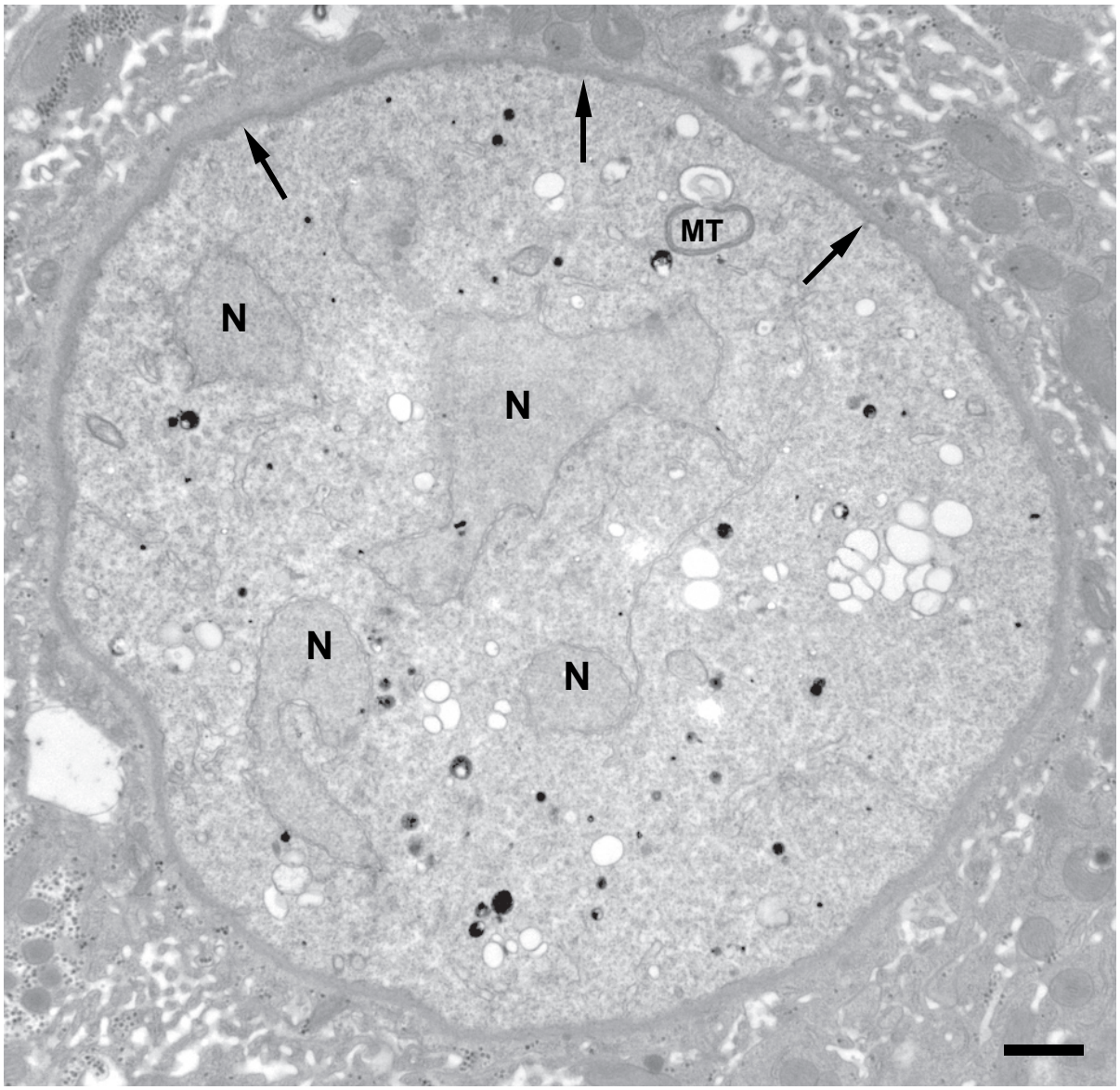


**Figure 3-15. Early stage of oocyst development.** The oocyst capsule is electron dense (arrows). Multiple nuclei (N) have a roughly oval or irregular polygonal shape. Mitochondria (MT) are randomly dispersed. Scale bar = 2 μm.

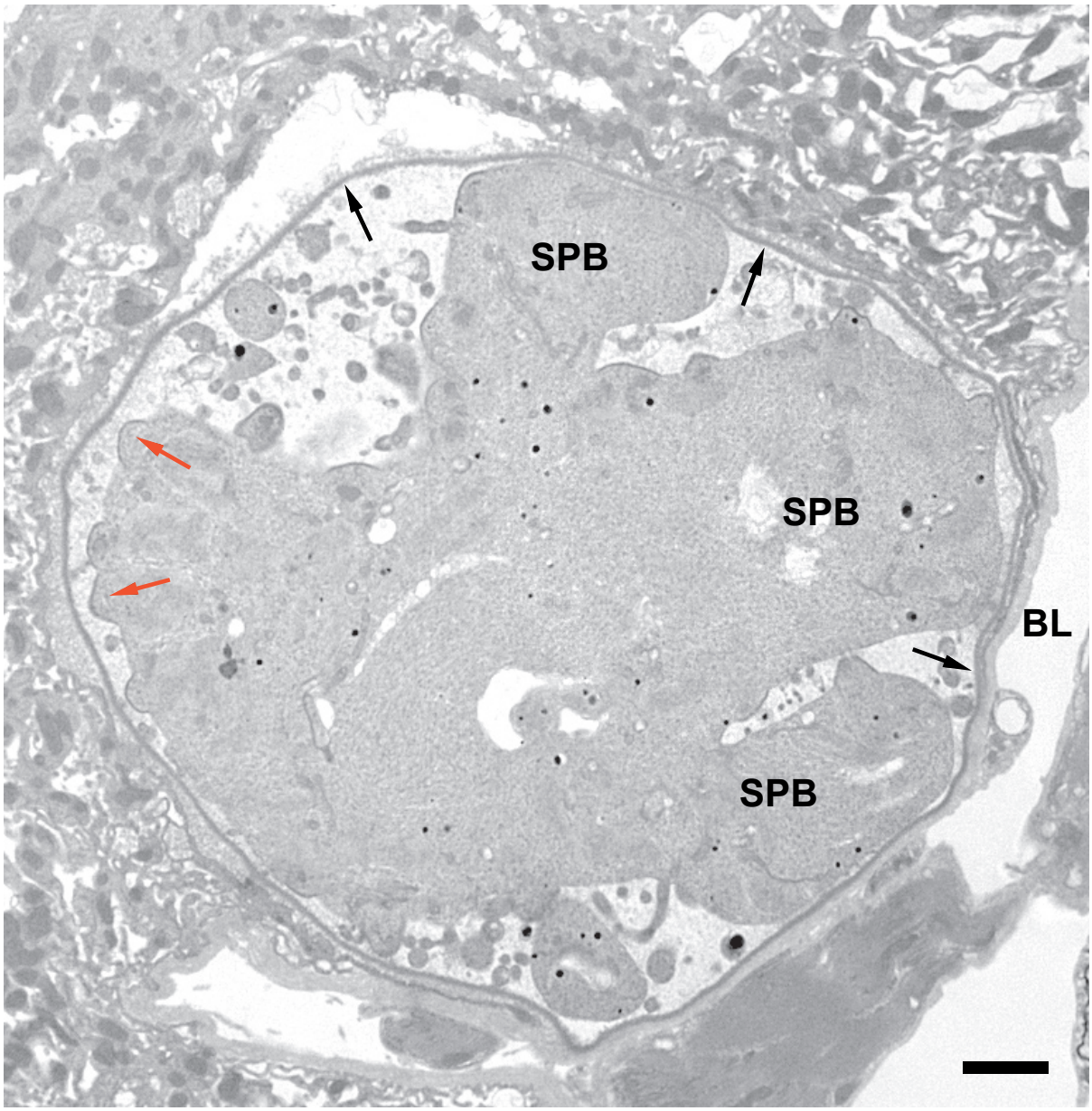


**Figure 3-16. Mid-stage oocyst.** The oocyst capsule is relatively electron-dense (black arrows). The sporoblast (SPB) is formed and sporozoites (red arrows) are budding out. BL: basal lamina. Scale bar = 2 μm.

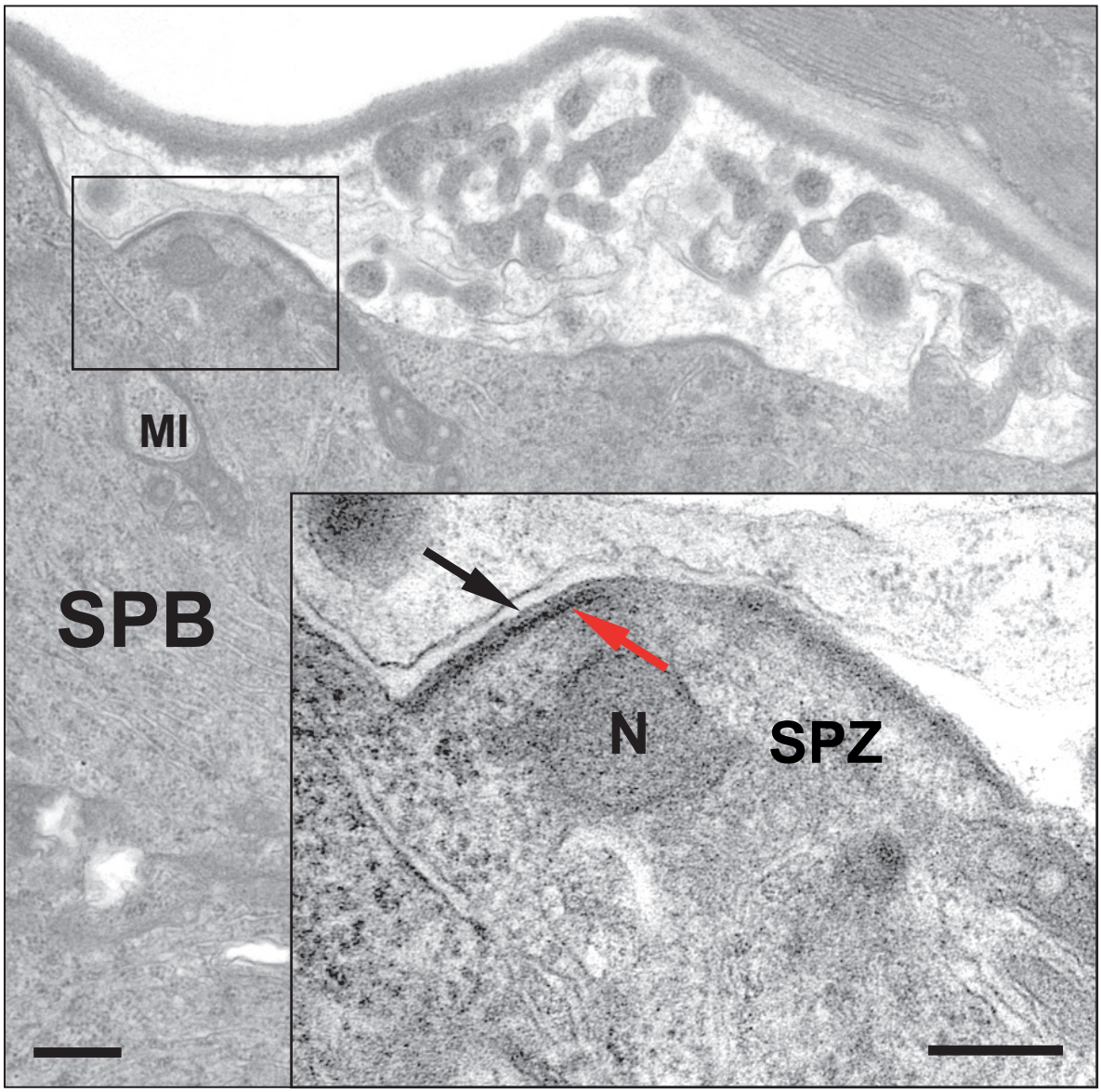


**Figure 3-17. Transmission electron micrograph showing a sporozoite (SPZ) in the process of budding from the sporoblast (SPB).** The sporoblast plasma membrane (black arrow) becomes the sporozoite plasma membrane. The inner membrane complex (red arrow) is assembled *de novo*. Nucleus (N) is located beneath the budding sporozoite and the tubular-like mitochondria (MI) are randomly dispersed. Inset is the higher magnification of the boxed region. Scale bars = 500 nm and 200 nm for the main graph and inset, respectively.

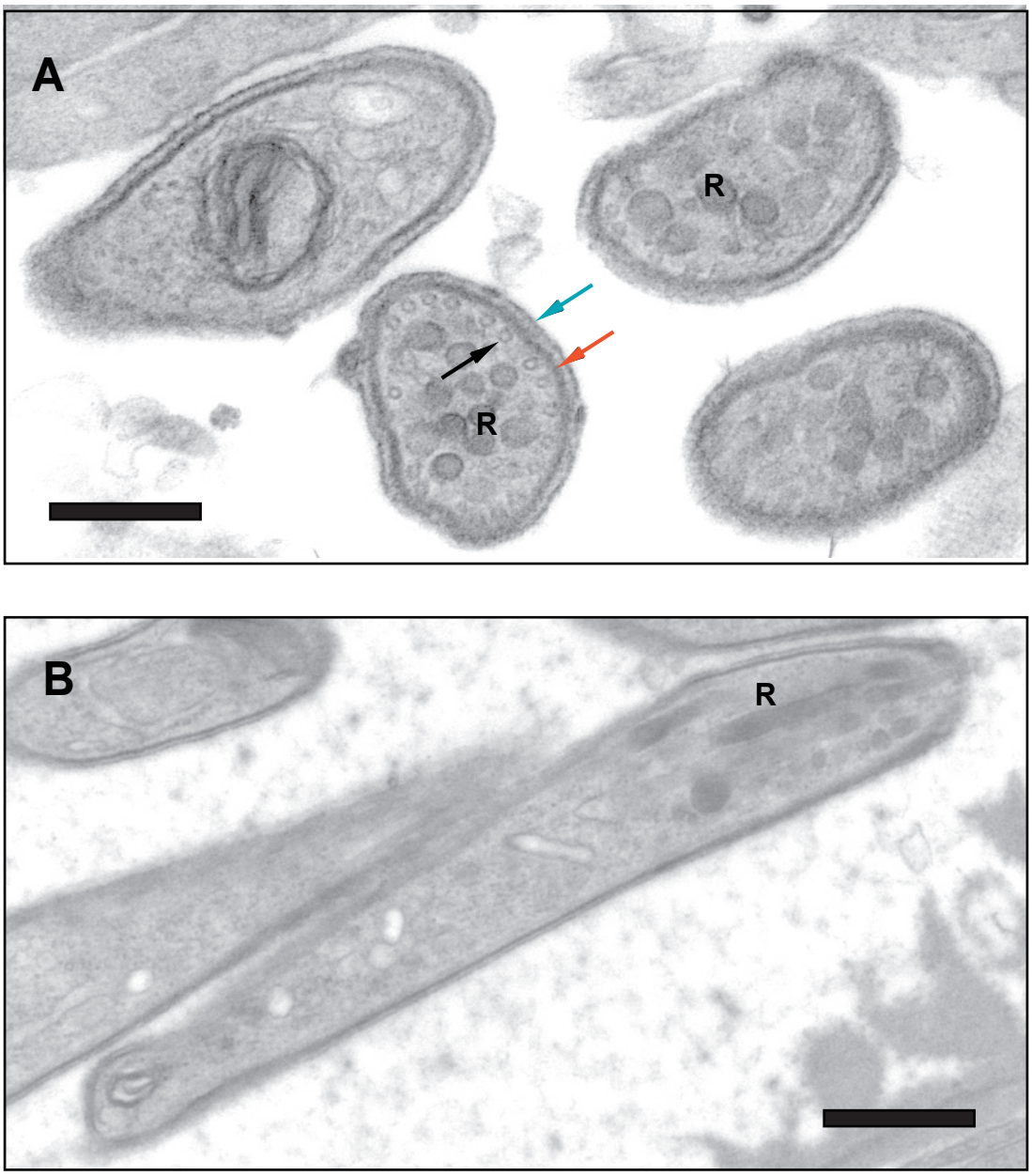


**Figure 3-18. Fine structure of the sporozoite.** Transverse section (A) and longitudinal section (B) of the sporozoites. The sporozoite shares a similar ultrastructure with ookinetes. The apical complex contains rhoptries (R) The outer (blue arrow) and inner membranes (red) are similar to that of the ookinete. A row of microtubules (black arrow) lie beneath the inner membrane. Scale bars in nm: (A), 100; (B), 500.

# CONCLUSIONS

In our study we attempted to provide a comprehensive description of the entire sporogonic development of *P. berghei* parasite in the *A. gambiae* mosquito by transmission electron microscopy. We were able to reinterpret several controversial theories. First, according to the reviews by Lehane, 1997 and Abraham et al., in 2004, the insect peritrophic matrix was thought to serve as a physical barrier to protect the midgut epithelium from mechanical damage and *Plasmodium* invasion. We report that in A. gambiae, the polymerization of the PM is completed at 28 h post infection. At that time, the majority of ookinetes have already entered the mosquito midgut and come to rest beneath the basal lamina. Therefore, we conclude that the PM is formed too late to prevent parasite penetration. It is still open whether the PM plays an important role in protection of the mosquito midgut from a physical damage or bacteria.

Our observations of the mosquito midgut before and after blood meal revealed the presence of highly aggregated secretory vesicles at the apical side of the epithelial cells before blood feeding. These vesicle disappear after feeding. The secretory vesicles are produced by the Golgi apparatus, and contain digestive enzymes (Billingsley et al., 1996). We propose that the secretory vesicles initially accumulate at the apical part of the cell, and then are released into the lumen through the apical edge of the epithelial cell. Since one of the important functions of midgut is the digestion of nutrients, secretory vesicles may play a role in digestion of the blood meal. Mosquito blood feeding is a very rapid process; the entire lumen cavity could be filled with blood in 1 to 5 min. Therefore, the accumulation of the enzymes for digestion in advance of feeding is an important physiological adaptation of the blood-sucking mosquitoes.

It was proposed that the invasion of ookinetes of the mosquito midgut cells causes severe damage, induces expression of nitric oxide synthase and leads to apoptosis (Han et al., 2000 and 2002, Kumar et al., 2004). These authors used immunofluorescent markers for nitric oxide synthase for analysis of the dissected midguts by confocal microscopy. However, the ultrastructural study of these tissues was not performed. In our study, we observed apoptotic cells by semi-thin sections stained with toluidine blue, both in non-infected and in infected mosquitoes. We propose that the apoptosis might be a general mechanism of cell turnover in the mosquito midgut. Further ultrastructural studies are required to examine the relevance of the parasite invasion to apoptosis of the epithelial cells.

The question of how and where the *P. berghei* parasites penetrate the mosquito midgut has long been a debatable issue. Recently, a theory of midgut wall entry was proposed in which the site of entry coincides with the site of convergence of at least three epithelial cells (Zieler et al., 2000a). However, this theory remains unproven from the ultrastructural point of view. We followed *P. berghei* ookinete invasion by electron microscopy. We do not find any evidence that parasite invades a specific type of midgut cell. Strikingly, we and others were not able to observe the parasites at the moment of midgut

cell invasion (Kadota et al., 2004, Vlachou et al., 2004). Although negative, these failures may indicate that the entry of parasites into the mosquito cells is a remarkably rapid process. Therefore, development of transgenic mosquitoes with fluorescently labeled membranes of the midgut epithelial cells could help to resolve this issue. This work is currently in progress in our laboratory.

Numerous studies using light and/or electron microscopy have investigated ookinete migration across the midgut epithelium (see Introduction). Malaria parasites are thought to enter the midgut epithelium intracellularly, but quickly exit invaded cells via the basolateral membrane, and migrate intercellularly to the basal surface of the midgut epithelium through the basolateral space between adjacent epithelial cells (reviewed by Baton et al., 2005). Previous electron microscopy studies are based upon a small number of invasion events, and thus are sensitive to biased and misleading observations. We performed systematic electron microscopy to examine the migration process of the *P. berghei* parasite in the mosquito midgut. Within a total of 124 ookinete examined, the majority of the ookinete (91%) took an extracellular route to pass through the midgut. However, there was still a minor portion of the parasites that were found intracellularly (9%). The majority of these "intracellular" parasites were located at the apical part of the cells, suggesting that these parasites might have been observed at the very early stages of the midgut invasion before their escape into the extracellular space. Therefore, we confirm that after a very rapid entry passage through the cell, *P. berghei* ookinetes preferably take an extracellular route to cross the *A. gambiae* midgut. This conclusion is important as it suggests that during midgut invasion the parasites are rather facing hostile environment of the extracellular space than the cytoplasmic milieu of the epithelial cells.

# CHAPTER 4

## The role of actin in parasite clearance

# INTRODUCTION

Several lines of evidence suggest that mosquitoes have evolved potent defence mechanisms against malaria parasites (reviewed by Sinden, 1999). Even in susceptible mosquitoes, *Plasmodium* undergoes several bottlenecks with massive losses occurring during its development. These include the transitions between gametocytes and ookinetes, between ookinetes and oocysts, and between midgut sporozoites and salivary gland sporozoites (see General Introduction for details). The greatest parasite losses occur in the midgut epithelial cells. It is known that insects defend themselves against bacteria and parasites using both cellular and humoral responses that are rapidly activated upon immune challenge. It has long been known that within the same species, mosquitoes display genetic variation in their susceptibility to parasites. Strains refractory to various malarias have been selected and studied. We made use of a refractory (R) strain of *A. gambiae*, which completely aborts the development of a number of malaria parasites, including the simian parasite *P. cynomolgi* B. In this strain, refractoriness is manifested by melanotic encapsulation of the ookinete, after it completes its passage through the mosquito midgut (Collins et al., 1986). A different refractory mechanism resulting in complete lysis of *P. gallinaceum* in the midgut was reported in another strain of *A. gambiae* (Vernick et al., 1995). These experiments are critical as they demonstrate that both susceptibility and refractoriness can be genetically selected in the mosquito, therefore, these complex features are encoded by the mosquito genes. However, the molecular identity of these genes remained for a long time unknown.

We identified *TEP1* as one of the mosquito genes which regulate parasite numbers in *A. gambiae* (See Chapter 2 for more details). This gene encodes a functional homolog of the mammalian complement factor C3. Binding of TEP1 to ookinetes mediates their killing through an unknown mechanism. To get better understanding of the effect of TEP1 on parasite survival, we set out to characterize ultrastructural features of the mosquito midgut in the context of the *TEP1* knockdown.

It has been previously reported that melanized ookinetes in the refractory mosquitoes are surrounded by an organelle-free zone that consists of finely fibrillar material (Torii et al., 1992; Vernick et al., 1995). Recently, a study based on the susceptible strain of *A. gambiae* and *A. stephensi* revealed that during the migration of *P. berghei* ookinetes in the mosquito midgut, the parasites are usually covered by a thickly stained membranous structure. This structure does not completely envelop the parasite. The authors described this structure as a lamellipodial “hood”, which is extended by the invaded cell to surround the parasite (Vlachou et al., 2004). Eventually, the invaded midgut cells undergo apoptosis and are expelled from the epithelium. During the expulsion of the invaded cell, the surrounding cells display a series of responses, including extensive lamellipodia crawling to restore the epithelial barrier beneath the damaged area. The authors speculated that the formation of the lamellipodial “hood” may be stimulated by the parasite and could represent a compromise that obstructs the egress of the ookinete and prevents draining of the invaded cells through the plasma membrane (Vlachou et al., 2004).

However, the significance and composition of this finely fibrillar material remained unknown. In our

experiments we addressed three questions: (1) What is the composition of the filamentous zone? (2) Is TEP1 involved in the formation of the filamentous zone? (3) What is the role of the filamentous zone in parasite killing?

# RESULTS

**1. Composition of the filamentous zone**

We performed transmission electron microscopy to study the fine structure of the filamentous zone. Both S and R mosquitoes were blood-fed with *P. berghei* infected mice. The mosquito midguts were then dissected at different time points post infection then fixed and embedded for transmission electron microscopy.

We observed an organelle-free fine filamentous zone surrounding melanized ookinetes in R mosquitoes (Figure 4-1 A). The appearance of this zone, and its size of around 500 nm, was very similar to those described by Torii et al. (1992) and Vernick et al. (1995). In R mosquitoes, the TEP1-labeled ookinetes were killed and melanized in the basal labyrinth or beneath the basal lamina (Blandin et al., 2004). The filamentous zone was predominantly observed on the sides of the apical end of the ookinete, often colocalizing with the site where melanization was initiated. Analysis of the zone at high magnification revealed that it was formed by fine filaments (Figure 4-1 A and B). It is important to note that the size and organization of the zone appeared structurally distinct from the previously described thin lamellipodium-like outgrowths or "hoods", which extend towards the ookinete from the cell (Vlachou et al., 2004).

In some cases, when a melanized ookinete was in contact with several epithelial cells, all cells were engaged in the formation of the filamentous zone, thus providing isolation of the parasite from live tissues (Figure 4-1 C and D). In some cases the intercellular location of the melanized parasites was revealed by melanin traces left by the ookinete in the intercellular space (Figure 4-1 D). Out of a total of 67 ookinetes observed in 8 refractory mosquitoes, 51 were melanized (76%). Interestingly, out of these 51 parasites, 32 were associated with the filamentous zone (62.7% of the melanized parasites). Vernick and colleagues reported that the filamentous zone was also found in susceptible mosquitoes but at a low frequency (Vernick et al., 1995). Therefore, we further examined the formation of the filamentous zone in susceptible mosquitoes.

Careful analysis confirmed the previous data and detected the filamentous zone surrounding ookinetes in S mosquitoes (Figure 4-2 A). The fine structure of this filamentous zone was identical to one observed in refractory mosquitoes. However, only a small fraction of ookinetes was associated with the filamentous zone (13 out of 88, or 14.8%). The majority of ookinetes surrounded by the filamentous zone were mostly alive as could be judged by their overall morphology and conservation of the orga-

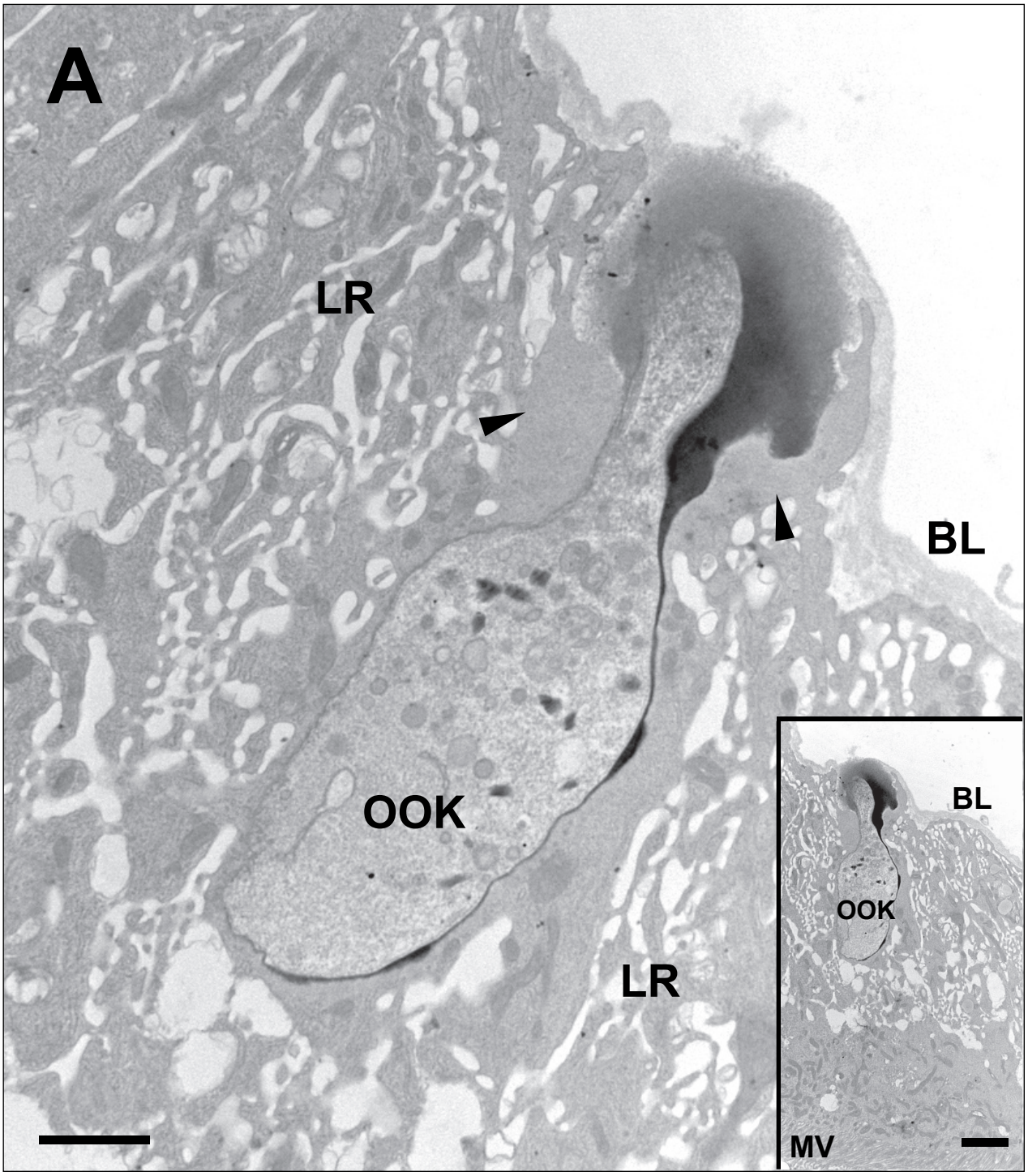


**Figure 4-1 A. Transmission electron micrograph of a melanized ookinete in the midgut of a refractory mosquito, 28 h post infection.** The ookinete is located in the extracellular space of the basal labyrinth and is surrounded by an organelle-free finely fibrillar material (arrow heads). Inset box: lower magnification view of the invaded epithelial cell. BL: basal lamina, OOK: ookinete, LR: basal labyrinth, MV: microvilli. Scale bar = 1 μm (2 μm in inset).

nelles (Figure 4-2 A). Additionally, the majority of the ookinetes in S mosquitoes were not associated with a filamentous zone, and remained in the extracelullar space of the basal labyrinth or beneath the basal lamina (Figure 4-2 B). Parasites without a filamentous zone were also mostly alive, and only few ookinetes were observed to undergo lysis (Figure 3-14).

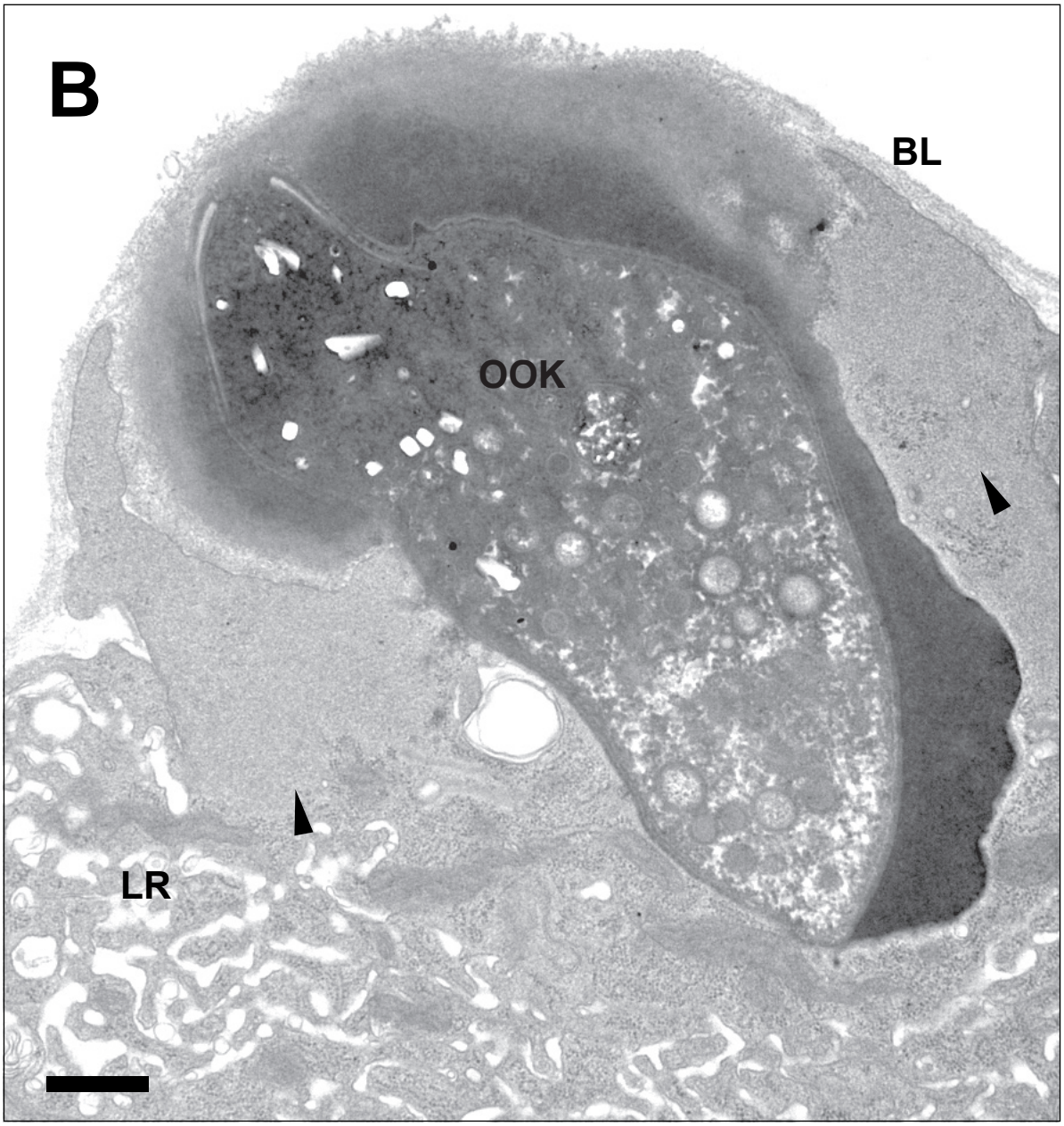


**Figure 4-1 B. Transmission electron micrograph of a melanized ookinete in the midgut of a refractory mosquito, 28 h post infection.** The ookinete is located beneath the basal lamina, surrounded by an organelle-free, finely fibrillar material (arrow heads). BL: basal lamina, OOK: ookinete, LR: basal labyrinth, MV: microvilli. Scale bar = 500 nm.

To demonstrate that the filamentous zone is indeed composed of polymerized actin, we attempted to immunohistochemical analysis using a specific antibody against the polymerized form of actin and immunogold labeling. This work is still in progress and requires optimization of the immunostaining conditions.

Simultaneously, we initiated immunofluorescence studies to confirm the composition of the filamentous zone. *A. gambiae* females from both S and R mosquitoes were infected with a transgenic parasite strain, PbGFPcon (kindly provided by Dr. A. P. Waters, LUMC, Leiden), which expresses GFP under control of the *elF1* gene promoter throughout its life cycle (Franke-Fayard et al., 2004). We used these

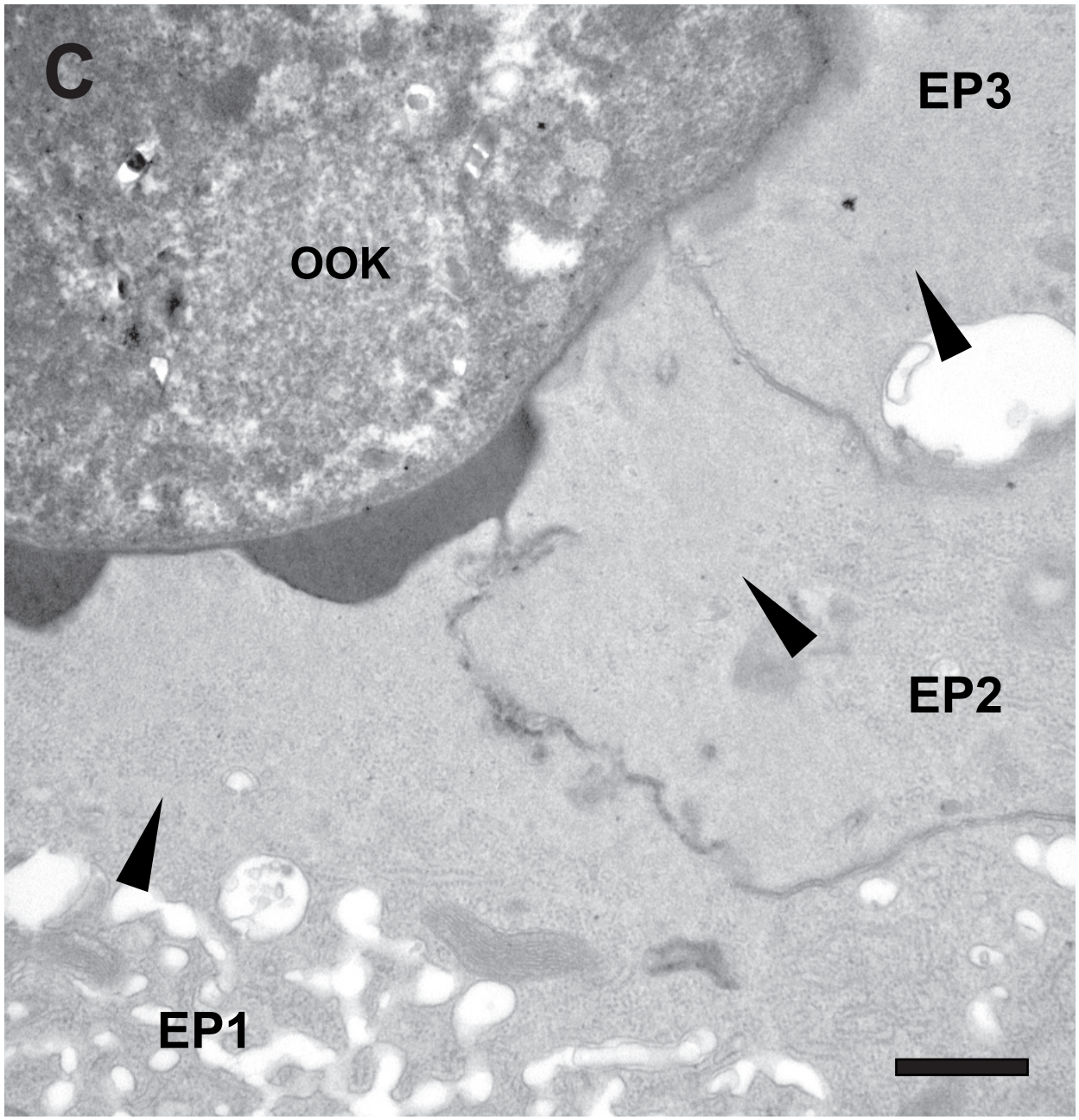


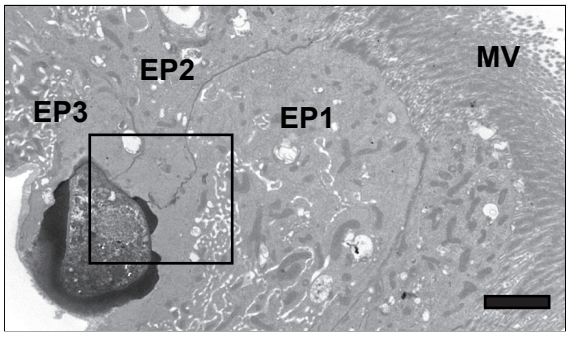


**Figure 4-1 C. The filamentous zone (arrow heads) is formed by three epithelial cells adjacent to the melanized ookinete.** EP: epithelial cell, OOK: ookinete, MV: microvilli. Inset is a low magnification view. Scale bar = 500 nm (2 μm in inset).

transgenic parasites to distinguish between live parasites (strong GFP fluorescence) and dead parasites (weak or absence of GFP fluorescence). To detect dead parasites, we used a polyclonal antibody directed against TEP1. This antibody recognizes TEP1 bound to the surface of parasites. Our previous studies demonstrated that TEP1 binding causes parasite killing and that the majority of TEP1-positive parasites are dead (Blandin et al., 2004).

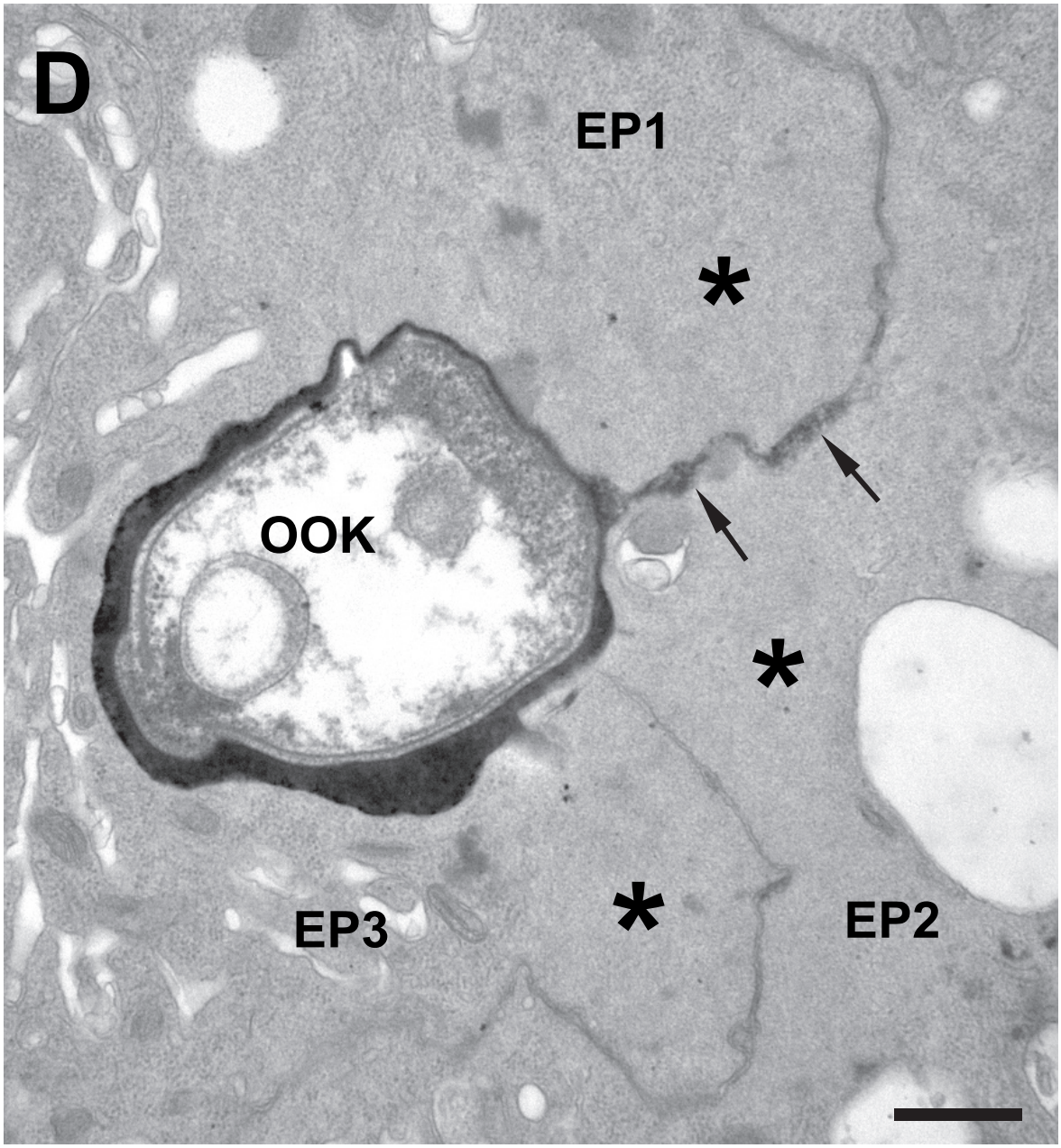


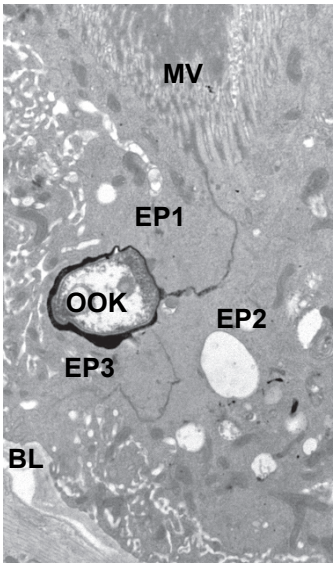


**Figure 4-1 D. A melanized ookinete (OOK) surrounded by the filamentous zone (asterisks) formed by three adjacent epithelial cells.** Note the melanin trail (arrows) left behind in the basolateral membrane separating two epithelial cells (EP1 and EP2) indicating that the ookinete is intercellular. Inset box: lower magnification view. MV: microvilli, EP: epithelial cell, BL: basal lamina. Scale bar = 500 nm.

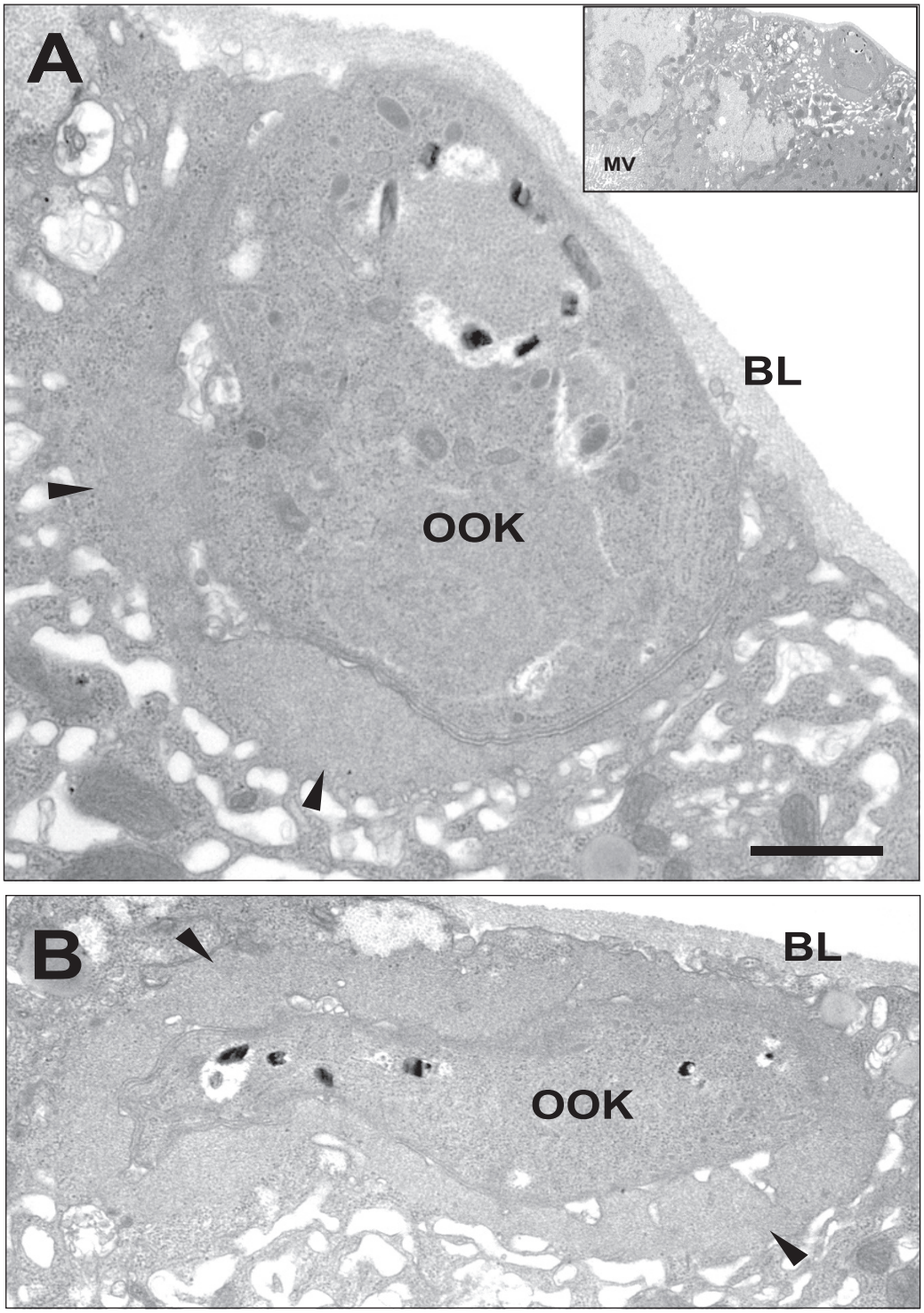


**Figure 4-2. The actin zone in the susceptible mosquitoes**.
Ookinetes (A and B) are located beneath the basal lamina and are surrounded by the actin zone (arrow head). Inset box: lower magnification of A. BL: basal lamina, OOK: ookinete, MV: microvilli. Scale bar = 500 nm.

The midguts of infected mosquitoes were dissected at 28 h post infection and analyzed by confocal microscopy. In these experiments, we used antibodies and probes that discriminate between the non-polymerized or globular actin (G-actin) and the polymerized or filamentous actin (F-actin). A monoclonal anti-alpha-actin antibody (Sigma) was used to recognize G-actin, whereas rhodamine-labeled

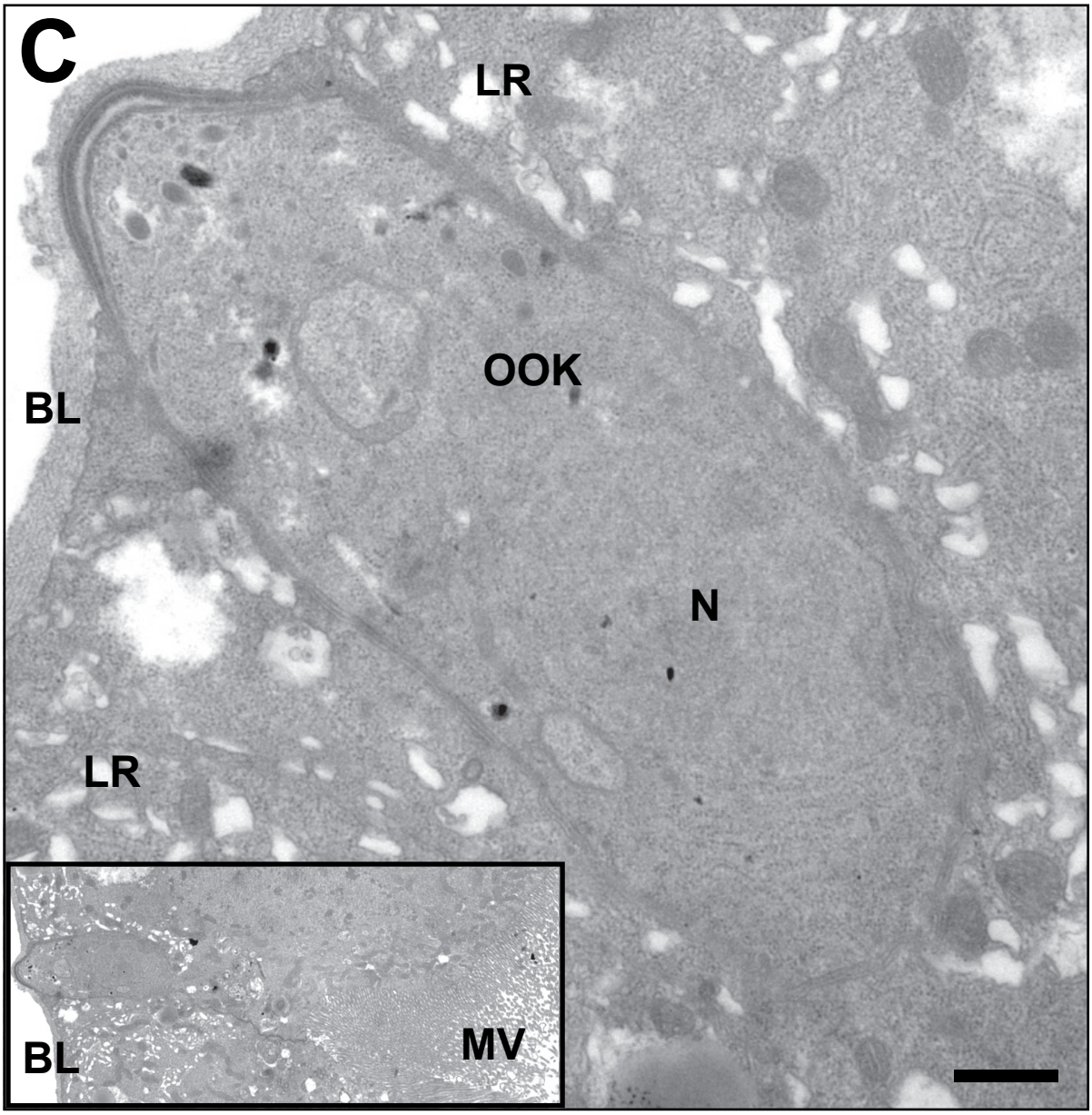


**Figure 4-2 C. The majority of ookinetes are not associated with the filamentous zone in susceptible mosquitoes**. The ookinete has successfully reached the basal lamina. Note the absence of polymerized actin around the parasite. BL: basal lamina, OOK: ookinete, N: nucleus, MV: microvilli, LR: basal labyrinth. Inset box: lower magnification view of the whole adjacent epithelial cell. Scale bar = 500 nm.

phalloidin (Molecular Probes) was used to recognize F-actin. Phalloidin is a cyclic peptide isolated from the death cap fungus *Amanita phalloides*, which specifically binds to F-actin and blocks its depolymerization (Becker et al., 2000). In S mosquitoes, the G-actin signal was observed aggregated at the tip of live ookinetes, where the microtubules and cytoskeleton are assembled (Figure 4-3). This signal was observed for both live (GFP expressing) and dead (negative for GFP but positive for TEP1 staining) ookinetes (Figure 4-3). We did not observe any G-actin-positive signals in the mosquito epithelial cells, neither in susceptible, nor in refractory mosquitoes. These results indicate that the anti-alpha-actin antibody recognizes elements of the ookinete cytoskeleton but does not react with the components of the filamentous zone.

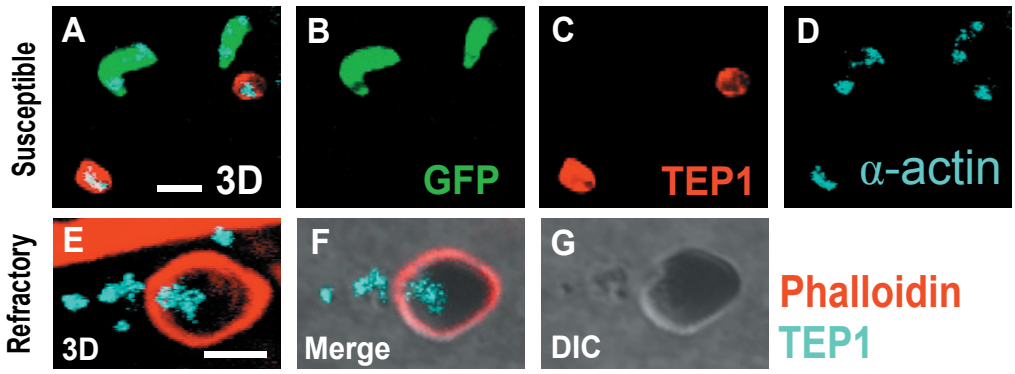


**Figure 4-3. Confocal images of actin staining.** Confocal sections and 3D reconstructions of midgut tissues from susceptible (A-D) and refractory (E-G) mosquitoes were fixed at 28 h post infection. Double staining shows TEP1 in red and a monoclonal antibody against non-polymerized α-actin in blue (A-D). Phalloidin labels polymerized actin, and TEP1 is shown in blue (E-G). Non-polymerized α-actin is detected both on live (GFP expressing) and dead (non GFP, but TEP1 positive) ookinetes (A-D). However, none of the live ookinetes are positive for phalloidin (not shown). A distinct polymerized actin ring forms around a melanized ookinete (E-G). Scale bar = 5 μm.

We next examined the distribution of F-actin in the midguts of susceptible mosquitoes using phalloidin. In these experiments, samples were collected at two time points, 24 and at 48 h after infection. We observed phalloidin-positive signals only around dead or dying parasites. The number of dead parasites surrounded by the phalloidin ring increased with time: 15.6% of dead parasites at 24 h and 28.2% at 48 h post infection. We never detected a phalloidin ring around live GFP-positive parasites.

Association of the phalloidin with dead or melanized parasites was even more spectacular in the refractory mosquitoes (Figure 4-3). Consistent with the ultrastructural observations, the polymerized actin detected by phalloidin staining in the confocal images seemed to be located at the anterior part of the ookinete, where melanization is usually initiated. Analysis of electron and confocal microscopy revealed that the filamentous zone was composed of polymerized actin, therefore, we propose to rename it the actin zone.

**2. Role of TEP1 in the formation of actin zone in susceptible and refractory *A. gambiae***

As discussed in the Chapter 2, TEP1 is an essential mosquito factor implicated in parasite killing. Therefore, we were interested to elucidate the relationship between TEP1 and the actin zone. We followed formation of the actin zone via transmission electron microscopy in TEP1-depleted mosquitoes. In these experiments *TEP1* knockdown was performed as described earlier in Chapter 2. Briefly, the expression of *TEP1* was silenced by direct injection of dsRNA corresponding to *TEP1* (*dsTEP1*) into the thorax of young susceptible and refractory mosquitoes (Blandin et al., 2002). The efficacy of the knockdown was confirmed by immunoblotting (Blandin et al., 2004). Four days after dsRNA injection, mosquitoes were fed on PbGFPcon-parasite infected mice. Infection prevalence and mean oocyst numbers per midgut were compared between control *dsLacZ* and *dsTEP1*-injected mosquitoes. The

*dsTEP1*-injected susceptible mosquitoes exhibited a five-fold increase in the mean number of oocysts, compared to the control (Blandin et al., 2004). *dsTEP1* injection in the refractory mosquitoes completely abolished melanotic refractoriness: no melanized parasites were detected and ookinetes developed into oocysts and released sporozoites normally (Blandin et al., 2004). For ultrastructural analysis, blood-fed *dsLacZ*- and *dsTEP1*-treated mosquitoes were dissected at different time points (21, 24, 28, 32, 44 and 48h) post infection, fixed and epoxy embedded.

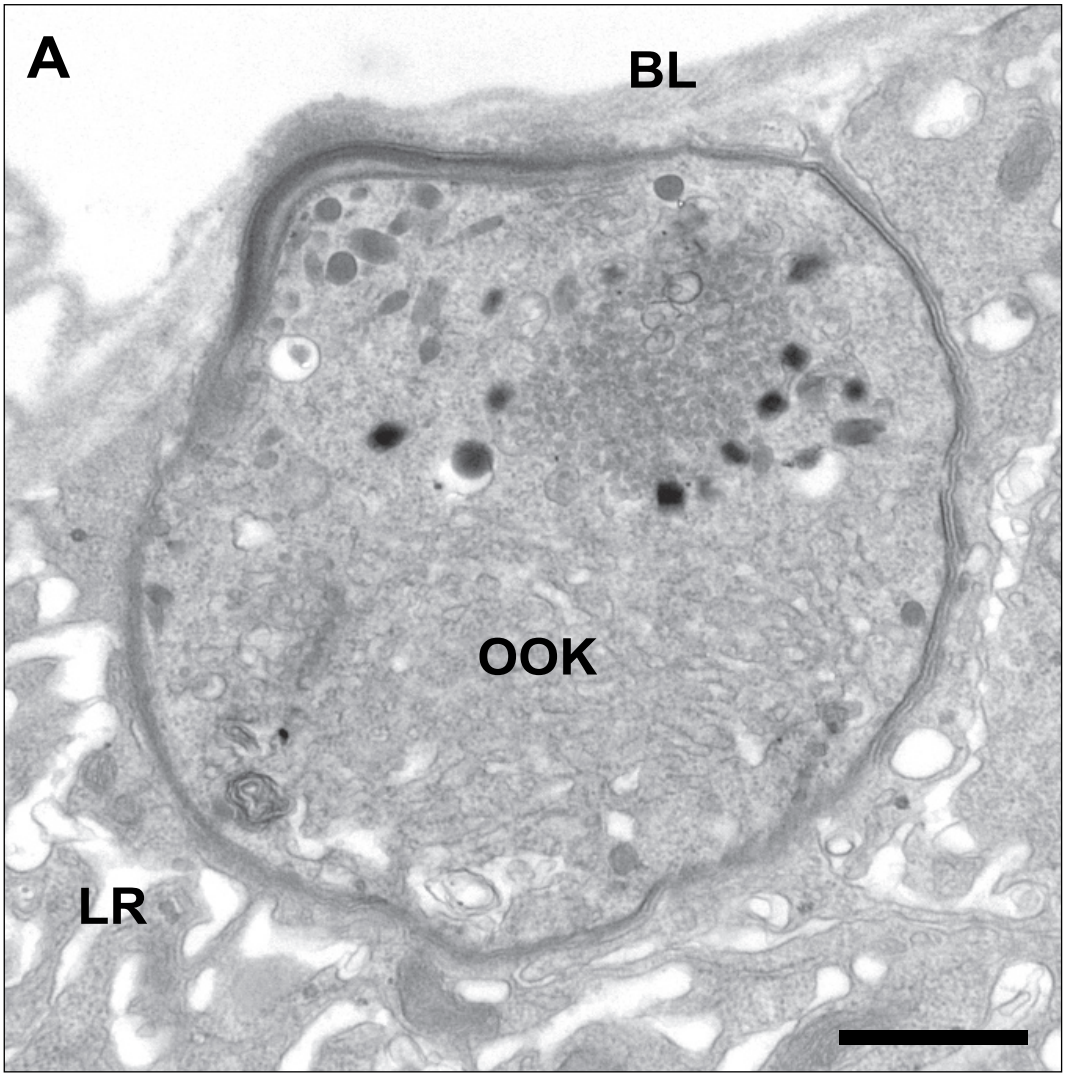


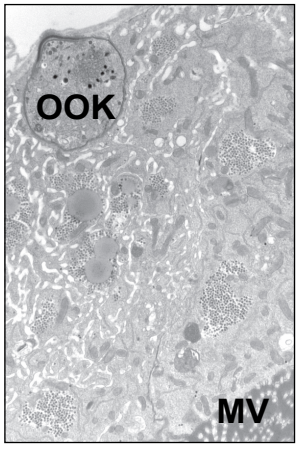


**Figure 4-4 A, B and C. Double stranded RNA knock-down of *TEP1* in the refractory mosquito abolishes both the melanization of ookinetes and the formation of the actin zone.** Ookinetes are located extracellularly beneath the basal lamina; note the absence of melanized parasites. Moreover, no actin zone is detected in the cells adjacent to the ookinetes. BL: basal lamina, LR: basal labyrinth, OOK: ookinete, MV: microvilli. Box = low magnification view. Scale bars = 500 nm.

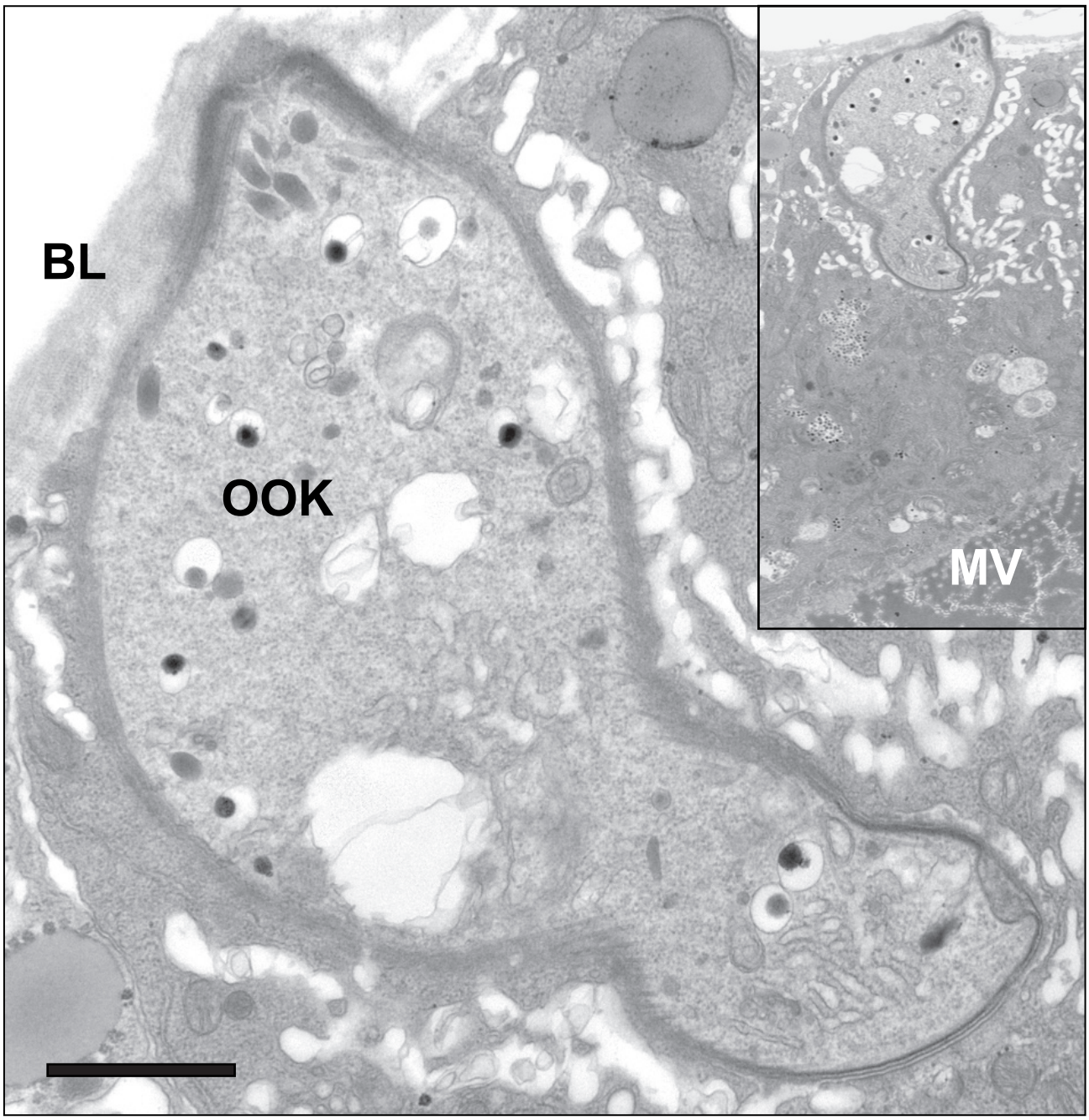


**Figure 4-4 B**. Legend as on previous page.

Electron microscopical analysis of dsRNA-injected mosquitoes revealed that dsRNA *per se* did not cause any structural modifications in the organization of the mosquito midgut. Slight differences in the abundance of the basal labyrinth were observed between control and *dsTEP1*-injected mosquitoes. However, further studies are needed before firm conclusions can be drawn from these observations. We conclude that *TEP1* knockdown does not cause significant changes in the midgut morphology. In both susceptible and refractory strains, normal parasite development was observed. Most of the detected parasites were alive with clearly visible intracellular organelles (Figure 4-4 for refractory and Figure 4-5 for susceptible mosquitoes). Melanotic encapsulation was abolished in the *dsTEP1* knockdown refractory mosquitoes, and the majority of ookinetes was observed beneath the basal lamina or in the extracellular space of the basal labyrinth. Strikingly, the formation of the actin zone

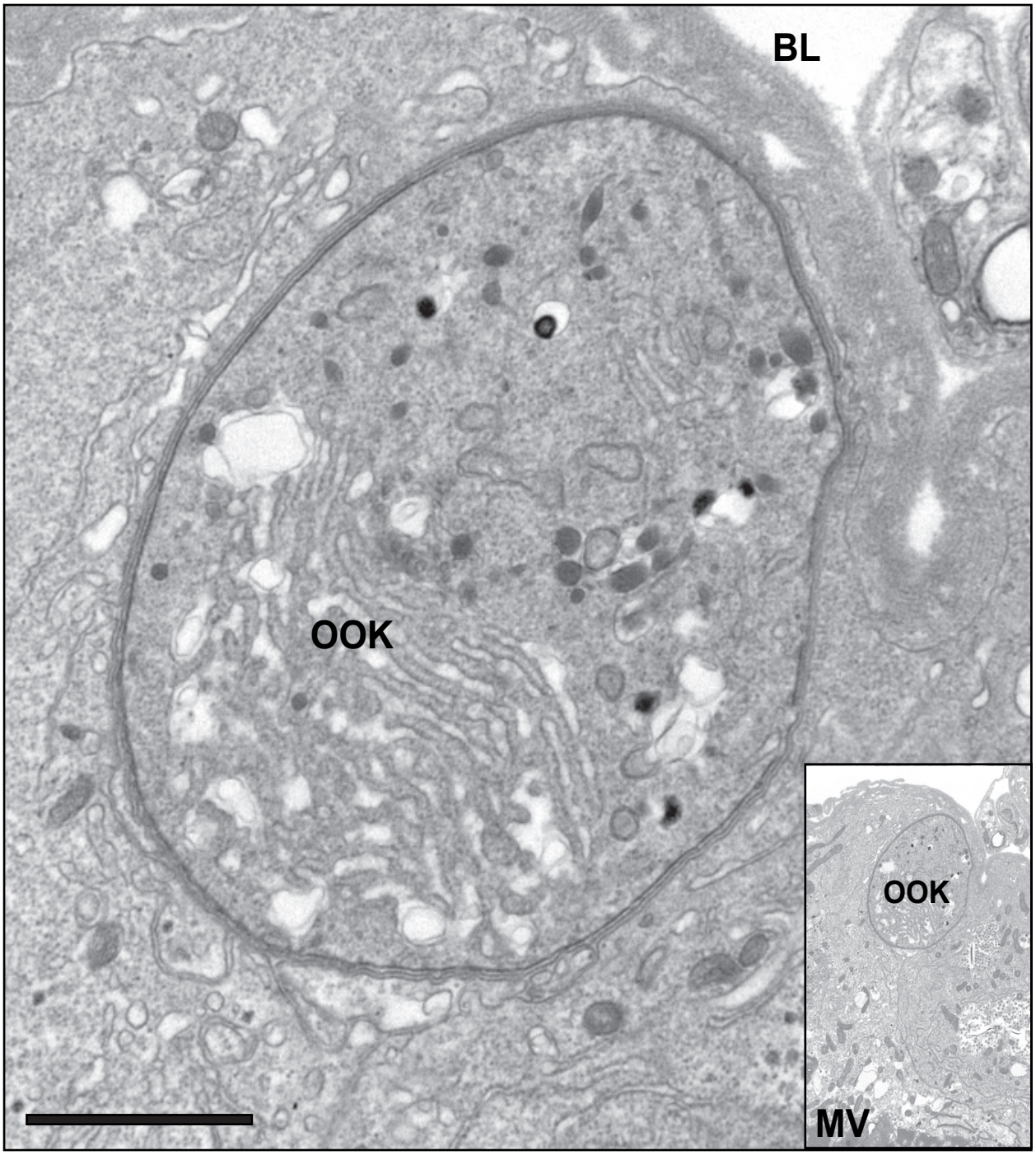


**Figure 4-4 C.** Legend as on page 97.

was completely abolished in *dsTEP* knockdown refractory mosquitoes. Epithelial cells adjacent to the ookinetes were regular, without any organelle-free actin zone (Figure 4-4). The same features were observed in the susceptible mosquitoes (Figure 4-5 and see also Table 4-1). Our results indicate that the presence of the actin zone correlates with *TEP1* function, and therefore, *TEP1* could be the genetic determinant of this structure.

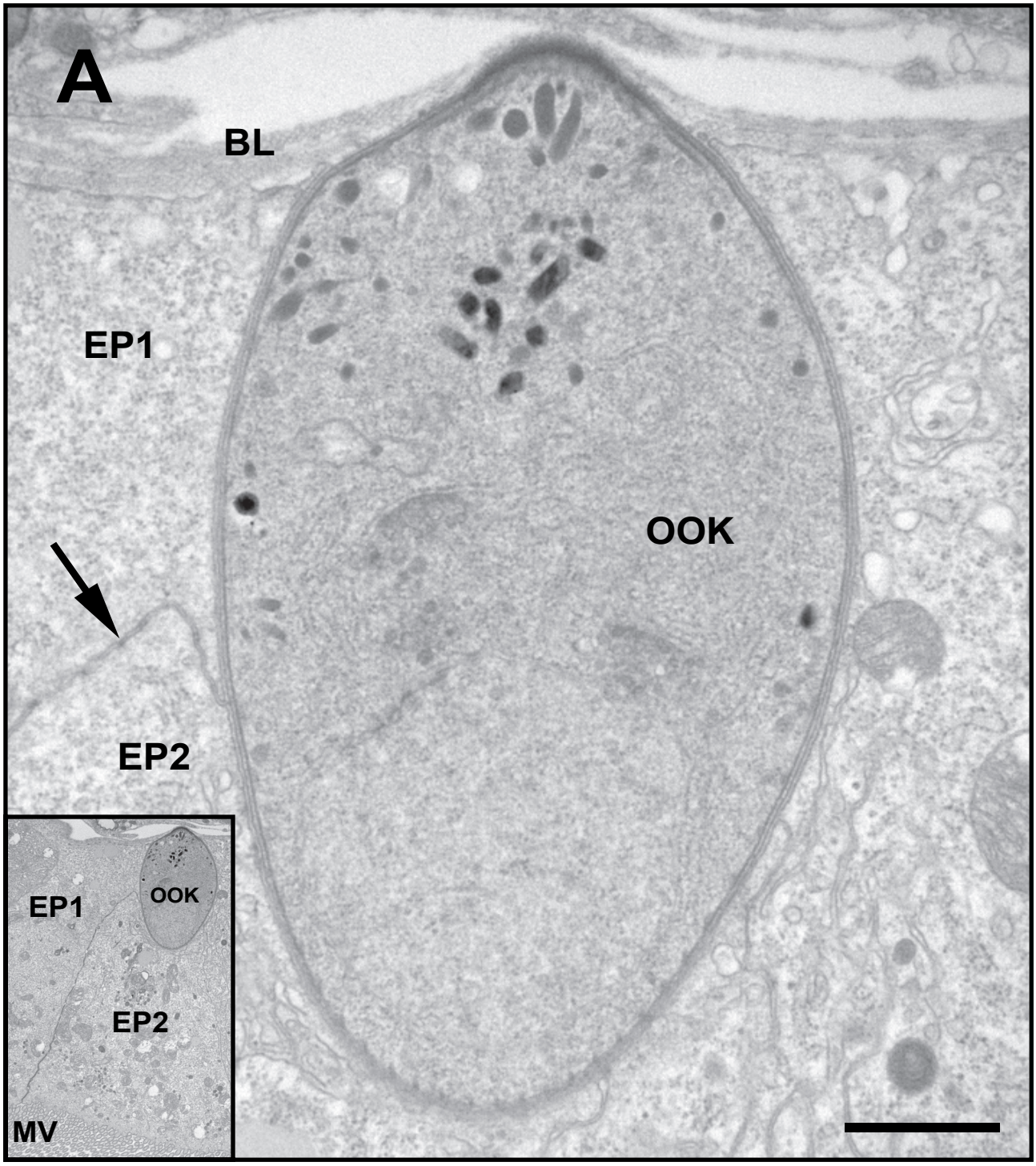


**Figure 4-5 A, B. dsRNA knock-down of *TEP1* abolishes formation of the actin zone in susceptible mosquitoes.** An ookinete is situated beneath the basal lamina. Note the basolateral membrane (arrows) separating two adjacent epithelial cells (EP1 and EP2) indicating that the ookinete is situated in an intercellular space. BL: basal lamina, EP: epithelial cell, OOK: ookinete, MV: microvilli. Box = lower magnification view. Scale bar = 500 nm.

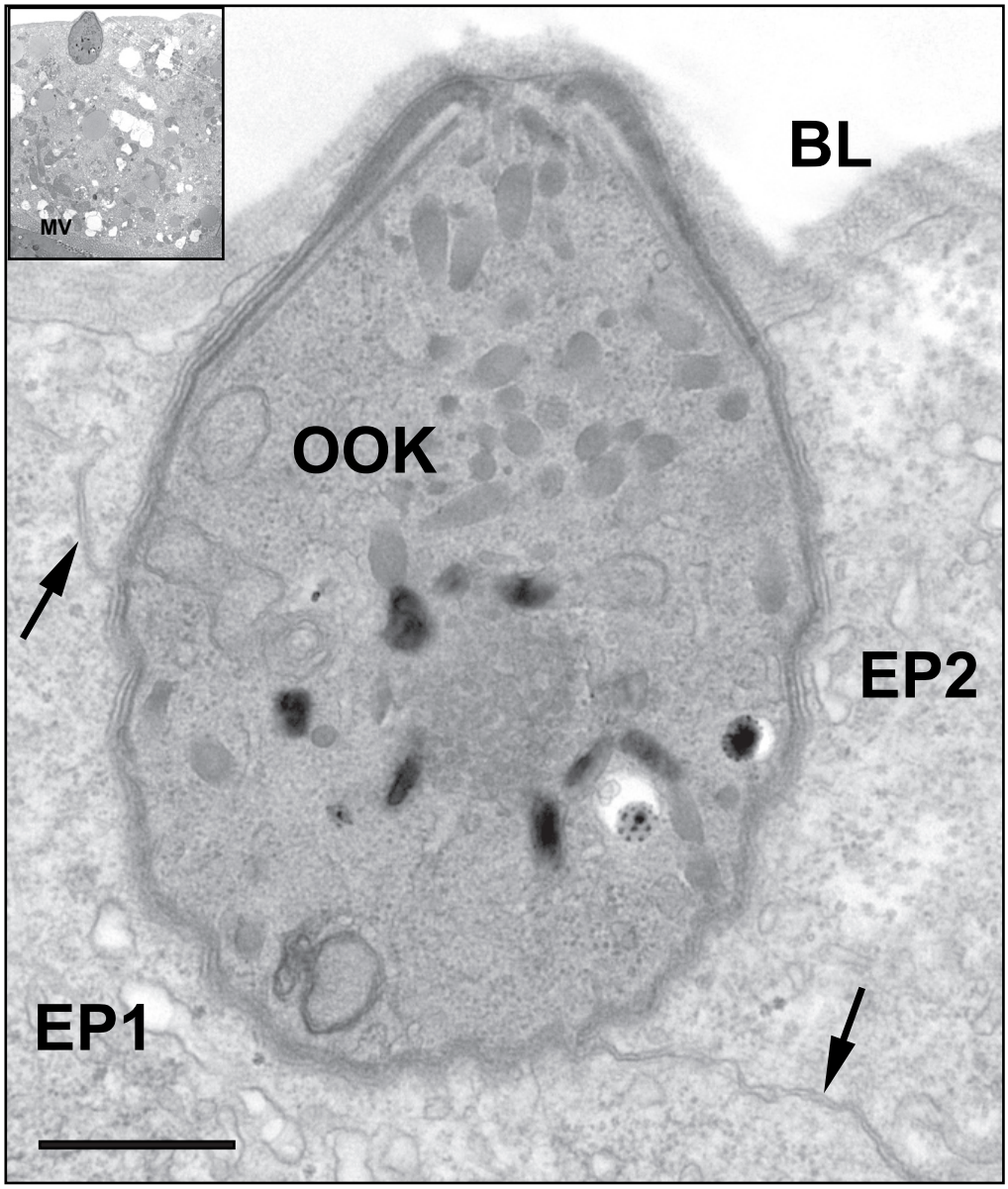


**Figure 4-5 B.** Legend as on previous page.

**Table 4-1. Comparison of actin zone formation in susceptible and refractory strain mosquitoes.**

| | No. of ookinete with an associated actin zone / total ookinetes in midgut ( no. of mosquitoes dissected) | |
|---|---|---|
| | S mosquitoes | R mosquitoes |
| *dsLacZ* KD | 13 / 88 (15) | 32 / 67 (8) * |
| *dsTEP1* KD | 1 / 36 (7) | 0 / 26 (5) |

* Of the 67 ookinetes recorded, 51 were melanized

### 3. Role of the actin zone in parasite killing

Previously we proposed that TEP1-dependent parasite killing is followed by a TEP1-independent clearance of dead parsites by lysis or melanization (Blandin et al., 2004). Moreover, results of our ultrastructural analysis strongly suggest that the formation of the actin zone is dependent on TEP1 function. These results taken together prompted us to examine whether the actin zone could be the mechanism by which binding of TEP1 causes parasite killing. Two possibilities can be considered: (i) TEP1, bound to the parasite surface, is recognized by receptors on the membranes of adjacent midgut cells, and activates local actin polymerization. The newly formed actin ring isolates parasites from necessary nutrient sources, thus causing parasite death. (ii) Actin polymerization is caused by the presence of dead parasites, which are killed by an unknown TEP1-dependent mechanism. As *TEP1* depletion results in better parasite survival, no actin zone is formed around live parasites.

To explore these hypotheses, we examined the kinetics of TEP1 binding to parasites and actin polymerization around parasites, using confocal microscopy. For these experiments, mosquitoes were blood-fed by PbGFPcon-parasite infected mice and specimens were prepared at 24 and 28 h post infection. We compared the number of live and dead parasites with and without a phalloidin ring. At least 10 mosquitoes at each time point were carefully examined by confocal or fluorescence microscopy. Each experiment was repeated 3 times. Within a total of 60 midguts collected at 24 and 48 hours post-infection, 8802 and 5696 ookinetes were observed, respectively (Figure 4-6). We did not detect an actin zone around live ookinetes except for one exceptional case (0.02% and 0% of the total ookinete number at 24 and 48 hours post-infection, respectively). However, the occurrence of the actin zone surrounding dead parasites increased over time (1.81% and 5.83% of the total ookinete count at 24 and 48 h post-infection, respectively). Our results indicate that the formation of the actin zone occurs after the death of the ookinetes and, therefore, cannot be responsible for parasite killing. Based on our observations, we propose that local actin polymerization is involved in the clearance of dead parasites by the mosquito epithelial cells.

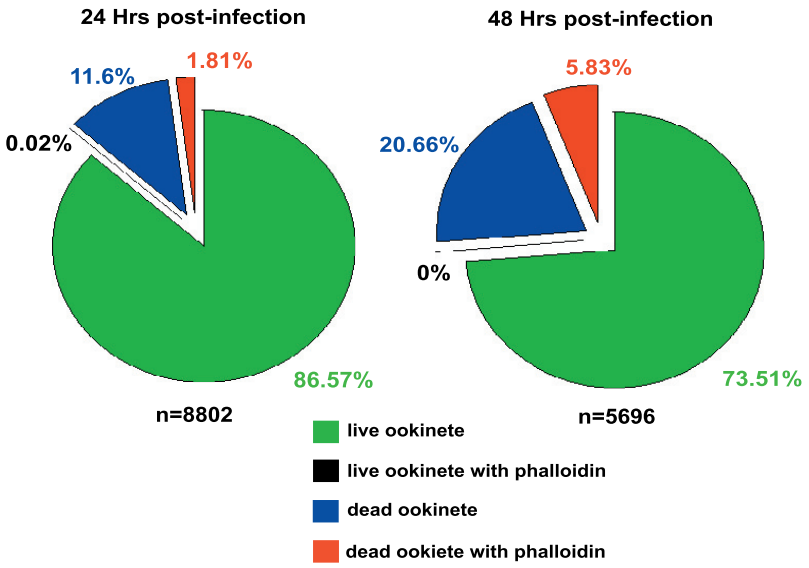


**Figure 4-6. Percentage of live and dead parasites in susceptible mosquitoes at 24 and 48 h post infection.**
The number of dead parasites with a phalloidin-positive signal increased over time (1.81% and 5.83% of all parasites at 24 and 48 h post infection, respectively).

# CONCLUSIONS

In this study, we demonstrated by transmission electron and confocal microscopy that the previously described filamentous zone surrounding melanized ookinetes is composed of polymerized actin and we rename it the "actin zone". Our study revealed that the actin zone is a result of local actin polymerization in the midgut epithelial cells induced by the presence of parasites. However, the actin zone is distinct from the lamellipodium "hood" previously described by Dr. Vlachou and colleagues (2004). Although both structures are associated with re-organization of the actin cytoskeleton, lamellipodia are specialized extensions at the front or leading edge of motile cells (e.g. macrophages). Their function is believed to allow persistent cellular protrusion over a surface (Mejillano et al., 2004). An alternative form of actin machinery called the filopodium, appears to perform sensory and exploratory functions to steer cells (Mejillano et al., 2004). As was discussed in the Chapter 1, lamellipodia in the cultured mosquito cells might play a role in phagocytosis of ookinetes. Morphologically, lamellipodia are thin sheets of actin filaments of 50 to 100 nm thickness (see Fig 1-4) and are thus distinct from the thick "actin zone" which measures 500 nm.

Using dsRNA knockdown of *TEP1* we demonstrate that formation of the actin zone is TEP1-dependent in both susceptible and refractory mosquitoes. *TEP1* knockdown leads to higher parasite numbers. However, at two examined time points after parasite infections, the number of actin-surrounded parasites was consistently lower than the number of dead parasites. To reach a final conclusion about the role of actin polymerization in parasite killing, we are in the process of analyzing how silencing of genes involved in actin polymerization affects development of the actin zone. Our preliminary data on the functional analysis of the mosquito genes potentially involved in actin polymerization suggest, that these genes do not play a major role in the killing of parasites. Further investigations aiming at the identification of genes that act downstream from *TEP1* in parasite killing, or of genes involved in the formation of the actin zone, will shed light on this issue.

Our data taken together indicate that formation of the actin zone occurs when parasites are dead or dying, suggesting that the actin zone is not associated directly with parasite killing. Therefore, we propose the following model of actin-based parasite clearance: the parasites are first killed by a TEP1-dependent mechanism, and subsequently the parasites are lysed or melanized. Dead or dying parasites are recognized by epithelial cells, and the actin zone is then formed to separate the dead or dying ookinetes from live tissues.

# GENERAL DISCUSSION

**Establishment of the *in vitro* co-culture system**

● We have established an *in vitro* co-culture system using a mosquito hemocyte-like cell line to remodel the mosquito-parasite interactions. Using transmission electron microscopy we demonstrate that the mosquito cells react to the parasites in the same fashion as towards inert megnetic beads. Beads and ookinetes are phagocytosed by a zipper-like mechanism by the mosquito cells.

● We attempted to use an *in vitro* co-culture system to perform the functional analysis of TEP1. Strikingly, TEP1 is not detected on the surface of banana-shaped ookinetes, whereas during the midgut invasion TEP1 is labeling up to 80% of ookinetes. Importantly, this binding *in vivo* mediates parasite killing. This observation impeded the further development of the co-culture system as a model to study TEP1 function.

● TEP1 is synthesized and secreted by hemocytes and binds to the surface of ookinetes in the midgut (Levashina et al., 2001, Blandin et al., 2004).This process involves two distinct types of the mosquito cells. The analysis of gene expressional profiles using cDNA microarrays revealed by that the ookinete and peptidoglycan treatments induced similar responses in the mosquito cells in co-culture. Moreover, *SRPN10*, which is strongly induced during the ookinete invasion in the midgut, is down regulated in the co-culture.

The detailed characterization of our *in vitro* system highlights several important differences with the *in vivo* midgut invasion process, and raises a note of caution for future studies relying solely on the co-culture system for analyses of host-parasite interactions.

**Functional analysis of mosquito TEP1 protein**

Functional analysis of TEP1 allowed us to demonstrate that TEP1 binds to and mediates killing of midgut stages of *P. berghei*. The binding of TEP1 and the consequent promotion of parasite killing in the midgut, are reminiscent of functions of complement factors in vertebrates. Importantly, our studies on the role of TEP1 during parasite invasion demonstrate that mosquitoes actively defend themselves against *Plasmodium* parasites, and that the dramatic losses undergone by parasites in the first days after infection are essentially due to this efficacious immune response. Thus, we demonstrate that TEP1 is an important player in the antiparasitic response in *A. gambiae*.

Therefore, we propose the following model of the immune responses of *A. gambiae* to *P. berghei*. After crossing the midgut epithelium, parasites come in contact (within the basal labyrinth) with soluble hemolymph components, but not with hemocytes. One of the hemolymph components, TEP1, recognizes and binds to the ookinetes, causing their death by an as yet unknown mechanism. The following step is the disposal of dead parasites by either lysis or, in the case of refractory mosquitoes, lysis and melanization. The model predicts that the processes of disposal of dead parasites (i.e. melanotic en-

capsulation and lysis) are controlled by genes other than *TEP1*. It is notable that TEP1 binding to and killing of parasites occurs in both R and S mosquitoes, albeit more slowly in the latter. Interestingly in susceptible mosquitoes, TEP1 does not bind to all parasites. A number of dead TEP1-negative ookinetes were detected in *TEP1*-deficient mosquitoes. This observation suggests that *TEP1* is not the only mosquito gene that controls parasite development and that other genes and gene cascades act in concert to keep the parasite load low during infection. Further functional studies should identify novel mosquito genes involved in the establishment of vectorial capacity.

**Ultrastructural study of interactions between *A. gambiae* and *P. berghei***

● The ultrastructural details of the parasite life cycle in the mosquito are not well understood. Reports on the complete cycle of one parasite inside one vector are still missing. Here, we followed the complete sporogonic development of *P. berghei* parasites in *A. gambiae* mosquito. Gametocytes fertilize in the blood meal within the mosquito midgut lumen and transform into zygotes and finally develop into motile ookinetes. The ookinetes then escape this environment and enter the midgut epithelial cells. A controversial question that has been addressed is whether the ookinetes have to cross the peritrophic matrix (PM) before entering a midgut cell. It was proposed that the PM plays an important role as a physical barrier to prevent the ookinete migration (reviewed by Abraham et al., 2004). We observed that the completely polymerized PM is only present after 28h post infection, whereas the majority of the ookinetes have already entered into the mosquito midgut and come to rest beneath the basal lamina. We conclude that in *A. gambiae*, the PM does not prevent invasion of the *P. berghei* parasites.

● It was proposed that the invasion of ookinetes of the mosquito midgut cells causes severe damage, induces expression of nitric oxide synthase (NOS) and leads to apoptosis (Han et al., 2000 and 2002; Kumar et al., 2004). Using semi-thin midgut sections, we detect extruded apoptotic cells in both non-infectious and infectious fed mosquito midguts, indicating the phenomenon of apoptosis is probably not parasite-dependent. A recent report of *P. falciparum* invasion of *A. stephensi* suggests that the epithelial cell extrusion may be a general mechanism of tissue repair rather than a parasite-specific response (Baton et al., 2004). Further immunofluorescent and electron microscopy might shed light on this issue.

● The passage of the motile, invasive ookinete across the mosquito midgut has remained controversial. The major arguments are how, and where does the parasite penetrate into the mosquito midgut, and the route of ookinete migration through the midgut. *Ex vivo* light microscope studies showed that ookinetes entered midgut cells through the apical lateral membrane close to the site of the intercellular junction (Zieler et al., 2000). However, the ultrastructural evidence was still missing. We followed ookinete invasion by fixation of *P. berghei* infected midguts at different time points post infection and observed by electron microscopy. We observed that parasites have no preference for invading a specific cell type. This confirms a recent report by Baton et al., (2004) that also found no evidence of preferential invasion of any morphologically distinct cells by ookinetes. Strikingly, we were not able

to observe the parasites at the moment of midgut cell invasion. As others (Kadota et al., 2004, Vlachou et al., 2004) also failed to capture the penetration process, we suggest that this is a remarkably rapid process. To examine this issue, other than electron microscopy cell biology tools are required. Thus a transgenic mosquito with a fluorescent marker for the epithelial cell membrane would be a great help to define this argument. Secondly, the route of ookinete migration has been reported to be either intercellular or intracellular depending on the parasite-mosquito species combinations. We demonstrate by electron microscopy that after a rapid entry through the cell, the ookinetes of *P. berghei* preferentially take an intercellular route to cross the *A. gambiae* midgut.

**Mechanism of parasite killing / clearance**

● We demonstrated that the previously described filamentous zone surrounding melanized ookinetes is composed of polymerized actin, and we renamed it the "actin zone". The formation of this zone occurs when parasites are dead or dying, suggesting that the actin zone is not associated with killing of parasites. In addition, the formation of the actin zone is TEP1-dependent, indicating that *TEP1* could be the genetic determinant of this structure.

● Taken together, our results lead us to re-evaluate the model of TEP1-dependent clearance of *P. berghei* ookinetes in *A. gambiae* (Figure 7). First, the parasites cross the midgut epithelium (preferentially by an intercellular route) and come into contact with soluble hemolymph components. TEP1 recognizes and binds to the ookinetes, causing them to die by an as yet unknown mechanism. The dead parasites are disposed of either by lysis or, in the case of R mosquitoes, lysis and melanization. Lysed parasites in both R and S mosquitoes and melanized parasites in R mosquitoes are then encircled by an organelle-free, finely fibrillar actin zone, and are thereby separated from the adjacent epithelial cells. The model predicts that the killing of parasites is controlled by TEP1 and that killed or dying ookinetes are separated by the actin zone from the epithelial environment. However, there are still questions to be answered: (1) How is TEP1 targeted to the parasite surface? (2) How does TEP1 binding trigger the destruction of parasites? (3) What is the destiny of the actin zone-encircled parasites?

**How is TEP1 targeted to parasite surface?**

We reported that TEP1 binds to the surfaces of bacteria and parasites, but we did not detect TEP1 on the surface of mosquito cells by immuno-histochemical analysis. The specific binding of TEP1 to pathogen surfaces could result from: (1) the specific recognition of pathogens by TEP1 or associated activating molecules from mosquito, (2) the localized activation of TEP1 by pathogen proteases that are either membrane-bound or secreted by pathogens and thus present in higher concentrations in the vicinity of the pathogen surface, (3) specific inhibitory molecules expressed by mosquito cells. These questions will undoubtedly form the basis of future investigations.

**How does TEP1 binding trigger the destruction of parasites?**

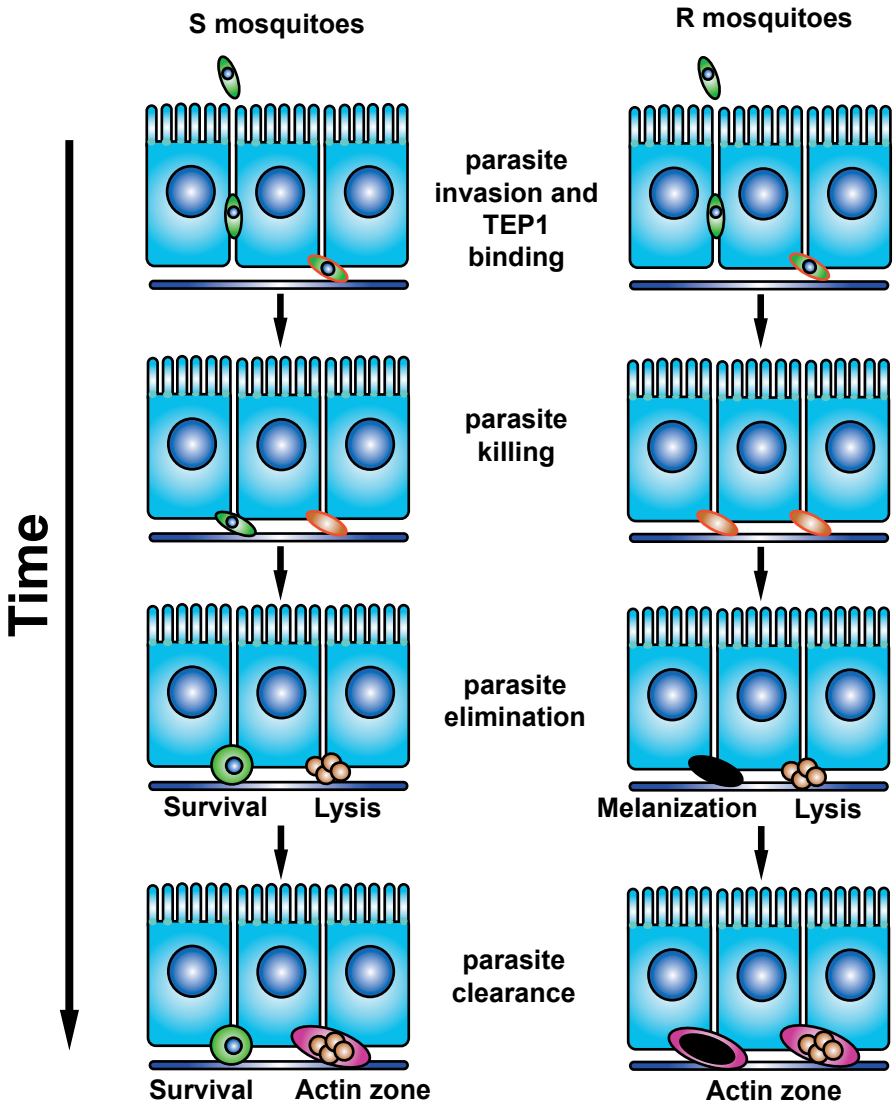


**Figure 7. Model for the TEP1-dependent antiparasitic response in refractory (R) and susceptible (S) mosquitoes**
Motile ookinetes (green) traverse the mosquito midgut (in light blue with microvilli on the lumen side) extracellularly for the most part and reach the basal lamina (thick blue line) where they become labelled with TEP1 (red line around ookinetes). This labelling targets parasites for killing. Dead parasites (brown) loose their nuclei (blue), and are eliminated. All parasites are killed in R mosquitoes whereas in S mosquitoes, some parasites survive and transform into oocysts (round and green). In S mosquitoes, dead parasites are disposed of by lysis (brown balls), whereas in R mosquitoes both lysis and melanization (black) are observed. Lysed parasites in both R and S mosquitoes, and melanized parasites in R mosquitoes are then encircled by an organelle-free, finely fibrillar actin zone (purple) to separate them from the adjacent epithelial cells.

Binding of TEP1 to bacteria promotes their uptake by hemocytes, probably via the interaction with a receptor that remains to be identified. We do not yet understand the mechanisms that are triggered by TEP1 binding to parasites. It is tempting to speculate that TEP1 may function as a complement-like

factor, with the covalent binding of its C-terminal part recruiting the formation of a structure similar to the membrane attack complex in mammals, and directing killing of the parasite.

In collaboration with EMBL, Heidelberg, we have recently established homozygous transgenic mosquito lines which phenotypically correspond to gain- (GOF) and loss-of-function (LOF) phenotypes for *TEP1*. We started analysis of these lines for transcriptional profiling using commercially-available Affymetrix mosquito genome arrays. We used two time points for comparative analysis of gene cohorts co-expressed with *TEP1* in control, in *TEP1* GOF and in *TEP1* LOF mosquitoes. We infected mosquitoes with GFP-expressing *P. berghei* and dissected their midguts at 24 h and 4 days post-infection for RNA extraction. We performed clustering of the microarray data and grouped genes according to their expression pattern in the three selected mosquito strains at these two time points. Our preliminary results show that a large number of genes are differentially expressed at the two time points. We hypothesize that genes positively involved in the activation of TEP1 should be up-regulated at both time points and should display the highest levels of expression in the GOF line, followed by the control mosquitoes, with minimal expression levels in the LOF line. Using this concept, we will select candidate genes for functional analysis by dsRNA silencing and examination of mosquito midgut for parasite survival. These results will hopefully shed light on the mechanisms of activation of the complement-like proteins in insects and provide insights on parasite recognition in the mosquito midgut.

**What is the destiny of the actin zone-encircled parasites?**

Dead parasites are eliminated by lysis and melanotic encapsulation and then separated by the actin zone from the adjacent epithelial cells. There are two possibilities for this issue: (1) The actin zone-encircled dead parasites will most probably stay in the zones, as melanized parasites in the refractory strain are still visible by light microscopy 10 days post infection. (2) The actin zone might degenerate and disappear after a certain number of days since its function is completed. Further ultrastructural studies focussing on later time points might bring answers for this issue.

Although some projects during my thesis produced negative results, the performed experiments were important to guide the development of adequate tools and acquisition of my expertise in the field of insect immunity. My hope is that results of the projects I was involved into will promote the identification of novel gene pathways that directly regulate mosquito-*Plasmodium* interactions. Identification of such genes and establishment of gene-specific tools (probes, antibodies etc) will be crucial for future studies on vector competence in the natural populations of *A. gambiae*.

# THÈSE EN FRANÇAIS

# Etude Cellulaire et Moléculaire des Interactions Entre le Parasite du Paludisme *Plasmodium berghei* et le Vecteur *Anopheles gambiae*

# INTRODUCTION

Le paludisme est de loin la maladie transmise par les insectes qui affecte le plus d'humains. Elle est provoquée par un parasite eucaryote unicellulaire, *Plasmodium*, et est transmise à l'homme par un moustique vecteur, *Anopheles*. Cette maladie, actuellement endémique en Afrique, en Amérique du sud et en Asie du sud-est, est particulièrement meurtrière en Afrique sub-saharienne, où elle fait au moins 90% de ses victimes. Chaque année, entre 300 et 500 millions de personnes contractent le paludisme et plus 2 millions en meurent, principalement des enfants de moins de 5 ans. Parmi les adultes, ce sont les femmes enceintes et les touristes non-immunisés qui sont les plus vulnérables. Outre les conséquences humaines, cette maladie est aussi un frein au développement économique des pays endémiques : la grande majorité de ces pays sont aussi ceux qui ont le plus faible produit national brut par habitant et les taux de croissance économique les plus bas (Sachs and Malaney, 2002).

### Le cycle de vie de *Plasmodium*

Les parasites responsables du paludisme sont transmis à l'homme par un moustique femelle infecté lorsque celle-ci prend un repas de sang. Afin de pouvoir infecter l'hôte suivant, le parasite doit suivre un cycle de développement complexe dans le moustique (Figure 8). À l'intérieur de l'intestin, les gamétocytes males et femelles se développent en gamètes ; la fécondation a alors lieu, quelques heures seulement après le repas de sang. Les zygotes ainsi formés se transforment en oocinètes mobiles qui envahissent et traversent l'épithélium intestinal 24 à 48h après l'infection. Une fois qu'ils ont atteint le côté basal, ils forment des kystes, appelés ookystes, entre l'épithélium intestinal et la membrane basale. Pendant les 10 jours qui suivent, à l'intérieur de chaque ookyste, une méiose suivie de nombreux cycles mitotiques, produisent des milliers de sporozoïtes haploïdes. Quatorze à 16 jours après infection, les sporozoites sont libérés dans l'hemocoele (équivalent du système circulatoire des vertébrés) du moustique, migrent et envahissent les glandes salivaires du moustique. Le cycle du parasite dans le moustique est achevé quand le moustique injecte ces sporozoïtes infectieux dans l'hôte suivant.

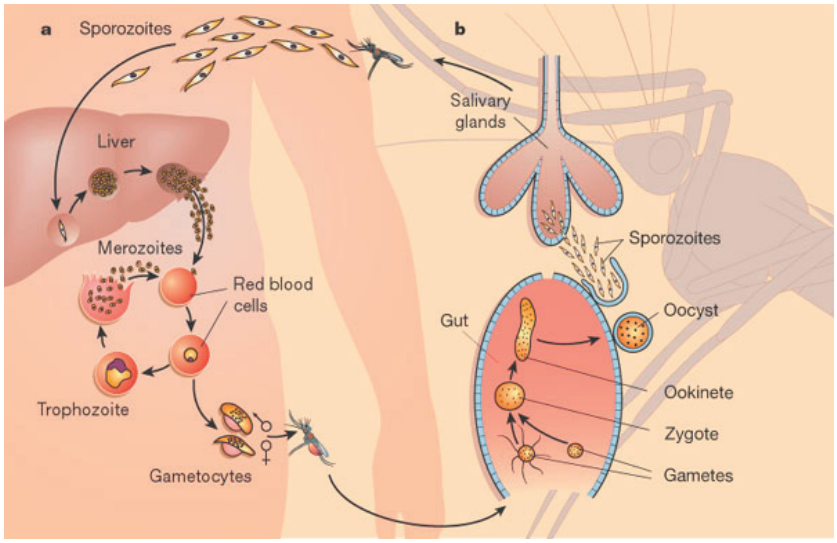


**Figure 8. Cycle de vie de Plasmodium.** Le parasite passe par de nombreux stades développementaux qui sont adaptés à l'invasion et à multiplication dans des types de cellules différents chez l'hôte humain et chez le moustique vecteur.

**Des moustiques susceptibles et des moustiques réfractaires**

À cause de la complexité des interactions entre le parasite et le moustique, la plupart des parasites ne peuvent se développer que dans un nombre très restreint d'espèces de moustiques et ainsi, seul un nombre limité de combinaisons *Plasmodium* - *Anopheles* peuvent transmettre le paludisme dans un groupe particulier de vertébrés. Outre ces variations interspécifiques, la capacité de chaque moustique à supporter le développement du parasite (ou capacité vectorielle) varie énormément entre individus d'une même espèce. Aussi, les interactions moustique – parasite constituent un aspect essentiel de la transmission de la maladie et représentent des cibles potentielles pour les stratégies visant à contrôler le paludisme. Les facteurs qui font qu'un moustique n'est pas capable de transmettre le parasite sont de deux ordres : le moustique est dépourvu d'un élément requis pour le développement du parasite, comme par exemple l'acide xanthurenic (Billker et al., 1998) qui est nécessaire à la gamétogénèse et/ou la réponse immunitaire du moustique est efficace pour supprimer le développement des parasites.

**La réponse immunitaire du moustique**

Plusieurs faits semblent en effet indiquer que les moustiques se sont dotés d'une réponse antiparasitaire efficace. Au cours de son développement chez le moustique, Plasmodium subit de nombreuses pertes et traverse plusieurs goulets d'étranglement, indiquant que le moustique est capable de limiter le développement du parasite. Ceci est confirmé par le cas extrême de deux souches de moustiques réfractaires sélectionnées au laboratoire, où le développement du parasite est bloqué par son encapsulation mélanotique (Collins et al., 1986) ou par sa lyse (Vernick et al., 1995) au niveau du tube digestif. Cependant les mécanismes moléculaires qui sous-tendent ces résistances, et plus généralement les défenses immunitaires du moustique restent à découvrir. L'étude du système immunitaire du moustique a très largement bénéficié de la connaissance plus précise que nous avions des systèmes immunitaires des vertébrés et d'autres Arthropodes, et plus particulièrement de la mouche *Drosophila melanogaster*, qui, comme le moustique, est un insecte diptère. De nombreux gènes potentiellement impliqués dans la réponse immunitaire du moustique ont été identifiés par homologie avec des gènes de l'immunité chez d'autres insectes, ou bien parce que leur expression est modulée lors d'une infection. Cependant, leur rôle dans la réponse immunitaire du moustique, et en particulier dans la défense antiparasitaire, n'avait pas été confirmé par une analyse fonctionnelle. Au moment où nous avons commencé ce projet, plusieurs laboratoires avaient déjà utilisé la méthode d'interférence à ARN pour supprimer spécifiquement l'expression des gènes dans différents organismes, et notamment, dans des cultures de cellules de drosophile. Aussi, nous avons décidé d'adapter cette méthode chez l'anophèle afin de pouvoir étudier la fonction des gènes. La mise en place de nouvelles techniques telles que l'interférence à ARN (Blandin et al., 2002), la transformation génétique (Catteruccia et al., 2000b; Grossman et al., 2001), l'analyse de l'expression des gènes à grande échelle grâce aux puces à ADN (Dimopoulos et al., 2002), couplée avec l'achèvement du séquençage du génome d'Anopheles gambiae (Holt et al., 2002) a amorcé une véritable révolution dans le domaine de l'immunité du mousti-

que. Dans une revue que nous avons récemment publié (Blandin and Levashina, 2004a), nous faisons état de nos connaissances antérieures et voyons en quoi ces progrès techniques ont changé notre vision du système immunitaire de l'anophèle.

**La famille des protéines à thioester**

Les bases moléculaires de la reconnaissance des pathogènes chez le moustique, comme chez la drosophile d'ailleurs, sont longtemps restées inconnues. Afin d'aborder ce problème, nous avons choisi d'étudier les protéines à thioester (TEPs pour "Thioester-containing proteins") en tant que molécules potentiellement impliquées dans la reconnaissance des pathogènes et dans l'activation des effecteurs de la réponse immunitaire. En effet, chez les vertébrés, les membres de cette famille sont d'importants acteurs de la réponse immunitaire, on y trouve :

• les α2-macroglobulines (α2Ms), qui sont des inhibiteurs universels de protéases, probablement impliqués dans l'élimination des protéases qui sont libérées lors d'une blessure ou qui sont produites par des pathogènes,

• les facteurs C3, C4 et C5 du complément, qui se lient à la surface des pathogènes et favorisent ainsi leur élimination par phagocytose ou par lyse cellulaire. Les TEPs ont en commun plusieurs caractéristiques: ces protéines de grande taille (~1500 acides aminés) sont (i) sécrétées sous forme inactive. (ii) Pour devenir fonctionnelles, elles doivent être activées par clivage protéolytique. (iii) Les TEPs se lient de façon covalente à la surface de leurs cibles (des pathogènes dans le cas des facteurs du complément, et des protéases dans le cas des α2Ms) via leur liaison thioester (iv) hautement réactive et très conservée parmi les TEPs. L'activation protéolytique ainsi que la liaison de la TEP à sa cible exposent son domaine Cterminal, permettant ainsi l'élimination du complex par phagocytose ou endocytose médiées par un récepteur. Dans le cas du complément, le clivage génère deux fragments: le fragment C-terminal qui contient le thioester et qui est lié à la cible et le fragment N-terminal (anaphylatoxine) qui déclenche l'inflammation au niveau du site d'infection. Toutes ces caractéristiques fonctionnelles imposent des contraintes particulières sur l'organisation structurale de ces protéines.

# BUTS DE L'ÉTUDE

Le parasite *Plasmodium* active la réponse immunitaire innée du vecteur moustique. Les lourdes pertes du nombre de parasites pendant le cycle de sporogonie montrent que les réponses immunitaires d'*A. gambiae* joue certainement un rôle important dans la compétence du vecteur. L'identification des mécanismes cellulaires et moléculaires appartenant à la recognition du non-soi et l'activation de la réponse immunitaire est une étape clé pour comprendre comment le vecteur limite l'invasion du parasite.Afin d'augmenter les connaissances des interactions parasite-vecteur, mon projet cible la caractérisation des interactions hôte-parasite au niveau cellulaire et moléculaire. Les principaux buts sont présentés ci-dessous.

**1. Développement d'un système *in vitro* pour l'étude des interactions entre une lignée cellulaire de moustique et le parasite**

L'étude de tout organisme pathogène est considérablement entravée par l'absence de modèle animal approprié et l'absence de système de culture. Avant le développement d'une méthode in vitro pour la maintenance au laboratoire du plus important parasite causant la malaria chez l'homme, i.e. *Plasmodium falciparum*, la recherche contre la malaria était sévèrement désavantagée. Plusieurs laboratoires ont étudié les étapes critiques des interactions hôte-parasite au niveau de l'invasion de l'estomac et des glandes salivaires. Ici, nous utilisons le système de co-culture *in vitro* pour l'analyse cellulaire et moléculaire des interactions des lignées cellulaires hémocytaires avec les étapes de sporogonie de *Plasmodium berghei*. La vue générale et l'analyse de l'ultrastructure détaillée des intéractions moustique-parasite ont été réalisées, respectivement, par microscope confocal et microscope à transmission électronique. De plus, l'expression génique au niveau transcriptionnel dans un système de co-culture a été analysée par puces à ADN.

**2. Analyse fonctionnelle de la protéine à site thioester 1, TEP1**

La première protéine à site thioester 1 (TEP1) chez le moustique a été identifiée et caractérisée (Levashina et al., 2001). TEP1 sert d'opsonine telle une protéine complément et promouvoit la phagocytose de certaines bactéries à Gram positif dans les lignées cellulaires de moustiques. Par conséquent, une question que l'on se pose est : « Est-ce que TEP1 est impliqué dans la défense immunitaire de moustique contre le parasite de la malaria ? » L'utilisation de la technique d'extinction de l'expression de gènes (silencing, en anglais) par injection d'ARN double brin a permis d'analyser les fonctions de TEP1 chez le moustique.

**3. Étude ultrastructurale du développement sporogonique de *Plasmodium berghei* chez *Anopheles gambiae***

Les actuelles descriptions du cycle de vie du parasite restent relativement schématiques et insatisfaisantes. Les documents du cycle complet d'un parasite à l'intérieur d'un vecteur sont manquants. Pour obtenir une meilleure compréhension de l'interaction d'une espèce spécifique de moustique avec le parasite, le développement de P.berghei au sein de l'estomac d'*A.gambiae* a été suivi par microscope à transmission électronique.

**4. Rôle de l'actine dans l'élimination du parasite chez le moustique *Anopheles***

Il a été reporté récemment qu'une zone filamentaire est présente autour de la majorité d'ookinètes mélanisés dans des lignées réfractaires au parasite. Cependant, l'importance et les composants de ce phénomène restent inconnus. Notre but a été de caractériser cette zone filamentaire en détail par microscopie confocale et microscopie à transmission électronique.

# CONCLUSION

**Mise en place d'un système de co-culture *in vitro***

Nous avons établi un système de co-culture *in vitro* en utilisant une lignée cellulaire semblable aux hémocytes pour modéliser les interactions moustique-parasite, et nous avons démontré par microscopie à transmission électronique que les cellules de moustiques réagissent aux parasites. Les parasites sont phagocytés par des protubérances formées en surface des cellules de moustiques, appelés lamellipodes. Nous supposons, dans ces systèmes de co-culture, que les parasites sont les premiers reconnus par la cellule de moustique et sont alors phagocytés par les lamellipodes protubérants et finalement engloutis par les cellules.

Nous tentons d'utiliser le système de co-culture in vitro pour une analyse fonctionnelle de TEP1. Remarquablement, TEP1 apparaissait à la surface de certains ookinètes seulement après 48 heures de co-culture, alors que TEP1 apparaît à la surface des parasites après 24 heures après infection *in vivo*. De plus, le signal TEP1 à la surface des parasites de l'intestin moyen de moustique était très homogène et au contraire faible, granulaire et épisodique au sein des systèmes de co-culture. Nous supposons que de telles différences sont dues à la différence d'environnement entre les systèmes in vivo et *in vitro*. Le contact d'un ookinète se fait premièrement avec une cellule intestinale puis avec TEP1 *in vivo* alors que c'est le contraire *in vitro*. D'ailleurs, TEP1 doit ne pas être activé en système de co-culture.TEP1 est synthétisé et sécrété par les hémocytes et se lie à la surface des ookinètes présentes dans l'intestin moyen (Levashina et al., 2001, Blandin et al., 2004); donc ce processus comprend deux types différents de lignées cellulaires de moustique est donc compliqué. Les profils d'expression de gènes de moustiques révélés par analyse de puces à ADN, ont suggéré des différences entre les systèmes in vitro et in vivo. Nous supposons que le système de co-culture in vitro n'est pas approprié pour une analyse fonctionnelle. Cependant, nous pouvons toujours utiliser ce système de co-culture pour interpréter les intéractions moléculaires de certains gènes induits par PGN, sans utiliser les ookinètes.

**Analyse fonctionnelle de la protéine TEP1**

L'analyse fonctionnelle de TEP1 permet de démontrer que TEP1 se lie et participe à l'élimination de *P. berghei* au niveau de l'intestin moyen. La liaison de TEP1 augmentant ainsi l'efficacité d'élimination du parasite au niveau de l'intestin moyen, nous rappelle les fonctions des facteurs complément chez les mammifères. De façon conséquente, nos études sur le rôle de TEP1 pendant l'invasion du parasite démontrent que les moustiques se défendent activement contre les parasites de type *Plasmodium*, et les pertes dramatiques en nombre de parasites pendant les premiers jours après infection sont essentiellement dû à l'efficacité de la réponse immunitaire. Ainsi, nous démontrons que TEP1 est un important participant de la réponse immunitaire.

Par conséquent, un modèle pour les réponses immunitaires chez *Anopheles gambiae* contre *P.berghei* est alors le suivant : après la traversée de l'épithélium intestinal, les parasites entrent en contact (au niveau du labyrinthe basal) avec les composants solubles de l'hémolymphe, mais pas avec les hémocytes. Un des composants solubles de l'hémolymphe, TEP1, reconnaît et se lie aux ookinètes, provoquant leur mort par un mécanisme encore inconnu. La prochaine étape est l'élimination des parasites morts, soit par lyse, soit par lyse et mélanisation dans le cas de moustiques réfractaires. Le modèle prédit que les processus d'élimination des parasites morts (i.e. encapsulation mélanique et lyse) sont controllés par d'autres gènes que TEP1. Il est à noter que la liaison de TEP1 induisant la mort des parasites a lieu à lafois dans les moustiques R et S, bien que le phénomène est moins rapide dans les moustiques S. Evidemment, un faible nombre d'ookinètes morts non marqués par TEP1 sont détectés chez les moustiques déficient en TEP1, ce qui suggère que TEP1 n'est pas le seul gène contrôlant le développement du parasite, mais que d'autres gènes et cascades d'induction de gènes doivent agir en concert pour garder le nombre de parasites faible pendant l'infection. Dans ce sens, une protéine immune riche en répétitions de Leucine, LRIM1, a récemment été montrée comme impliquée dans la réponse antiparasitaire chez le moustique (Osta et al., 2004).

**Étude ultrastructurale des interactions *P. berghei-A. gambiae***

La description du cycle de vie du parasite chez le moustique reste quelque part schématique et incomplète. Des rapports sur le cycle complet d'un parasite à l'intérieur d'un vecteur sont toujours manquants. Ici, nous suivons le développement sporogonique complet du parasite *P. berghei* au sein du moustique *A. gambiae*. Les gamétocytes sont fertilisés au niveau de la lumière intestinale pendant le repas sanguin et transformés en zygotes pour finalement se développer en ookinètes mobiles. Les ookinètes s'échappent de cet environnement pour entrer dans les cellules épithéliales intestinales. Une question controversée peut alors être adressée : est-ce que les ookinètes doivent traverser la matrice péritrophique (MP) avant d'entrer au niveau de la cellule intestinale ? Il a été proposé que la MP joue un rôle important en tant que barrière physique afin d'empêcher la migration des ookinètes (Abraham et al., 2004). Nous avons observé que la MP complètement polymérisée est seulement présente audessus des microvilli, et ceci 28 heures après infection ; tandis que la majorité des ookinètes sont déjà entrés dans l'intestin moyen du moustique et s'arrêtent plus bas, au niveau de la lame basale, 24 heures après infection. Il a aussi été décrit que plus de 85% des ookinètes étaient déjà présents au niveau de la lame basale seulement 22 heures après infection (Kadota et al., 2004). Nous supposons que la MP joue un rôle de barrière protectrice pour l'intestin moyen contre d'autres pathogènes (e.g. bactéries) mais pas contre l'invasion parasitaire.

Il a été proposé que l'invasion des ookinètes au niveau des cellules intestinales de moustiques provoque de sérieux dommages, induisant notamment l'expression de la synthase d'acide nitrique et conduisant à l'apoptose (Han et al., 2000 and 2002; Kumar et al., 2004). Cependant, l'évidence ultrastructurale pour cette hypothèse est toujours manquante. Nous avons observé, au niveau de sections d'estomac,

la présence de cellules apoptotiques à la fois dans les intestins moyens de moustiques infectés et non infectés, ce qui indique que le phénomène d'apoptose est probablement indépendant du parasite. Un récent rapport sur l'invasion de *P. falciparum* dans *A.stephensi* suggère que l'invasion des cellules épithéliales doit être un mécanisme général de la réparation tissulaire, plus qu'une réponse spécifique au parasite (Baton et al., 2004). Plus d'analyses par microscopie électronique à immunofluorescence doivent être entreprises pour répondre à cette question.

Le passage d'un ookinete mobile et invasif à travers la paroi intestinale de moustique reste controversé. Les principaux arguments sont comment, où le parasite pénètre dans l'intestin moyen de moustique et quel est le chemin que prend l'ookinète pour migrer au sein de l'intestin. Des études in vitro sous microscope ont montré que les ookinètes pénètrent les cellules intestinales par la membrane latérale apicale adjacente aux jonctions intercellulaires (Zieler et al., 2000). Cependant, l'évidence de l'ultrastructure est toujours manquante. Il a été possible de suivre l'invasion d'un ookinète sous microscope électronique, en fixant des intestins infectés par *P. berghei* à différents points après infection. Nous avons observé que les parasites n'ont pas de préférence pour envahir un type de cellule particulier. Ceci confirme un papier récent de Baton et al. (2004). Remarquablement, nous n'avons pas pu observer les parasites au moment de l'invasion de la cellule intestinale par les parasites. Des rapports similaires (Kadota et al., 2004, Vlachou et al., 2004) montrent que plusieurs tentatives à capturer le processus de pénétration ont échouées, suggérant que ce processus est très rapide. Ainsi, un moustique transgénique avec un marqueur fluorescent pour la membrane de cellule épithéliale serait d'une grande aide pour répondre à cette question. Deuxièmement, la route de la migration d'un ookinète a été décrite étant soit intercellulaire ou intracellulaire, dépendant de la combinaison des espèces parasite-moustique. Nous avons démontré par microscopie électronique que les ookinètes de *P. berghei* préfèrent prendre un chemin extracellulaire pour traverser l'intestin moyen d'*A. gambiae*.

**Mécanisme pour tuer et éliminer le parasite**

Nous avons démontré que la zone filamenteuse entourant les ookinètes mélanisés est composée d'actine polymérisée et nous l'avons surnommée « la zone d'actine ». La formation de cette zone a lieu quand les parasites sont morts ou mourants, ce qui suggère que cette zone d'actine n'est pas la cause de la mort des parasites. De plus, la formation de cette zone est dépendante de TEP1, indiquant que TEP1 pourrait être un déterminant génétique de cette structure.

Tous ensemble, ces résultats nous conduisent à proposer un modèle dépendant de TEP1 permettent l'élimination via l'actine des ookinètes de *P. berghei* chez *A. gambiae*. Premièrement, les parasites traversent l'épithélium intestinal (préférentiellement par un chemin extracellulaire) et arrivent en contact (au niveau du labyrinthe basal) avec des composants de l'hémolymphe soluble, mais pas avec les hémocytes. Un de ces composants, TEP1, reconnaît et se lie aux ookinètes, provoquant leur morts par un mécanisme encore inconnu.

Les parasites morts sont éliminés soit par lyse ou, dans le cas des moustiques R, lyse et mélanisation. Les parasites lysés retrouvés chez les moustiques R et S et les parasites mélanisés retrouvés uniquement chez les moustiques R sont alors encerclés par une zone d'actine finement fibreuse, dépourvue d'organelles. Les parasites sont ainsi isolés des cellules épithéliales adjacentes. Le modèle prédit que la destinée des parasites morts (i.e. lyse et encapsulation mélanique) est contrôlée par TEP1 et que les parasites sont séparés de l'environnement épithélial par une zone d'actine. Cependant, plusieurs questions ne sont toujours pas résolues : (1) Comment TEP1 est ciblé sur la surface des parasites ? (2) Comment la liaison de TEP1 dirige la destruction des parasites ? (3) Quelle est la destinée des parasites encerclés par cette zone d'actine ?

**Comment TEP1 est ciblé sur la surface des parasites ?**

Nous avons prouvé que TEP1 se lie à la surface des bactéries et des parasites mais il est impossible de détecter TEP1 sur la surface des cellules de moustique par analyse immuno-histochimique. La liaison spécifique de TEP1 sur la surface des pathogènes pourrait être due à : (1) la reconnaissance spécifique des pathogènes par TEP1 ou de molécules associées activatrices au niveau du moustique, (2) l'activation localisée de TEP1 par les protéases pathogènes qui seraient soit liées à la membrane ou sécrétées par les pathogènes et donc présentes à de fortes concentrations autour de la surface du pathogène, (3) des molécules inhibitrices spécifiques exprimées par les cellules de moustique. Ces questions vont certainement être à la base de futurs travaux.

**Comment la liaison de TEP1 dirige la destruction des parasites ?**

L'attachement de TEP1 sur des bactéries promouvoit leur emprisonnement par les hémocytes, certainement par l'interaction avec un récepteur qui reste à identifier. Nous ne savons toujours pas quels sont les mécanismes qui sont responsables de la liaison de TEP1 aux parasites. Il est tentant d'imaginer que TEP1 doit fonctionner comme un facteur tel le complément, avec une liaison covalente par sa partie C-terminale et formant ainsi une structure similaire au complexe d'attaque de membrane présent chez les mammifères, tuant ainsi directement le parasite. En collaboration avec l'EMBL, Heidelberg, nous avons récemment établi des lignées de moustiques transgéniques homozygotes qui correspondent phénotypiquement à un gain (GOF) ou une perte de fonction (LOF) pour TEP1. Nous proposons d'utiliser ces lignées pour une analyse des profils transcriptionnels en utilisant des puces à ADN d'A.gambiae, commercialisée par Affymetrix. Nous avons utilisé deux temps de contrôle pour comparer les différentes analyses d'expression de gènes co-exprimés avec TEP1, au niveau de moustiques contrôles, de moustiques GOF et LOF. Les moustiques ont été infectés par le P.berghei exprimant la GFP et les intestins moyens ont été disséqués 24h ou 4 jours après infection, pour une extraction d'ARN. Les données des puces à ADN ont été triées par groupes de gènes correspondant à leur niveau d'expression dans les trois lignées de moustiques sélectionnées et aux deux points de contrôle. Nos résultats préliminaires ont montré qu'un grand nombre de gènes étaient différemment exprimés aux niveaux

de ces deux temps de contrôle. Nous supposons que les gènes impliqués dans l'activation de TEP1 devraient être régulé de façon positive au niveau des deux temps de contrôle et devraient présenter de plus forts taux d'expression au niveau, dans l'ordre, dans la lignée GOF, la lignée contrôle et enfon la lignée LOF. En utilisant ce concept, nous sélectionnerons des gènes candidats pour une analyse fonctionnelle via la technique d'extinction de l'expression de gènes par injection d'ARN double brin et examinerons la survie des parasites au niveau de l'estomac de moustique. Ces résultats vont améliorer les connaissances de l'activation des protéines ressemblantes au complément présent chez les mammifères, et fournir des indications sur la reconnaissance du parasite dans l'intestin moyen de moustique.

**Quelle est la destinée des parasites encerclés par cette zone d'actine ?**

Les parasites morts sont éliminés par lyse et encapsulation mélanique, puis séparés des cellules adjacentes épithéliales par une zone d'actine. Il y a deux possibilités pour se faire : (1) Les parasites morts encerclés par la zone d'actine doivent certainement rester dans cette zone, puisque les parasites mélanisés retrouvés au sein des lignées de moustiques réfractaires sont toujours visibles sous microscopie 10 jours après infection. (2) La zone d'actine devrait dégénérer et disparaître après un certain nombre de jours puisque sa fonction est remplie. Des études ultrastructurales à des temps plus tard après infection seraient  à envisager afin de répondre à cette question.

# MATERIALS AND METHODS

## 1. Mosquito and parasite techniques

*Anopheles gambiae* mosquito maintenance

The susceptible G3 and the refractory L3-5 colonies were reared at 28˚C at a relative humidity of 80%, with a 12/12 h night/day cycle. Larva were raised in 0.1% salt water and fed with powdered fish food. Adult were fed on wet cotton, soaked in a 10% sucrose solution. To complete the lifecycle, females were allowed to take a blood meal on anaesthetized Balb/C or ICR (CD1) mice. The mosquitoes layed eggs two days after blood meal on a wet filter paper.

Parasite maintenance

*P. berghei* (ANKA strain) clone 2.34, a non-gametocyte producing clone 2.33 (both kindly provided by Prof. R. E. Sinden), and a transgenic *P. berghei* PbGFPconline (Frankle Fayard et al., 2004, kindly provided by Dr. A. Waters) were maintained in ICR mice followed the protocoles established by Sinden (1997). The parasitemia of the infected mice was determined from blood films stained with Diff-Quik I (Dade Behring) or Giemsa solution (Merck) under a light microscope. For blood stage passages, 100-150 µl of blood from an infected mouse (parasitaemia ~ 10%) was subcutaneous injected into a healthy mouse. A maximum of 8 passages was performed, and then a fresh aliquot of blood stage parasite was de-frozen. Only mice in which the infection rate of erythrocytes reached levels above 5% in 3 days were used for infection experiments. For infections, females were allowed to take a blood meal on infected ICR mice at 20˚C for 30 minutes or until the majority of the mosquitoes were fed. Infected mosquitoes were kept in an incubator at 20˚C at a relative humidity of 80% with 12/12 night/day cycle to allow the development of parasites until dissection.

## 2. *In vitro* co-culture methods

Ookinete Culture

*P. berghei* (ANKA clone 2.34 and non-gametocyte producing clone 2.33) infected blood was collected from anaesthetized Balb/C mice by heart puncture. The anaesthetizing solution (0.2% ketamine and 5% xylazine in 1X PBS) was subcutaneously injected into infected mice (100 µL/10g of mouse body weight). The infection of the mice and the ookinete culture conditions has previous been described (Sinden, 1997). Briefly, parasitized blood drawn by cardiac puncture from infected mice was immediately 10 times diluted in precooled RPMI-1640 medium (pH 7.4) containing 10% FCS, and passed through a column (Plasmodifur) to remove the white blood cells. The blood was then transferred into a 75 ml culture flask and incubated at 20˚C for 24 h. Mature ookinetes were purified either using Nycodenz gradient (Carter et al., 1987) or magnetic beads (Dynabead®) coated with 13.1 monoclonal antibody against P28 (Kind gift of Prof. R.E. Sinden).

Cell Line

The cell line used was Sua 5.1* isolated from smashed trypsinized larvae of *A. gambiae* Suakoko strain (Müller et al., 1999) kindly supplied by Dr. Hans-Michael Müller, EMBL, Heidelberg. The Sua 5.1* cell line was cultured in Schneider medium (Gibco) supplemented with 10% fetal calf serum (FCS, Sigma, heat-inactivated for 2 h at 56˚C, ) and antibiotics (100 units/ml of penicillin and 100 µg/ml of streptomycin, Sigma). Cells were split regularly every 4 to 6 days, and seeded at 50% confluency in

disposable plastic cell culture flasks (Nunc) under a tissue culture hood at 25˚C.

Co-culture System

To establish the *in vitro* co-culture system, a basement membrane-like Matrigel (Sigma) was used. Pre-cooled Matrigel were gently spread on the surface of sterile coverslip in a 24-well culture plate. The mosquito cells were added into the wells after the Matrigel was completely polymerized. After incubation for 24 hours at 25˚C, the cells attached to the Matrigel and the purified ookinetes were then directly added into the well at a ratio of 1:10 (ookinete: culture cells). The co-cultures were incubated at 25˚C until further analysis. The immunofluorescence staining and analysis was directly performed in the culture plate.

**3. Immunological techniques**

Immunofluorescence staining and confocal microscopy of the co-culture system

Antibodies used were 13.1 monoclonal antibody directed against P28 (Tirawanchai and Sinden, 1990) and TEP1 polyclonal antibody (Levashina et al., 2001). The staining was done directly on the 24-well plate. The medium of the co-culture was removed, and the cells were fixed for 30 minutes with 4% formaldehyde in phosphate buffered saline (PBS), then washed three times with PBS. The primary antibodies were then added at a dilution of 1:1000 and 1:300 for 13.1 monoclonal and TEP1 polyclonal antibody, respectively. Samples were incubated either at 4˚C overnight or room temperature for 1 h, and then washed three times with PBS. The secondary antibody was added and incubated for 1 h and washed three times with PBS. The nuclei were stained either with DAPI (1:1000) or with TO-PRO-3 (1:1000) (Molecular Probes). All the procedures were performed at room temperature and avoided light after the secondary antibody was added. Samples were mounted using the ProLong Antifade Kit (Molecular Probes) and analyzed under a Zeiss LSM 510 confocal microscope. Several laser lines were used for the excitation of the fluorescent probes: Ar for Alexa-488 (wavelength 488 nm), He-Ne for Rhodamine-Phalloidin and Cy3 (wavelength 543 nm), Kr-Ar for Cy5 or TO-PRO3 (wavelength 633 nm) and UV for DAPI (wavelength 650 nm). The reconstruction of the 3-dimentional image was obtained from a Z-series (usually 20-30 slices) of 2-dimentional images. The 2-dimentioned images was collected in the size of 1024 X 1024, and using Z-stack for series scanning for certain depths of the sample. The thickness of each 2-dimentional images should be corresponded to the pinhole, usually set around 0.9 μm. The final assembling of the 2-and 3-dimensional images was processed by the Zeiss LSM 510 Image Browser.

Immunofluorescence staining and confocal microscopy of mosquito midgut

The dissected mosquito midguts were prefixed for 15 seconds in fixative (4% formaldehyde in PBS), then cut open with a microdissection scissors on an ice-cold glass plate. The blood meal was removed and the epithelium was fixed for another 1 h. The sample was washed three times in PBS for 15 min. Phalloidin staining (2 μM) was performed before permeabilization. The sample was then permeabilized in PBS-T (0.1% Triton-100 in 1X PBS, pH 7.2) and blocked (0.1% Triton-100 and 1% Bovine Serum Albumin in 1X PBS, pH 7.2). The primary antibodies were then added at a dilution of 1:1000 and 1:300 for monoclonal alpha-actin and polyclonal TEP1 antibody, respectively. The following procedures were as described above for the co-culture system.

**4. Transmission electron microscopy**

Transmission Electron Microscopy (TEM) for the co-culture system

The co-culture samples were directly fixed with 4% glutaraldehyde in 0.1 M phosphate buffer (pH 7.2) for 1 h, rinsed with 0.1M phosphate buffer and post-fixed with 1% osmium tetroxide for 1 h. After post-fixation, the sample was rinsed with 0.1 M phosphate buffer, dehydrated through a graded ethanol series until 100% ethanol, and embedded in an epoxy resin. Ultrathin sections were cut on a Reichert Om U3 ultramicrotome and observed using a BioTwin, Phillips transmission electron microscope operating at 60 kV accelerating voltage.

Immuno-electron microscoy

The mosquito midguts were dissected 30 h postinfection and fixed in 1% formaldehyde, 0.5% glutaraldehyde for 1 h and rinsed with 0.1 M phosphate buffer (pH 7.2). The samples were then permeabilized in PBS-T (0.1% Triton-100 in 1X PBS, pH 7.2) and blocked (0.1% Triton-100 and 1% Bovine Serum Albumin in 1X PBS, pH 7.2). Midguts were incubated overnight at 4˚C with rabbit polyclonal antibody against TEP1 at 1:100, followed by 1 h incubation with a 10 nm gold particle-conjugated secondary antibody (British BioCell International, 1:60). The samples were then dehydrated, embedded in epoxy resin and sectioned for examination with an electron microscope (BioTwin, Phillips) at 60kV accelerating voltage.

Toluidine blue staining

The semi-thin sections were stained by toluidine blue, a basophilic dye, for pre-examination of the embedding samples. The samples were sectioned by glass knife in the thickness of 400 -500 nm, and transferred to a glass slide within a drop of water. The section was fixed on the glass slide by evaporating the water on a hot plate. The toluidine blue solution (0.1 g of toluidine blue, and 1 g of borax in 100 ml H2O) was drop onto the section and leave for 2 min on the hot plate. The glass slide was then rinsed with water and dried for light microscope observation.

Transmission electron microscopy for mosquito midgut

The mosquito midguts were carefully dissected in 0.1 M phosphate buffer and fixed by 4% glutaraldehyde. The sample was postfixed in 1% osmium tetroxide, rinsed, dehydrated through a graded ethanol series and embedded in an epoxy resine. Ultrathin sections were cut on a Reichert ultramicrotome and transferred to 150-mesh grids. Sections were stained with uranyl acetate and lead citrate (Reynold's lead) and examined by a Hitachi TEM operating at 60 kV accelerating voltage.

**5. cDNA microarray methods**

Construction of Anopheles cDNA Microarrays

A two-step PCR amplication of 3840 EST clone inserts was performed using T3 and T7 primers and LB cultures as primary templates. Ethanol-precipitated PCR products were resuspended in ArrayIt Microspotting solution (Telechem International, Sunnyvale, CA) and spotted on aminosilane-coated glass slides with the Omnigrid microarray spotter (GeneMachines, San Carlos, CA). The slides then were incubated at 60˚C for 3 h and at 100˚C for 10 min to cross-link the DNA and kept dry under vacuum until hybridization.

Probe Preparation and Microarray Hybridization

cmRNA was synthesized with an Ambion MEGAscript T7 RNA synthesis kit (Ambion, Austin TX) from double-stranded cDNA primed with an oligo d(T)-T7 promoter sequence. Complementary cDNA probes were synthesized and labeled with Cy-3-dUTP and Cy-5-dUTP fluorescent nucleotide analogs, in a random primed first-strand reverse-transcription reaction. After removal of unincorporated dNTPs with a Qiagen PCR purification kit (Qiagen, Chatsworth, CA), the probes were combined, lyophilized, and resuspended in hybridization buffer containing 50% formamide, 6X SSC, 0.5% SDS, 5X Denhardt's reagent, and 0.5 mg/ml poly(A) DNA. Arrays were prehybridized in 6X SSC, 0.5% SDS and 1% (v/v) BSA at 42˚C for 90 min, hybridized overnight at 42˚C in humidified hybridization chambers, washed twice in 0.1X SSC, 0.1%SDS (5 minutes), twice in 0.1X SSC (5 minutes), then rinsed with de-ionized water and air dried.

Microarray Data Analysis

Intensities of hybridized probes were estimated with GenePix 4000b (AXON Instruments, Foster City, CA) semiconfocal microarray scanner and corresponding software. The hybridization ratio for each probe was calculated using the estimated ratio of medians after normalization of the total array intensity. The estimated fold regulation value of each clone was expressed as the log-2 value of the normalized ratio of medians. To ensure reproducible regulation profiles, genes were only selected for cluster analysis if regulated above a threshold, set as 2-fold in at least two experiments. Clustering analysis and graphic presentations were performed by using the CLUSTER and TREEVIEW software (available at http://rana.lbl.gov/index.htm?software/).

# References

Abraham, E. G., and Jacobs-Lorena, M. (2004). Mosquito midgut barriers to malaria parasite development. Insect Biochem. Molec. Biol. *34*, 667–671.

Aderem, A., and Underhill, D. M. (1999). Mechanisms of phagocytosis in macrophages. Annu Rev Immunol. *17*, 593-623.

Aikawa, M. (1971). *Plasmodium*: The fine structure of malaria parasites. Experimental Parasitology *30*, 284-320.

Al-Olayan, E. M., Beetsma, A. L., Butcher, G. A., Sinden, R. E., and Hurd, H. (2002). Complete development of mosquito phases of the malaria parasite *in vitro*. Science *295*, 677–679.

Alavi, Y., Arai, M., Mendoza, J., Tufet-Bayona, M., Sinha, R., Fowler, K., Billker, O., Franke-Fayard, B., Janse, C. J., Waters, A., Sinden, R.E. (2003). The dynamics of interactions between *Plasmodium* and the mosquito: a study of the infectivity of *Plasmodium berghei* and *Plasmodium gallinaceum*, and their transmission by *Anopheles stephensi*, *Anopheles gambiae* and *Aedes aegypti*. International Journal for Parasitology *33*, 933-943.

Baton, L. A., and Ranford-Cartwright, L. C. (2004). *Plasmodium falciparum* ookinete invasion of the midgut epithelium of *Anopheles stephensi* is consistent with the Time Bomb model. Parasitology *129*, 663-676.

Baton, L. A., and Ranford-Cartwright, L. C. (2005).How do malaria ookinetes cross the mosquito midgut wall? Trends in Parasitology *21*, 22-28.

Becker, W., and Hardin, J. (2000). The cytoskeleton and cell motility. Becker, W., Kleinsmith, L. J., and Hardin, J. (Eds) The world of the cell. The Benjamin/Cummings Publishing Company. *pp*752-780.

Beernsten, B. T., Lames, A. A., and Christensen, B. M. (2000). Genetics of mosquito vector competence. Microbiol Mol. Biol. Rev. *64*, 115-137.

Billker, O., Lindo, V., Panico, M., Etienne, A. E., Paxton, T., Dell, A. Rogers, M. Sinden, R. E., and Morris, H. R. (1998). Identification of xanthurenic acid as the putative inducer of malaria development in the mosquito. Nature *392*, 289–292.

Billingsley, P. F. (1990). The midgut ultrastructure of hematophagous insects. Annu. Rev. Entomol.

*35*, 219-248.

Billingsley, P. F., and Lehane, M. J. (1996). Structure and ultrastructure of the insect midgut. Billingsley, P. F., and Lehane, M. J. (Eds) Chapman and Hall. *pp*3-30.

Blandin, S., Moita, L.F., Koecher, T., Wilm, M., Kafatos, F.C., and Levashina, E.A., (2002). Reverse genetics in the mosquito *Anopheles gambiae*: targeted disruption of the Defensin gene. EMBO reports *3*, 852-856.

Blandin, S., and Levashina, E. A. (2004a). Thioester-containing proteins and insect immunity. Mol Immunol *40*, 903-908.

Blandin, S., Shiao, S.-H., Moita, L. F., Janse, C., Waters, A. P., Kafatos, F. C., and Levashina, E. A. (2004b). Complement-like protein TEP1 is a determinant of vectorial capacity in the malaria vector *Anopheles gambiae*. Cell *116*, 661–670.

Canning, E. U., and Sinden, R. E. (1973). The organization of the ookinete and observation on nuclear division in oocysts of *Plasmodium berghei*. Parasitology *67*, 29-40.

Carter, F. H., Suhrbier, A., Beckers, P. J. A., and Sinden, R. E. (1987). The *in vitro* cultivation of *Plasmodium falciparum* ookinetes, and their enrichment on Nycodenz density gradients, Parasitology *95*, 25-30.

Catteruccia, F., Nolan, T., Blass, C., Müller, H. M., Crisanti, A., Kafatos, F. C. (2000). Toward *Anopheles* transformation : Minos element activity in anopheline cells and embryos. Proc. Natl. Acad. Sci. USA. *97*, 2157-2162.

Cerenius, L., and Soderhall, K. (2004). The prophenoloxidase-activating system in invertebrates. Immunol Rev. *198*, 116-26.

Chitnis, C. E. and Blackman, M. J. (2000). Host cell invasion by malaria parasites. Parasitology Today *16*, 411-415.

Choe, K. M., Werner, T., Stoven, S., Hultmark, D., and Anderson, K. V. (2002). Requirement for a peptidoglycan recognition protein (PGRP) in Relish activation and antibacterial immune responses in *Drosophila*. Science *296*, 359-362.

Christophides, G.K., Zdobnov, E., Barillas-Mury, C., Birney, E., Blandin, S., Blass, C., Brey, P.T., Collins, F.H., Danielli, A., Dimopoulos, G., Hetru, C., Hoa, N.T., Hoffmann, J.A., Kanzok, S.M., Letunic,

I., Levashina, E.A., Loukeris, T.G., Lycett, G., Meister, S., Michel, K., Moita, L.F., Müller, H.M., Osta, M.A., Paskewitz, S.M., Reichhart, J.M., Rzhetsky, A., Troxler, L., Vernick, K.D., Vlachou, D., Volz, J., von Mering, C., Xu, J., Zheng, L., Bork, P., Kafatos, F.C., 2002. Immunity-related genes and gene families in *Anopheles gambiae*. Science *298*, 159–165.

Chu, C. T., and Pizzo, S. V. (1994). alpha 2-Macroglobulin, complement, and biologic defense: antigens, growth factors, microbial proteases, and receptor ligation. Lab Invest. *71*, 792-812.

Collins, F. H., Sakai, R. K., Vernick, K. D., Paskewitz, S., Seeley, D. C., Miller, L. H., Collins, W. E., Campbell, C. C., and Gwadz, R. W. (1986). Genetic selection of a *Plasmodium*-refractory strain of the malaria vector *Anopheles gambiae*. Science *234*, 607-610.

Coluzzi, M. (1999). The clay feet of the malaria giant and its African roots: hypotheses and inferences about origin, spread and control of *Plasmodium falciparum*. Parasitologia *41*, 277-183.

Crowley, T. E., Hoey, T., Liu, J. K., Jan, Y. N., Jan, L. Y., and Tjian, R. (1993). A new factor related to TATA-binding protein has highly restricted expression patterns in *Drosophila*. Nature *361*, 557-561.

Danielli, A., Kafatos, F.C., and Loukeris, T.G. (2003). Cloning and characterization of four *Anopheles gambiae* serpin isoforms, differentially induced in the midgut by *Plasmodium berghei* invasion. J Biol Chem *278*, 4184–4193.

Danielli, A., Barillas-Mury, C., Kumar, S., Kafatos, F. C., and Loukeris, T. G. (2005). Overexpression and altered nucleocytoplasmic distribution of *Anopheles* ovalbumin-like SRPN10 serpins in *Plasmodium*-infected midgut cells. Cellular Microbiology *7*, 181–190.

Devenport, M., Fujioka, H., and Jacobs-Lorena, M. (2004). Storage and secretion of the peritrophic matrix protein Ag-Aper1 and trypsin in the midgut of *Anopheles gambiae*. Insect Molecular Biology *13*, 349–358.

Dimopoulos, G., Seeley, D., Wolf, A., and Kafatos, F. C. (1998). Malaria infection of the mosquito *Anopheles gambiae* activates immune-responsive genes during critical transition stages of the parasite life cycle. Embo J *17*, 6115-6123.

Dimopoulos, G., Müller, H. -M., and Kafatos, F. C. (1999). How does *Anopheles gambiae* kill malaria parasites Parassitologia. *41*, 169-175.

Dimopoulos, G., Casavant, T. L., Chang, S., Scheetz, T., Robertss, C., Donohue, M., Schultz, J., Benes, V., Bork, P., Ansorge, W. et al., (2000). *Anopheles gambiae* pilot gene discovery project: identification

of mosquito innate immunity genes from expressed sequence tags generated from immune-competent cell lines. Proc. Natl. Acad. Sci. USA *97*, 6619–6624.

Dimopoulos, G., Christophides, G. K., Meister, S., Schultz, J., White, K. P., Barillas-Mury, C., and Kafatos, F. C. (2002). Genome expression analysis of *Anopheles gambiae*: Responses to injury, bacterial challenge, and malaria infection. Proc. Natl. Acad. Sci. USA *99*, 8814–8819.

Duffy, P. E., and Kaslow, D. C. (1997). A novel malaria protein, Pfs28, and Pfs25 are genetically linked and synergistic as falciparum malaria transmission-blocking vaccines. Infect. Immun. *65*, 1109-1113.

Ferrandon, D., Jung, A. C., Criqui, M., Lemaitre, B., Uttenweiler-Joseph, S., Michaut, L., Reichhart, J., and Hoffmann, J. A. (1998). A drosomycin-GFP reporter transgene reveals a local immune response in *Drosophila* that is not dependent on the Toll pathway. Embo J *17*, 1217-1227.

Franke-Fayard, B., Khan, S. M., Ramesar, J., Mendoza, J., van der Keur, M., van der Linden, R., Sinden, R. E., Waters, A. P., and Janse, C. J. (2004). A *Plasmodium berghei* reference line that constitutively expresses GFP at a high level throughout the complete life cycle. Mol Biochem Parasitol. *137*, 23-33.

Fujioka, H., and Aikawa, M. (2002). Structure and life cycle. Malaria Immunology. *80*, 1-26.

Gantt, S., Persson, C., Rose, K., Birkett, A. J., Abagyan, R., and Nussenzweig. V. (2000). Antibodies against thrombospondin-related anonymous protein do not inhibit *Plasmodium* sporozoite infectivity in vivo. Infect. Immun. *68*, 3667-3673.

Ghosh, A., Edwards, M. J., and Jacobs-Lorena, M. (2000). The journey of malaria parasite in the mosquito: hopes for the new century. Parasitol. Today *16*, 196–201.

Gokudan, S., Muta, T., Tsuda, R., Koori, K., Kawahara, T., Seki, N., Mizunoe, Y., Wai, S. N., Iwanaga, S. and Kawabata, S. (1999). Horseshoe crab acetyl group-recognizing lectins involved in innate immunity are structurally related to fibrinogen. Proc. Natl. Acad. Sci. USA *96*, 10086–10091.

Gottar, M., Gobert, V., Michel, T., Belvin, M., Duyk, G., Hoffmann, J. A., Ferrandon, D., and Royet, J. (2002). The *Drosophila* immune response against Gram-negative bacteria is mediated by a peptidoglycan recognition protein. Nature *416*, 640-644.

Gwadz, R., and Collins, F. (1996). Anopheline mosquito and the agents they transmit. Beaty, B., and Marquardt, W. (Eds) The Biology of Disease Vectors. University Press of Colorado, *pp*73-84.

Han, Y. S., Thompson, J., Kafatos, F. C., and Barrilas-Mury, C. (2000). Molecular interaction between *Anopheles stephensi* midgut cells and *Plasmodium berghei*: the time bomb theory of ookinete invasion of mosquitoes. The EMBO J. *19*, 6030-6040.

Han, Y. S., and Barillas-Mury, C. (2002). Implications of Time Bomb model of ookinete invasion of midgut cells Insect Biochem Mol Biol. *32*, 1311-1316.

Hoffmann, J. A., Reichhart, J. -M., and Hetru, C. (1996). Innate immunity in higher insects. Curr. Opin. Immunol. *8*, 8-13.

Hoffmann J. A., and Reichhart, J. -M., (2002). *Drosophila* innate immunity: an evolutionary perspective Nat. Immunol. *3*, 121-126.

Hoffmann, J. A., Kafatos, F. C., Janeway, C. A., and Ezekowitz, R. A. (1999). Phylogenetic perspectives in innate immunity. Science *284*, 1313-1318.

Hoffmann, J. A. (2003). The immune response of *Drosophila*. Nature *426*, 33-38.

Hurd, H., Al-Olayan, E., and Butcher, G. A. (2003). *In vitro* methods for culturing vertebrate and mosquito stages of *Plasmodium*. Microbes and Infection *5*, 321-327.

Imler, J. -L. and Hoffmann, J. A. (2001). Toll receptors in innate immunity Trends Cell *11*, 304–311.

Ishino, T., Yano, K., Chinzei, Y., and Yuda, M. (2004). Cell-passage activity is required for the malarial parasite to cross the liver sinusoidal cell layer. PLoS Biol. *1*, 13-20.

Ishino, T., Chinzei, Y., and Yuda, M. (2005). A *Plasmodium* sporozoite protein with a membrane attack complex domain is required for breaching the liver sinusoidal cell layer prior to hepatocyte infection. Cellular Microbiology *7*, 199–208.

Ito, J., Ghosh, A., Moreira, L. A., Wimmer, E. A., and Jacobs-Lorena, M. (2002). Transgenic anopheline mosquitoes impaired in transmission of a malaria parasite. Nature *417*, 452-455.

Janse, C., Mons, B., Rouwenhorst, R., Van, D. X. P., Overdulve, J., and Van, D. K. H. (1985). *In vitro* formation of ookinetes and functions and functional maturity of *Plasmodium berghei* gametocytes. Parasitology *91*, 19-29.

Kadota, K., Ishino, T., Matsuyama, T., Chinzei, Y., and Yuda, M. (2004). Essential role of membrane-attack protein in malarial transmission to mosquito host. Proc. Natl. Acad. Sci. USA. *101*, 16310-

16315.

Kappe, S., Bruderer, T., Gantt, S., Fujioka, H., Nussenzweig, V., and Menard, R. (1999). Conservation of gliding motility and cell invasion machinery in apicomplexan parasites. J. Cell Biol. *147*, 937-943.

Kappe, S., Kaiser, K., and Matuschewski, K. (2003). The *Plasmodium* sporozoite journey: a rite of passage. Trends Parasitol. *19*, 135-143.

Krotoski, W. A., Collins, W. E., Bray, R. S., Garnham, P. C. C., Cogswell, F. B., Gwadz, R., Killick-Kendrick, R., Wolf, R. H., Sinden, R. E., Koontz, L. C., and Stantfill P. S. (1982) Demonstration of hypnozoites in sporozoite-transmitted *Plasmodium vivax* infection. Am. J. Trop. Med. Hyg. *31*, 1291-1293.

Khush, R. S., Leulier, F., and Lemaitre, B. (2001). *Drosophila* immunity: two paths to NF-kappa B. Trends Immunol. *22*, 260-264.

Kumar, S., Gupta, L., Han, Y. S., and Barillas-Mury, C. (2004). Inducible peroxidase mediate nitration of *Anopheles* midgut cells undergoing apoptosis in response to *Plasmodium* invasion. J Biol. Chem. *279*, 53475-53482.

Lagueux, M., Perrodou, E., Levashina, E. A., Capovilla, M., and Hoffmann, J. A. (2000). Constitutive expression of a complement-like protein in toll and JAK gain-of-function mutants of *Drosophila*. Proc Natl Acad Sci U S A *97*, 11427-11432.

Lane, N. J., Dallai, R., and Ashhurst, D. E. (1996). Structural macromolecules of the cell membranes and the extracellular matrices of the insect midgut. Billingsley, P. F., and Lehane, M. J. (Eds) Chapman and Hall *pp*115-152.

Lee, S. Y., Wang, R. and Soderhall, K. (2000). A lipopolysaccharide- and beta-1, 3-glucan-binding protein from hemocytes of the freshwater crayfish *Pacifastacus leniusculus*. Purification, characterization, and cDNA cloning J. Biol. Chem. *275*, 1337–1343.

Lehane, M. J. (1997). Peritrophic matrix structure and function. Annu. Rev. Entomol. *42*, 525–50.

Lehane, M., Aksoy, S., and Levashina, E. A. (2004). Immune responses and parasite transmission in blood-feeding insects. Trends Parasitol. *20*, 433-439.

Lemaitre, B., Nicolas, E., Michaut, L., Reichhart, J. M., and Hoffmann, J. A. (1996). The dorsoventralregulatory gene cassette spatzle/Toll/cactus controls the potent antifungal response in *Drosophila*

adults. Cell *86*, 973-983.

Levashina, E. A., Moita, L. F., Blandin, S., Vriend, G., Lagueux M., and Kafatos, F.C. (2001). Conserved role of a complement-like protein in phagocytosis revealed by dsRNA knockout in cultured cells of the mosquito, *Anopheles gambiae*. Cell *104*, 709-718.

Mazzacano, C. A., Vargas, J. C., Mackay, A. J., and Beier, J. C. (1998). *Plasmodium gallinaceum*: Effect of insect cells on ookinete development *in vitro*. Experimental Parasitology *88*, 210-216.

Meis, J. F. G. M., and Ponnudurai, T. (1987). Ultrastructural studies on the interaction of *Plasmodium falciparum* ookinetes with the midgut epithelium of *Anopheles stephensi* mosquitoes. Parasitilogy Research *73*, 500-506.

Meis, J. F. G. M., Pool, G., van Gemert, G. J., Lensen, A. H. W., Ponnudurai, T., and Meuwissen, J. H. E. T. (1989). *Plasmodium falciparum* ookinetes migrate intercellularly through *Anopheles stephensi* midgut epithelium. Parasitology Research *76*, 13-19.

Meister, M. (2004). Blood cells of *Drosophila*: cell lineages and role in host defence. Curr Opin Immunol *16*, 1-6.

Meister, M., and Lagueux, M. (2003). *Drosophila* blood cells. Cellular Microbiology *5*, 573–580.

Mejillano, M. R., Kojima, S. I., Applewhite, D.A. Gertler, F. B. Svitkina, T. M., and Borisy, G. G. (2004). Lamellipodial versus filopodial mode of the actin nanomachinery: Pivotal role of the filament barbed end. Cell *118*, 363-373.

Menard, R. (2001). Gliding motility and cell invasion by Apicomplexa: insights from the *Plasmodium* sporozoite. Cellular Microbiology *3*, 63-73.

Mota, M. M., Pradel, G., Vanderberg, J. P., Hafalla, J. C., Frevert, U., and Nussenzweig, R. S., et al. (2001). Migration of *Plasmodium* sporozoites through cells before infection. Science *291*, 141–144.

Mota, M. M., and Rodriguez, A. (2004). Migration through host cells: the first steps of *Plasmodium* sporozoites in the mammalian host. Cellular Microbiology *6*, 1113–1118.

Müller, A. K., Labaied. M., Kappe, S. H. I., and Matuschewski1, K. (2005). Genetically modified *Plasmodium* parasites as a protective experimental malaria vaccine. Nature *433*, 164-167.

Müller, H. M., Dimopoulos, G., Blass, C., and Kafatos, F. C. (1999). A hemocyte-like cell line established from the malaria vector *Anopheles gambiae* express six prophenoloxidase genes. J Biol Chem *274*, 11727-11735.

Nappi, A. J., Vass, E. (1998). Hydrogen peroxide production in immune-reactive *Drosophila melanogaster.* J Parasitol. *84*, 1150-1157.

Nonaka, M., and Yoshizaki, F. (2004). Evolution of the complement system. Mol Immunol *40*, 897-902.

Nussenzweig, V., and Nussenzweig, R. S. (1985). Circumsporozoite proteins of malaria parasites. Cell *42*, 401-403.

Nusslein-Volhard, C., and Wieschaus, E. (1980). Mutations affecting segment number and polarity in *Drosophila*. Nature *287*, 795-801.

Ochiai, M., and Ashida, M. (2000). A pattern-recognition protein for beta-1,3-glucan. The binding domain and the cDNA cloning of beta-1,3-glucan recognition protein from the silkworm, *Bombyx mori*. J. Biol. Chem. *275*, 4995-5002.

Osta, M. A. Christophides, G. K., and Kafatos, F. C. (2004). Effects of Mosquito Genes on *Plasmodium* Development. Science *303*, 2030-2032.

Paskewitz, S. M., Brown, M. R., Lea, A. O., and Collins, F. H. (1988). Ultrastructure of the encapsulation of *Plasmodium cynomolgi* (B strain) on the midgut of a refractory strain of *Anopheles gambiae*. J. Parasitol. *74*, 432-439.

Pollard, T. D., and Earnshaw, W. C. (2002). Programmed cell death. Schmitt, W. (Ed). Cell Biology. Elsevier Science. *pp*767-782.

Raikhel, A. S., Kokoza, V. A., Zhu, J., Martin, D., Wang, S. F., Li, C., Sun, G., Ahmed, A., Dittmer, N., and Attardo, G. (2002). Molecular biology of mosquito vitellogenesis: from basic studies to genetic engineering of anti-pathogen immunity. Insect Biochem. Molec. Biol. *32*, 1275-1286.

Ramet, M., Manfruelli, P., Pearson, A., Mathey-Prevot, B., and Ezekowitz, R. A. (2002). Functional genomic analysis of phagocytosis and identification of a *Drosophila* receptor for *E. coli*. Nature *416*, 644-648.

Rodriguez, M. C., Gerold, P., Dessens, J., Kurtenbach, K., Schwartz, R. T., Sinden, R. E. and Margos,

G. (2000). Characterization and expression of Pbs25, a sexual and sporogonic stage specific protein of *Plasmodium berghei*. Mol. Biochem. Parasitol. *110*, 147-59

Rogers, W. O., Malik, A., Mellouk, S., Nakamura, K., Rogers M.D. Szarfmann A. (1992). Characterization of *Plasmodium falciparum* sporozoite surface protein 2. Proc. Natl. Acad. Sci. USA *89*, 9176-9180.

Salvesen, G. S., Sayers, C. A., and Barrett, A. J. (1981). Further characterization of the covalent linking reaction of alpha 2-macroglobulin. Biochem J. *195*, 453-461.

Shahabuddin, M., Kaidoh, T., Aikawa, M., Kaslow, D. C. (1995). *Plasmodium gallinaceum*: mosquito peritrophic matrix and the parasite-vector compatibility. Exp Parasitol. *81*, 386-393.

Shahabuddin, M., and Pimenta, P. F. (1998). *Plasmodium gallinaceum* preferentially invades vesicular ATPase-expressing cells in *Aedes aegypti* midgut. Proc. Natl. Acad. Sci. USA *95*, 3385-3389.

Shao, L., Devenport, M., and Jacobs-Lorena, M. (2001). The peritrophic matrix of hematophagous insects. Arch Insect Biochem Physiol. *47*, 119-125.

Sim, E., and Sim, R. B. (1981). Binding of fluid-phase complement components C3 and C3b to human lymphocytes. Biochem J. *198*, 509-518.

Simonetti, A. B., Billingsley, P. F., Winger, L. A. and Sinden, R. E. (1993). Kinetics of expression of two major *Plasmodium berghei* antigens in the mosquito vector, *Anopheles stephensi*. J. Eukaryot. Microbiol. *40*, 569-576.

Sidén-Kiamos, I., Vlachou, D., Margos, G., Beetsma, A., Waters, A. P., Sinden, R. E., and Louis, C. (2000). Distinct roles for Pbs21 and Pbs25 in the *in vitro* ookinete to oocyst transformation to *Plasmodium berghei*. Journal of Cell Science *113*, 3419-3426.

Sinden, R. E., and Canning, E. U. (1972). The ultrastructure of *Plasmodium berghei* ookinetes in the midgut wall of *Anopheles stephensi.* Trans R Soc Trop Med Hyg. *66*, 6

Sinden, R. E., and Strong, K. (1978). An ultrastructural study of the sporogonic development of *Plasmodium falciparum* in *Anopheles gambiae*. Transaction of the Royal Society of Tropical Medicine and Hygiene. *72*, 477-491.

Sinden, R. E. (1997). Infection of mosquitoes with rodent malaria. In The Molecular Biology of Insect Disease Vectors: a Methods Manual. Crampton, J. M., Beard, C. B., and Louis, C. (Eds). London:

Chapman and Hall. *pp*67-91.

Sinden, R. E. (1999). *Plasmodium* differentiation in the mosquito. Parasitologia *41*, 139-148.

Sinden, R. E., and Billingsley, P. F. (2001). *Plasmodium* invasion of mosquito cells: hawk or dove? Trends Parasitol. *17*, 209-212.

Sinden, R. E. (2002). Molecular interactions between *Plasmodium* and its insect vectors. Cellular Microbiology *4*, 713-724

Syafruddin, Arakawa, R., Kamimura, K., and Kawamoto, F. (1992). Development of *Plasmodium berghei* ookinetes to young oocysts *in vitro*. Journal of Protozoology *39*, 333-338.

Sultan, A. A., Thathy, V., Frevert, U., Robson, K. J., Crisanti, A., Nussenzweig, V., Nussenzweig, R. S., and Menard, R. (1997). TRAP is necessary for gliding motility and infectivity of *Plasmodium* sporozoites. Cell *90*, 511-522.

Tamayo, P., Slonim, D., Mesirov, J., Zhu, Q., Kitareewan, S., Dmitrovsky, E., Lander, E. S., and Golub, T. R. (1999). Interpreting patterns of gene expression with self-organizing maps: methods and application to hematopoietic differentiation Proc. Natl. Acad. Sci. USA *96*, 2907–2912.

Tellam, R. L., and Willadsen, W. G. (1999). Peritrophic matrix proteins. Insect Biochem Mol Biol. *29*, 87-101.

Tirawanchai, N., and Sinden, R. E. (1990). Three non-repeated transmission blocking epitopes recognized in the 21 kD surface antigen of zygotes-ookinete of *Plasmodium berghei*. Parasite Immunol *12*, 435-446.

Torii, M., Nakamura, K.-I., Sieber, K. P., Miller, L. H., and Aikawa, M. (1992). Penetration of the mosquito (*Aedes aegypti*) midgut wall by the ookinetes of *Plasmodium gallinaceum*. J. Protozool. *39*, 449-454.

Vizioli, J., Bulet, P., Charlet, M., Lowenberger, C., Blass, C., Müller, H.-M., Dimopoulos, G., Hoffmann, J. A., Kafatos, F. C., and Richman, A. (2000). Cloning and analysis of a cecropin gene from the malariavector mosquito, *Anopheles gambiae.* Insect Molecular Biology *9*, 75–84.

Vizioli, J., Richman, A. M., Uttenweiler-Joseph, S., Blass, C., and Bulet, P. (2001a). The defensin peptide of the malaria vector mosquito *Anopheles gambiae*: antimicrobial activities and expression in adult mosquitoes. Insect Biochem. Molec. Biol. *31*, 241–248.

Vizioli, J., Bulet, P., Hoffmann, J. A., Kafatos, F. C., Müller, H.-M., and Dimopoulos, G. (2001b). Gambicin: A novel immune responsive antimicrobial peptide from the malaria vector *Anopheles gambiae*. Proc. Natl. Acad. Sci. USA *98*, 12630-12635.

Vernick, K. D., Fujioka, H., Seeley, D. C., Tandler, B., Aikawa, M., and Miller, L. H. (1995). *Plasmodium gallinaceum*: A refractory mechanism of ookinete killing in the mosquito, *Anopheles gambiae*. Experimental Parasitology *80*, 583-595.

Vlachou, D., Zimmermann, T., Cantera, R., Janse, C. J., Waters, A. P., and Kafatos, F. C. (2004). Real-time, *in vivo* analysis of malaria ookinete locomotion and mosquito midgut invasion. Cellular Microbiology *6*, 671-685.

Volanakis, J E., (1995). Transcriptional regulation of complement genes. Annu. Rev. Immunol. *13*, 277-305.

Werner, T., Liu,G., Kang, D., Ekengren, S., Steiner, H., and Hultmark, D. (2000) Proc. Natl. Acad. Sci. USA. *97*, 13772–13777.

Warburg, A., and Miller, L. H. (1992). Sporogonic development of a malaria parasite *in vitro*. Science *255*, 448-450.

Warburg, A., and Schneider, I. (1993). *In vitro* culture of the mosquito stages of *Plasmodium falciparum*. Experimental Parasitology *76*, 121-126.

Wirth, D. F. (2002). Biological revelations. Nature *419*, 495-496.

Zheng, L., Cornel, A. J., Wang, R., Erfle, H., Voss, H., Ansorge, W., Kafatos, F. C., and Collins, F.H. (1997). Quantitative trait loci for refractoriness of *Anopheles gambiae* to *Plasmodium cynomolgi* B. Science *276*, 425-428.

Zheng, L., Wang, S., Romans, P., Zhao, H., Luna, C., and Benedict, M. Q. (2003). Quantitative trait loci in *Anopheles gambiae* controlling the encapsulation response against *Plasmodium cynomolgi* Ceylon. BMC Genet *4*, 16.

Zieler, H., and Dvorak, J. A. (2000a) Invasion in vitro of mosquito midgut cells by the malaria parasite proceeds by a conserved mechanism and results in death of the invaded midgut cells. Proc. Natl. Acad. Sci. USA. *97*, 11516-11521.

Zieler, H., Garon, C. F., Fischer, E. R., and Shahabuddin, M. (2000b). A tubular network associated with the brush-border surface of the *Aedes aegypti* midgut: implications for pathogen transmission by mosquitoes. The J. Exp. Biol. *203*, 1599-1611.

Zhou, Z., Hartwieg, E. and Horvitz, H. R. (2001). CED-1 is a transmembrane receptor that mediates cell corpse engulfment in *C. elegans*. Cell *104*, 43-56.